

AJUR

American Journal of
Undergraduate Research

Volume 20 | Issue 1 | June 2023

www.ajuronline.org

Print Edition ISSN 1536-4585
Online Edition ISSN 2375-8732

AJUR

American Journal of
Undergraduate Research

Volume 20 | Issue 1 | June 2023

- 2 **AJUR History and Editorial Board**
- 3 **Divestment Movements over Environmental Issues: The Brazilian Amazon Case**
Pedro Eymael
- 27 **Using Coral Color to Indicate Coral Health in Five Caribbean Species**
Gabriella Herrera, Alexandra M. Good, Alexander Hirota, Catherine Razal, Nicole Gaertner, Justin Sefcik, Jesse Gilbert, & Keisha D. Bahr
- 37 **Synthesis and Palladium-Catalyzed Cross-Coupling of an Alkyl-Substituted Alkenylboronic Acid Pinacol Ester with Aryl Bromides**
Shoma Mukai & Nathan S. Werner
- 47 **Spawning Conditions Affect Clutch Probability and Size in Laboratory-Housed Zebrafish (*Danio rerio*)**
Sydni Anderson, Elizabeth Sipes, Megan Franke, & Dena R. Hammond-Weinberger
- 59 **Color Saturation: Upper and Lower Percentage Histogram Manipulation**
Kyra Obert, Maria Schudt, & Ian Bentley
- 77 **Overexpression of MMACHC Prevents Craniofacial Phenotypes Caused by Knockdown of *znf143b***
Isaiab Perez, Nayeli G. Reyes-Nava, Briana E. Pinales, & Anita M. Quintana

American Journal of Undergraduate Research (AJUR) is a national, independent, peer-reviewed, open-source, quarterly, multidisciplinary student research journal. Each manuscript of AJUR receives a DOI number. AJUR is archived by the US Library of Congress. AJUR was established in 2002, incorporated as a charitable not-for-profit organization in 2018. AJUR is indexed internationally by EBSCO and Crossref with ISSNs of 1536-4585 (print) and 2375-8732 (web).

EDITORIAL TEAM

Dr. Peter Newell, Editor-in-Chief
Dr. Kestutis Bendinskas, Executive Editor
Dr. Anthony Contento, Copy Editor

EDITORIAL BOARD *by subject area*

ACCOUNTING

Dr. Dean Crawford,
dean.crawford@oswego.edu

ARCHEOLOGY

Dr. Richard Redding,
rredding@umich.edu

ART HISTORY

Dr. Lisa Seppi,
lisa.seppi@oswego.edu

BEHAVIORAL NEUROSCIENCE

Dr. Aileen M. Bailey,
ambailey@smcm.edu

BIOCHEMISTRY

Dr. Kestutis Bendinskas,
kestutis.bendinskas@oswego.edu

BIOENGINEERING

Dr. Nin Dingra,
ndingra@alaska.edu

BIOENGINEERING

Dr. Jorge I. Rodriguez,
jorger@uga.edu

BIOINFORMATICS

Dr. John R. Jungck,
jungck@udel.edu

BIOINFORMATICS

Dr. Isabelle Bichindaritz,
ibichind@oswego.edu

BIOLOGY, PHYSIOLOGY

Dr. David Dunn,
david.dunn@oswego.edu

BIOLOGY, DEVELOPMENTAL

Dr. Poongodi Geetha-Loganathan,
p.geethaloganathan@oswego.edu

BIOLOGY, MICROBIOLOGY

Dr. Peter Newell,
peter.newell@oswego.edu

BOTANY

Dr. Julien Bachelier,
julien.bachelier@fu-berlin.de

CHEMISTRY

Dr. Alfredo Castro,
castroa@felician.edu

Dr. Charles Kriley,
ckriley@gcc.edu

Dr. Vadoud Niri,
vadoud.niri@oswego.edu

COMPUTER SCIENCES

Dr. Dele Oluwade,
deleoluwade@yahoo.com

Dr. Mais W Nijim,
Mais.Nijim@tamuk.edu

COMPUTER SCIENCES

Dr. Bastian Tenbergen,
bastian.tenbergen@oswego.edu

COMPUTATIONAL CHEMISTRY

Dr. Alexander Soudackov,
alexander.soudackov@yale.edu

ECOLOGY

Dr. Chloe Lash,
CLash@stfrancis.edu

ECONOMICS

Dr. Elizabeth Schmitt,
elizabeth.schmitt@oswego.edu

EDUCATION

Dr. Charity Dacey,
cdacey@touro.edu

Dr. Marcia Burrell,
marcia.burrell@oswego.edu

EDUCATION, PHYSICS

Dr. Andrew D. Gavrin,
agavrin@iupui.edu

ENGINEERING, ELECTRICAL

Dr. Michael Omidiora,
momidior@bridgeport.edu

ENGINEERING, ENVIRONMENTAL

Dr. Félix L Santiago-Collazo,
fsantiago@uga.edu

FILM AND MEDIA STUDIES

Dr. Lauren Steimer,
lsteimer@mailbox.sc.edu

GEOLOGY

Dr. Rachel Lee,
rachel.lee@oswego.edu

HISTORY

Dr. Richard Weyhing,
richard.weyhing@oswego.edu

Dr. Murat Yasar,
murat.yasar@oswego.edu

HONORARY EDITORIAL

BOARD MEMBER

Dr. Lorrie Clemo,
lorrie.a.clemo@gmail.com

JURISPRUDENCE

Bill Wickard, Esq.,
William.Wickard@KLGates.com

KINESIOLOGY

Dr. David Senchina,
david.senchina@drake.edu

LITERARY STUDIES

Dr. Melissa Ames,
mames@ein.edu

Dr. Douglas Guerra,
douglas.guerra@oswego.edu

MATHEMATICS

Dr. John Emert,
emert@bsu.edu

Dr. Jeffrey J. Boats,
boatsjj@udmercy.edu

Dr. Dele Oluwade,
deleoluwade@yahoo.com

Dr. Christopher Baltus,
christopher.baltus@oswego.edu

Dr. Mark Baker,
mark.baker@oswego.edu

MEDICAL SCIENCES

Dr. Thomas Mahl,
Thomas.Mahl@va.gov

Dr. Jessica Amber Jennings,
jjennings@memphis.edu

METEOROLOGY

Dr. Steven Skubis,
steven.skubis@oswego.edu

NANOSCIENCE AND CHEMISTRY

Dr. Gary Baker,
bakergar@missouri.edu

PHYSICS

Dr. Priyanka Rupasinghe,
priyanka.rupasinghe@oswego.edu

POLITICAL SCIENCE

Dr. Kaden Paulson-Smith,
Paulsonk@unwg.edu

Dr. Katia Levintova,
levintoe@unwg.edu

PSYCHOLOGY

Dr. Matthew Dykas,
matt.dykas@oswego.edu

SOCIAL SCIENCES

Dr. Rena Zito,
rzito@elon.edu

STATISTICS

Dr. Mark Baker,
mark.baker@oswego.edu

TECHNOLOGY, ENGINEERING

Dr. Reg Pecen,
regpecen@sbsu.edu

ZOOLOGY

Dr. Chloe Lash,
CLash@stfrancis.edu

Divestment Movements over Environmental Issues: The Brazilian Amazon Case

Pedro Eymael

School of International Relations, Getulio Vargas Foundation, São Paulo, SP, Brazil

<https://doi.org/10.33697/ajur.2023.076>

Student: pedroeymael15@gmail.com

Mentor: carolina.moehlecke@fgv.br

ABSTRACT

Devastating forest fires in Brazil's Amazon rainforest, one of the most important biomes for Earth's climate balance, have captured the world's attention in 2019 and 2020. Foreign governments, non-governmental organizations and institutional investors pressured Brazilian President Jair Bolsonaro to act and control the situation. Within this context, institutional investors threatened to divest from companies potentially linked to the wildfires and to sell government bonds, creating a divestment movement. Against this background, this article shows that Bolsonaro's responses varied for each of the groups criticizing the handling of the environmental situation. It is argued that the Brazilian government adopted a more conciliatory tone and took more concrete actions when responding to institutional investors' demands, compared to the responses for foreign governments and non-governmental organizations (NGOs). Based on fifteen in-depth interviews conducted in 2021 with professionals involved in this divestment case, the paper concludes that institutional investors played a key role in Bolsonaro's winning coalition and electoral aspirations. Moreover, the shortage of financial capital due to the COVID-19 pandemic created further incentives for Bolsonaro to avoid conflicts with institutional investors.

KEYWORDS

Divestment; Amazon Rainforest; Wildfires; Investors; Climate Change; Brazil; Politics

INTRODUCTION

In 2019 and 2020, the Amazon wildfires took the headlines as the number of destroyed wildlife areas kept breaking records in Brazil. Brazilian President Jair Bolsonaro's administration was accused of being responsible for these events after adopting a series of deregulations on environmental protection, such as rolling back illegal deforestation laws, scaling down the operational ability of the main Brazilian environmental supervisory agency, the Brazilian Institute of the Environment and Natural Resources (IBAMA), and even firing the head of the Brazilian space monitoring organization, the National Institute for Spatial Researches (INPE), who denounced the overwhelming growth of Amazon rainforest loss.¹⁻⁶ These actions not only prompted domestic responses, but also generated reactions from foreign countries, international civil society, and the private sector. However, even though all these actors pressured for better environmental protection, the Brazilian government reacted differently to each one of them, being more responsive to the private sector than others.

Studying the influence that the private sector can exert on governments in comparison to other states and civil society can provide insights about power, decision-making processes, and transnational private governance. The strategy adopted by the financial sector in the Brazilian case was to threaten to divest from activities related to the Amazon destruction and sell bonds from the Brazilian government and state-owned companies. From a broader perspective, divestment occurs when investment funds, pension funds, governments, and any other organizations dealing with investments decide to sell their assets, such as stocks and bonds, from specific companies, sectors, and even countries.⁷⁻⁹ This decision can be either motivated by financial reasons, such as increased governmental regulation on a specific sector undermining a company's performance, or/ and social and ethical reasons, such as investors reallocating their investments out of companies known for employing forced child labor.⁸

This article contributes to the divestment literature. While companies have experienced divestments after violating human rights, harming the environment, and having negative public perception,¹⁰⁻¹⁶ institutional investors have never blamed nor threatened to divest from governments over environmental issues. The Carmichael mine project, in Australia, did suffer with divestment movements against it, and the Australian government intervened to subsidize it. However, the government did not become a target of the movement.¹¹ Other governments were indeed the main focus of divestment efforts, such as in Myanmar, Sudan, and the

Apartheid regime in South Africa. However, these cases were motivated by human rights abuses, not environmental issues.^{9, 17-19} The Brazilian case, on the other hand, presents a different scenario in which a federal government is the main target of a divestment movement due to environmental motives. In this context, Bolsonaro has adopted a more conciliatory reaction to the private financial sector relative to other players, both in terms of actions to address the demands and of discursive tone. Therefore, it is important to do an in-depth study of the Brazilian case to further develop knowledge of how divestment movements unfold and to better understand the private sector's ability to influence governments in a globalized world facing more and more environmental challenges.

Given these events, this article will answer the following question: why did the Brazilian government vary its reaction to external pressures from foreign governments, civil society, and institutional investors regarding the Amazon wildfires? This article's hypothesis is that governments are more responsive to institutional investors' pressure than foreign governments' and NGOs' pressure when investors play a major role in the incumbent winning coalition and when financial capital is scarce. Drawing from interviews with key players involved with the Brazilian divestment case, the article will first show that Bolsonaro's government indeed crafted different responses to different actors pressuring Brazil due to the Amazon wildfires, and then argue that the Brazilian government was more responsive to the pressure from institutional investors because they played a key role in Bolsonaro's winning coalition stability and his electoral concerns, and because Brazilian financial capital was scarce due to the COVID-19 pandemic. Therefore, the private sector was able to have their critiques more recognized due to three main reasons: electoral concerns, economic need, and winning coalition bonds.

LITERATURE REVIEW

Three branches of the literature explore the functioning, achievements, and implications of divestment movements: the study area of the demand side of divestment, carried out by actors such as activists; the area focused on the supply side of divestment, embodied by institutional and non-institutional investors; and the branch concentrated on the consequences and reactions of divestment-targeted firms and governments.

One strand of scholarship identifies NGOs; coalitions of civil rights, student, environmental, and labor activists; religious organizations; and consumers as the protagonists of the demand side of divestment.^{10, 17, 18} They operate as norm entrepreneurs to pressure institutional investors to divest, which threatens their target's social license to operate by stigmatizing and delegitimizing them and also questioning their financial performance.^{9, 10, 11, 18-21} Another group of scholars investigates which factors can lead the supply side of divestment, mainly constituted by institutional investors, such as public and private banks, insurance firms, universities, public-sector pension funds, and asset management firms to divest. These actors assess political, institutional, economic, environmental, and any other relevant uncertainties in order to manage financial risks and guarantee the financial performance of their clients' invested capital.^{22, 23} Once they get targeted by divestment movements, they are pressured to apply exclusionary screening to their investment decisions, which is the practice of using a "set of filters to determine which companies, sectors or activities are eligible or ineligible to be included in a specific portfolio" based on different criteria.²⁴ In this context, they may consider various aspects to perform this exclusionary screening: reputational and legitimacy risks for their businesses, the financial performance of an investment (if an activity is profitable, investors will hardly divest from it, but if it has high financial instability and volatility, a value-maximizing strategy would be to divest), their fiduciary duties, the structural characteristics of their investments, such as long-time temporality investments, their willingness to use their shareholders "voice" by engaging with companies, the possession of calculative models capable of adequately price new kinds of financial risks, such as climate change risks, as well as the heterogeneity of organizational design.^{13, 15, 16, 20, 22, 25-27} A final group of scholars examines how firms and industries targeted by divestment movements to be stigmatized are affected and how they react. These affected companies and industries perceive this matter as a legitimacy contest for survival. Thus, maintaining their social license to operate through strategies, such as delegitimizing divestment movements, means fortifying their standing with regulators and keeping with the ability to raise capital for expansion and usual business, besides not losing clients.^{9, 12, 15, 17, 21, 28, 29}

More generally, there is a consensus in the academic literature that divestment movements are not very efficient in generating relevant financial impact for targeted companies and industries, especially in the short term.²² Sectors with high demand will continue to be profitable regardless of whether some investors sell their shares or assets, and these stocks will continue with the same prices as long as there are other investors willing to buy what divestors have sold, or governments willing to reduce divestment impacts.^{14, 21} Nevertheless, these limitations are acknowledged by divestment activists, who argue that their main short- and medium-term goals are raising awareness, producing knowledge, shifting attention, and stigmatizing certain industries, governments, and activities. In the long-term, these outcomes may eventually increase market uncertainty by making shareholders doubtful about ventures' future profitability, strengthening the chances of cessation of engagement by customers, contractors, and suppliers, and promoting more governmental restrictive regulatory measures that, in the aggregate, would impose enormous costs on the targeted activities and sectors if they continue with "business as usual."^{8, 10, 11, 18, 20, 21, 23} Besides the aforementioned conditions, divestment movements are the most successful in altering their targets' activities when they manage to combine

normative with financial factors. The former can cause the second, for example, when the movement convinces consumers that buying products from a specific company is not socially acceptable: the demand diminishes and so does the targeted business's overall operation. Consequently, its financial performance becomes uncertain, and investors decide to divest.

This article contributes to a gap in the literature on how governments react to divestment movements. It builds on studies of how the Sudanese, South African, and Australian governments reacted to such movements. For example, the Sudanese government defended itself against U.S. student divestment movements against human rights violations in 2005 by publishing a defense letter in the *New York Times*.⁹ Moreover, U.S. opponents of divestment movements to overthrow the racist Apartheid regime in South Africa countered that continued corporate presence in the country served to improve the conditions of black workers through social responsibility accounting.^{17, 19, 27} While these studies contribute to understanding government (re)action in the context of divestment dynamics, they do not analyze in depth the role of national governments in defending themselves in such events, nor do they propose theoretical frameworks to examine their views and motivations on the subject. The Australian divestment case regarding the Carmichael Mine and its governmental influence has received more scholarly attention because the government sheltered the energy sector from divestment movements.^{14, 21} However, the divestment unrest was not primarily focused on challenging the government itself, but rather a specific project supported by it.

This paper will tackle the subject of how governments react to divestment pressures through the analysis of the Brazilian divestment case, which is to the best of my knowledge the first time in history that a federal government is the main target of a divestment movement due to environmental degradation. Although other governments were indeed the main focus of divestment efforts, such as in Myanmar and Sudan, these cases were motivated by human rights violations, not environmental issues.^{9, 17, 19, 27} The Brazilian and Australian cases have some similarities: in both cases, the motivation for divestment pressure was mainly environmental, and important sectors for the respective economies were targeted (coal in Australia and livestock, soy, and other products in Brazil). However, there are important differences as well: first, the efforts against the Carmichael mine were part of a broader international climate action movement (anti-mining campaign), while in Brazil it was a more singular movement, highlighting the different levels of interaction between civil society and the private sector. Second, in Brazil, the Amazon rainforest issue is contentious, with different parties attacking each other for the topic, while in Australia, the coal sector was supported by both major political parties. Finally, in Australia, divestment pressure was directed at a specific project of a multinational company supported by the government, while in Brazil the pressure was broader, directed at the government itself and at various companies from different sectors that could be benefiting from the forest fires.^{8, 11, 21} Therefore, studying the extent to which a government may be affected by divestment pressures related to environmental contentious issues and how it responds to them, particularly in a globalized financial world facing increasing challenges from the climate crisis, can provide valuable contributions for the literature. Such analysis also provides insights into current trends within the private financial sector related to environmental, social, and governance (ESG) parameters, and how they are changing the incentives of private organizations when making investment and divestment decisions, in line with the developments and dynamics of the Brazilian case.

OVERVIEW - THE BRAZILIAN DIVESTMENT CASE

Jair Bolsonaro, a seasoned congressman with more than twenty years of political experience, took office as Brazil's president in January 2019. During his election campaign, he shared polemical statements about his planned environmental policies, such as Brazil's withdrawal from the Paris Agreement and the dissolution of the Ministry of Environment (neither of which happened).³⁰ ³¹ The first indications that Bolsonaro's environmental policies were flawed came when eight former environment ministries from past administrations released a manifesto criticizing them,³² and the National Institute for Spatial Researches (INPE) publicly highlighted the 278% year-on-year increase in deforestation in the Amazon rainforest in July.⁶ Soon came news of forest fires in the Amazon, such as an 82% increase in wildfires between January and August compared to the same period in 2018,³³ the "Day of Fire" when farmers and ranchers set a coordinated series of fires in the Amazon rainforest and adjacent lands to show their support for Bolsonaro,³⁴ and when the sky suddenly darkened in the middle of the day in São Paulo, Brazil's largest city, located nearly 1800 kilometers from the Amazon rainforest, because of the smoke coming from the Amazon fires.³⁵

This situation attracted the world's attention, including from foreign countries, international NGOs, multinational companies, and investment funds, among others. They began to criticize the Brazilian federal government's handling of the forest fires and demanded action to solve the problem by publishing statements and reports, writing petitions, and taking other actions that will be later detailed in this essay. On the other hand, the Bolsonaro government responded to these criticisms with a series of reactions, such as the deployment of the army to control the fires,³⁶ the enactment of a ban on forest fires in the Amazon,³⁷ and the creation of the Amazon Council.³⁸

The private sector, and institutional investors in particular, exerted a range of pressures, threatening to divest from the government, as well as from companies potentially linked to the fires, such as the livestock, soybean, and cellulose sectors with large companies like Marfrig Global Foods, Cargill, and Suzano. One example of this pressure was when 251 institutional

investors with approximately \$17.7 trillion in assets under management, such as the California Public Employees’ Retirement System (CalPERS), China Asset Management Co., and the Church of Sweden, demanded action on deforestation from companies in Brazil. They stated, “We are concerned about the financial impact deforestation may have on investee companies, by potentially increasing reputational, operational, and regulatory risks. Considering increasing deforestation rates and recent fires in the Amazon, we are concerned that companies exposed to potential deforestation in their Brazilian operations and supply chains will face increasing difficulty accessing international markets.”³⁹

Further evidence was that 34 international financial institutions managing \$4.5 trillion in assets sent letters to Brazilian embassies in seven countries calling for meetings and expressing concern that Brazil was removing protections for the environment and indigenous communities, therefore “creating widespread uncertainty about the conditions for investing.”⁴⁰ In addition, the investors wrote, “[We] urge the government of Brazil to demonstrate clear commitment to eliminating deforestation and protecting the rights of indigenous peoples.”⁴⁰ However, after more than a year of pressure, the only divestment that occurred was by the public limited company Nordea Asset Management, which withdrew its \$47 million investment in the Brazilian meat company JBS and suspended the purchases of Brazilian government bonds.^{41, 42}

The timelines below provide a chronological overview of key events within this dynamic of external and internal pressures, and government responses to them. They cover events between 2019 and 2020, with a focus on the months of August and September, when higher rates of wildfire typically occur. Pressures emanating from various groups are shown below the x-axis, while government responses to them are depicted above it. A variety of sources were used to produce them, including newspaper articles and official statements from organizations, which can be found in the appendix.

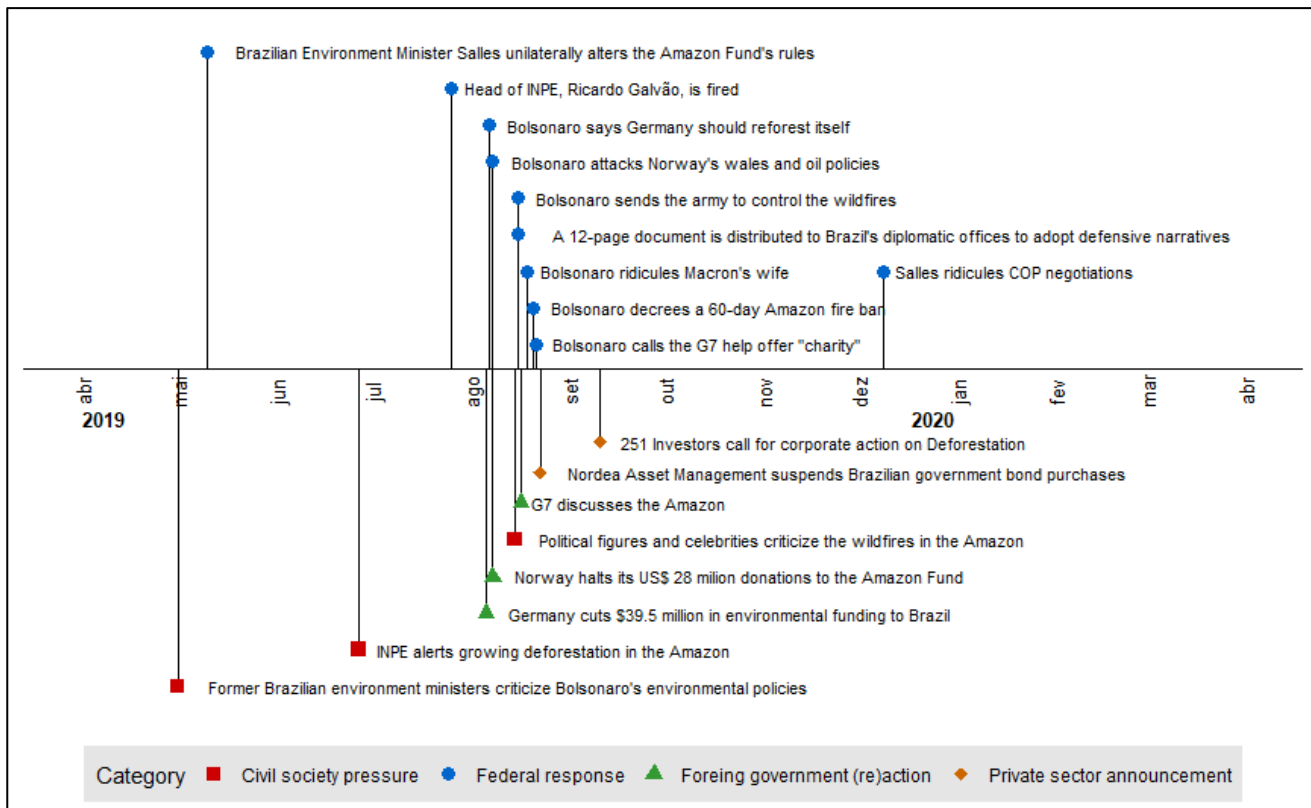


Figure 1. Key events during 2019.

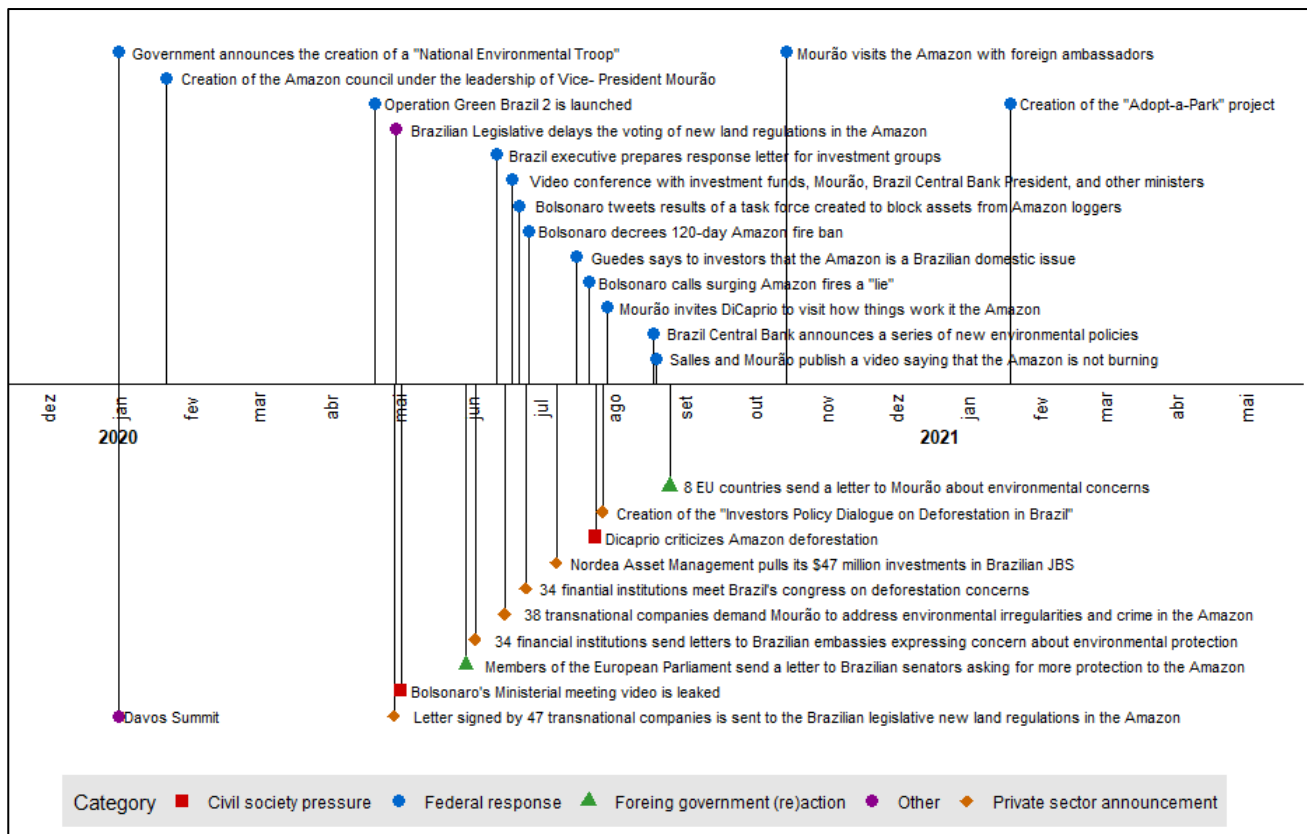


Figure 2. Key events during 2020 and 2021.

The timelines demonstrate that Bolsonaro’s government adopted a range of reactions to the demands and criticisms of various groups, some of which were more aggressive while others had a more serious and conciliatory tone. The following sections analyze these responses and explore the reasons why particular responses were chosen to address the pressures of each group.

METHODS AND PROCEDURES

This paper’s research methodology is based on in-depth virtual interviews conducted during the second half of 2021 with a group of investment portfolio managers, high-level government officials, and civil society representatives all directly and indirectly involved with the Brazilian divestment dynamics, in a methodological similar way to the work done by Christophers,²² which attempted to interview various and diverse institutional investor representatives and stopped seeking further interviews once the information gathered began to repeat itself. Since the Brazilian case is still very recent, this interview method was the preferred strategy because it not only enabled the author to get a more detailed and clearer picture of the whole dynamic by comparing and examining different statements from people coming from different organizations with conflicting interests, but also gave him access to information that is not otherwise available to the public, not even in newspapers and official reports. These, in turn, were useful in evaluating this paper’s hypothesis that governments are more responsive to institutional investors’ pressure in comparison to foreign governments and NGOs when investors play a major role in the incumbent winning coalition and financial capital is scarce.

All interview materials (questions, explanations, and scripts) were submitted to the analysis of the Ethics Compliance Committee on Research Involving Human Beings of the Getulio Vargas Foundation. After receiving their approval (Decision n. 161/2021 emitted on the 2nd of August 2021), the author proceeded to send out the invitations and conduct the interviews. More than 210 invitations to different professionals were made both through intermediaries known to the researcher as well as through institutional contact points in each interviewee’s respective organization. The interview invitations were sent by email, followed by websites’ contact forms, and LinkedIn, Facebook, Twitter, and Instagram account messages. The choice of which organizations and persons to invite was first based on the relevance to the divestment dynamics in Brazil (if the organization was directly involved with exercising divestment pressures, suffering with them, or speaking either in favor or against them, for example), and

secondly with the use of the snowball method. The ratio of invitations made, response rate, and acceptance rate can be seen in the table below (different invited professionals at the same organization were counted separately for all these invitations' numbers).

Area/ Sector	Invites sent	Non-response rate	Rejection rate	Acceptance rate	Interviews conducted
Civil society	64	68.75%	21.87%	9.37%	7
Bolsonaro government areas	21	80.95%	9.52%	9.52%	2
Financial sector	38	71.05%	18.42%	10.52%	4
Political opposition to Bolsonaro	7	71.42%	14.28%	14.28%	1
Brazilian agribusiness sector	37	62.16%	35.13%	2.70%	1

Table 1. Invitations to interviews and response, rejection, and acceptance rates.

The overall acceptance rates were low, but this was already expected since all invitations were made online during the COVID-19 pandemic. However, two groups stand out: first, there was a slightly higher acceptance rate for invitations to the political opposition to Bolsonaro. Since the author had more direct connections with people from this sector, it was easier for him to get efficient recommendations and also have invitations accepted. Second, the acceptance rate was much lower in the Brazilian agribusiness sector. Being one of the sectors most affected by this divestment dynamic, one might assume that they prefer not to talk about the issue unless absolutely necessary.

The fifteen interviews are listed on the table below. These were of fundamental importance for the following points: providing detailed descriptions of processes and mechanisms observed in the context of divestment pressures; perform the process tracing of these mechanisms, thus adding micro-foundations for events and patterns observed at the macro level; empirically verify actors' interests and preferences as well as their initially observed relationships; and analyze the validity of this paper's hypothesis. In order to identify and highlight narrative biases by respondents, a triangulation method was used with information from multiple sources coming from distinct organizations and backgrounds to assess and confirm the convergence of information.⁴³ In addition, to ensure the professional integrity of the interviewees, no more information will be given at the risk of hurting their anonymity.⁴⁴ Seven people related to the civil society (A1 - A7), three people related to the Brazilian government and legislative politics (B1 - B3), and five people associated with the national and international private and financial sector (C1 - C5) were interviewed. All interviewees come from different organizations. The interviews were semi-structured, conducted via videoconference, with a leverage duration of one hour, and with some of the questions, which can be found in the appendix, varying according to the interviewee's background.

Interviewee	Sector
A1	Campaigner at an international environmental NGO
A2	Coordinator of a transnational environmental coalition
A3	Environmental grassroots activist
A4	CEO of a Brazilian environmental NGO
A5	Coordinator at an international foundation and professor at a Brazilian university
A6	Head of the Centre for Sustainability Studies at a Brazilian university
A7	Science director at a research institute focused on the Amazon
B1	Advisor for a Brazilian senator part of the opposition against Bolsonaro
B2	Chief of environment at a Brazilian federal bureau
B3	Member at the Bolsonaro’s Brazilian executive power sphere
C1	Sustainability manager at a Brazilian agribusiness association
C2	Portfolio manager at an investment fund A that threatened to divest
C3	Associate portfolio manager at an investment fund B that threatened to divest
C4	Portfolio manager at an asset management firm that threatened to divest
C5	Director of sustainable investing at an asset management firm that threatened to divest

Table 2. List of interviewees and their backgrounds.

RESULTS

Through the period between 2019 and 2021, different players pursued to pressure the Brazilian government to alter its policies regarding environmental protection, specially concerning the Amazon rainforest and the wildfires happening there. The following sections present the results of this research, particularly in relation to the motivations and strategies of the actors involved in the divestment pressures, the different governmental reactions of the Bolsonaro government, and the overall leverage of divestment threats in the Brazilian case. The interviews were particularly useful in gaining the knowledge and information necessary to understand how the pressures and government reactions within the Brazilian divestment case relate to the hypothesis defended by this paper that governments are more likely to respond to institutional investor pressure when they play a more important role in the incumbent winning coalition, compared to foreign governments and NGOs, and when financial capital is scarce.

MOTIVATIONS AND STRATEGIES

This section analyses the reasons and strategies employed to pressure Bolsonaro’s policies. In order to do that, news, reports, and official statements will be used, besides the interviewees’ perceptions of their own and each other’s categories.

CIVIL SOCIETY

Civil society was one of the players that pursued to pressure the Brazilian government to change its behaviors concerning environmental protection in the Amazon. International NGOs, such as Greenpeace and World Wildlife Fund (WWF), local Brazilian networks, such as the Brazilian Indigenous People Articulation (APIB), and celebrities, like Leonardo DiCaprio, are some examples of players who publicized their dissatisfaction with the wildfires.^{1, 45-50} When it comes to their interests, three environmental activists (A1, A2, A5) stated that these actors focus on democratic agendas related to the vulnerable people and on

the defense of the “common good”, arguing that many of them do have honest concerns about the well-being of nature and the preservation of our world’s climate stability. One of them (A1) emphasized that NGOs are not interested in maximizing profits, which in turn elevates their moral standards. On the other hand, a person of the Bolsonaro’s Brazilian federal government (B3) argued that some of these groups are financed by external players and countries with doubtful intentions to gain power and undermine Brazil’s sovereignty, besides wanting to get more publicity and enhance their popularity.

Concerning their strategies, interviewees from the three branches (A3, A6, B1, C1) highlighted the capacity that NGOs and celebrities have at the communicative arena as their actions shape narratives and share ideas through the media, boosting a topic’s relevance and scope. Moreover, these actors can engage in legislative advocacy by pressuring representatives to demand changes from the federal government within the political system (A3). Besides that, civil society actors also seek to increase the pressure from other players at the Brazilian government. They met and encouraged state representatives from foreign countries to change their positions regarding the Amazon (C5) and pursued to facilitate coordination and cooperation between local networks and international organizations, other NGOs, and governments (C1). The “naming and shaming” method targeted at companies and institutional investors in order to raise their reputational costs of operating or being related to activities linked to the Amazon destruction was also used (A5, B2).

A great number of the interviewees (A1, A4, B1, B2, C2, C4, C5) pointed out to this indirect reputational link between civil society activism and divestment pressures: since NGOs and celebrities influence how society thinks about deforestation and wildfires in the Amazon by shining light on the issue, many clients of the institutional investors organizations can be stimulated to start pressuring them to alter their investment policies (besides constraining other businesses as well by not buying their products). Another important shared view among interviewees (A3, C3, C4, C5) was the existence of a more direct relationship: many NGOs have a direct dialogue with institutional investors through which they make presentations, present research and reports, and even help these investors to monitor the activities of their invested businesses by denouncing when a producer is related to illegal forest destruction in the Amazon. Two environmental activists (A2, A3) even argued that without the civil society pressure, the financial sector would not have engaged with the divestment threats in the first place.

One good illustration given by one interviewed (A5) of the relationship between the civil society activism and the Amazon wildfires was the “Sangue Indígena: Nenhuma Gota a Mais” (“Indigenous Blood: No Drop More”), a one-month tour organized by APIB at the end of 2019.⁵¹ This campaign took a Brazilian indigenous group to visit twelve different countries in Europe, such as Germany and Spain, in order to raise awareness of the situation in Brazil and denounce the environmental and human rights violations happening under Bolsonaro’s presidency. They met with other activists, legislative and executive representatives, agents of companies that had operations in Brazil, and institutional investors with investments in the Brazilian agribusiness sector, besides organizing demonstrations.⁵² Moreover, two of their main activities were denouncing the relationship between the finance sector and the Amazon destruction and highlighting the harmful effects the EU-Mercosur trade agreement could have on the environment.⁵³ Another example was the campaign “Defund Bolsonaro”,⁵⁴ which was launched in September 2020 by a coalition of NGOs calling for more actions from companies, governments, banks, and society to stop financing activities related to the wildfires.

Therefore, it emerged from the interviews that civil society tried to act as norm entrepreneurs in the Brazilian case, stressing that it was wrong to do business with some Brazilian sectors. NGOs and other groups tried to influence the middle players, the institutional investors, to take a stricter stance on forest fires in the Amazon, while also pursuing to influence other governments and public opinion as a whole.

FOREIGN GOVERNMENTS

Different countries have adopted distinct positions in the face of the fires in the Amazon. Some leaders adopted indifferent positions and sent messages of support wishing the situation would improve, sometimes even disposing of resources to help the Brazilian government. This was the case for countries such as the United States and Israel.^{55, 56} However, most of the external state involvement in the issue came from governments placing the blame for the wildfires on Bolsonaro’s decisions, such as France, Germany, and Norway.⁵⁷⁻⁵⁹

These more critical countries had varied reasons to adopt such stances: first, according to some of the interviewees (A2, A3, C4), in some of these countries, large groups of society are genuinely preoccupied with the climate crisis, and therefore demand that their leaders employ diplomacy aimed at combating further environmental destruction. Second, some of them have already invested a great amount of money for environmental protection in Brazil in the last decade through multilateral schemes, such as the Amazon Fund. One professor at a Brazilian university (A5) argued that to see decisions dismantling all the achievements accomplished with the invested resources must feel like a disappointment, and that is why some leaders reprimanded the situation. Third, a senior member of Bolsonaro’s government and two representatives of civil society (A6, A7, B3) emphasized that interest

groups inside those countries might benefit from a damaged Brazilian commodities export-sector, leading them to pressure for actions of their governments. Finally, since climate change can threaten the national security of nations due to extreme weather events, and the balance of the Amazon rainforest is also important for agriculture and climate stability in other countries, some governments could be acting in ways to defend their own economic and national security (A2, A4).^{60, 61}

Foreign countries can exert their pressure through different channels. First, five interviewees with civil society and political backgrounds (A1, A4, A6, B1, B2) highlighted that nations can use diplomatic ways to show their discontent, such as official statements in forums, at conferences, on social media, and on television, as well as by symbolically isolating countries by limiting visits by heads of state to those countries. Second, interviewees from the three branches (A1, A6, B1, B2, C1) pointed out that external states can make use of issue linkage to halt negotiations on other matters such as international commerce. One Environmental grassroots activist (A3) cited the discussions on Brazil's accession to the Organization for Economic Cooperation and Development (OECD) and the EU-Mercosur agreement as two examples of this dynamic, pointing out that Bolsonaro's actions regarding the environment were convenient to delay such conversations because of protectionist groups in countries like France. Third, these governments may bypass the federal government and seek to establish links with subnational leaders, such as governors and mayors (A4, A7). Fourth, as already mentioned, developed countries can invest and have invested money in Brazil, be it by investing in funds, sponsoring programs and initiatives, or purchasing bonds. In this way, they can threaten to stop their investments and even divest what they already have invested, at least according to a science director at a Brazilian research institute focused on the Amazon (A7).

Overall, the interviews provided evidence that foreign countries may have very different interests in pressuring the Brazilian government regarding the Amazon rainforest fires, and that their strategies range from more traditional diplomatic measures to a more invasive approach by reaching out to internal opposition leaderships.

INSTITUTIONAL INVESTORS

The motivations of institutional investors to divest from companies and state-owned enterprises operating in Brazil due to the Amazon rainforest fires are directly related to the notion of "reputation": the reputation of institutional investors, the reputation of the companies in which they invest, and the reputation of the Brazilian government (in this case, the term "reputation" represents the opinions from different audiences, such as customers, that are held about these different actors). Institutional investors depend, among other things, on their clients' preferences. Both the media and the civil society can shape reputations of companies and organizations by deciding which information they are going to spread, which strategies will be used to do it, and who they are going "target" (at least in the case of civil society, according to one campaigner at an international environmental NGO (A1)). Therefore, clients of institutional investors can demand the divestment of specific companies, sectors, and even governments because of these targets' reputations, which in turn might be influenced by the media and the civil society through their communicative capabilities and spread networks.

This direct relationship between the reputation of institutional investors and the reputation of the companies and activities in which they invest is one of the reasons why divestment and the associated pressures can occur. Almost all the interviewees (A1, A2, A5, A6, A7, B1, B2, C1, C2, C4, C5) emphasized that reputational risks create incentives for such institutional investors to pressure to divest, since universities, governments, investment funds, and pension funds have each one specific audiences to whom they are held accountable for. In the case of investment and pension funds, for example, each of them must respond to their client's demands accordingly. If customers or other relevant groups on which they rely do not want their money invested in a company suspected of using child labor, they have the right to ask those responsible for managing their capital to stop investing in that company. Another example of this bottom-up dynamic is when a person concerned about climate change decides to become a client of an investment management company: The person will look for a company that does not invest in fossil fuels or is associated with them in any way. Representatives from the three branches (A6, B2, C1, C2) explained this by arguing that the reputation of an institutional investor organization associated with negative issues, such as deforestation, can generate negative economic consequences for the organization by decreasing its brand value, making it experience lower market performance compared to its competitors due to the difficulty to retain customers and attract new ones, and even suffering from boycotts.

In addition to reputation, one chief of environment at a Brazilian federal bureau and one coordinator of a transnational environmental coalition (A2, B2) argued that uncontrolled deforestation and wildfires in the Amazon rainforest create material financial risks for institutional investors, since the companies they invest that operate in the region suffer from increased reputational and regulatory risks, resulting in exacerbated systemic risk across portfolios. Thus, they fear that their invested assets will drop value as the companies lose access to markets and suffer from reputational damages. Moreover, three experts with civil society backgrounds (A2, A3, A6) mentioned that new regulatory frameworks with stricter laws, such as the new EU taxonomy and climate litigation, are increasingly creating more incentives for institutional investors to consider sustainability aspects when analyzing their investments in order to avoid taxes and fines.⁶² As a result, five participants (A1, A6, C2, C3, C5) pointed out that

institutional investors seeking to avoid negative associations can use divestment threats to demand more transparent disclosures and more effective measures to diminish environmental risks from the companies in which they invest.⁶³

Moreover, the Brazilian case shows that it was not only private companies that had to handle with these pressures: Bolsonaro's government also had to deal with criticism from institutional investors regarding the Amazon wildfires. One example was when 251 Investors with USD \$17.7 trillion in assets under management called for corporate action on deforestation and fires in the Amazon and supported the efforts of Brazilian groups that "pledged the national government to regain control of the situation as a matter of urgency."^{39, 63} An advisor to a Brazilian senator who is part of the opposition to Bolsonaro and one chief of environment at a Brazilian federal bureau (B1, B2) agreed that investors want to invest in countries with stable and foreseeable political, institutional, economic, and environmental regulatory contexts. Both of them further argued that the fact that institutional investors not only pressured the companies related to the Amazon context, but also the Brazilian government itself, demonstrates that they attribute part of the blame for the wildfires and the lack of stability in Brazil to Bolsonaro's policy as well.

At the same time, this aspect shows that the financial sector and institutional investors also believed that changing government behavior was necessary to guarantee a greater stability for their investments, since altering their invested companies' attitudes alone would not be enough to safeguard their reputation. This happens because investors cannot control every single activity in the Amazon, as there are millions of people living near the forest and hundreds of thousands economic activities happening in the region. Every single one of these activities can propagate deforestation and wildfires, and although a certain company might not be related to them, it still is vulnerable to the negative reputational contagion since it operates in the same region.²¹ Because of that, institutional investors also demand policy changes from the Brazilian government in order to control all the activities they cannot control themselves, thus pursuing to mitigate the risk of negative contagion to their investments.

Another motivation raised by some interviewees is the increased societal preoccupation related to the increasing number of extreme weather occurrences. Floods, droughts, and wildfires, among others, have become more frequent in the last few years, obliging people from all around the world to already struggle with the effects of climate change.⁶⁴ Consequently, a greater portion of societies start to preoccupy themselves with such themes, and companies from distinct sectors are now having to respond to more pressure coming from consumers, governments, and shareholders regarding their environmental impacts.^{65, 66} As a result, three interviewees (B1, B3, C3) commented that the environmental, social, and governance (ESG) parameter has been developing in recent years which has led to more scrutiny over companies and organizations, and at the same time has allowed them to use ESG strategies to improve their reputations. A senior member of Bolsonaro's executive government (B3) even argued that this international ESG investment trend was one of the main reasons for the divestment pressures related to the Amazon wildfires, rather than the government's actions or the numbers of forest fires and deforestation. Therefore, the Brazilian divestment pressures also can be understood as an effect of additional concern from individuals and the private sector, especially since Amazon's equilibrium and tipping point are not only essential for Brazil's climate and economic stability, but also for the rest of the world due to the transnational aspect of climate change.^{61, 67}

Institutional investors dispose of powerful strategies to pressure their invested companies and governments. As already mentioned, they can use their assets and the threat to divest to gain leverage in bargains and engagements with linked businesses. This same dynamic can be used when trying to influence governmental decisions through the sale of sovereign bonds, and it takes part within the usual divestment process: investors threaten to divest if they are unsatisfied and their demands are not considered, then the company might accept the exigences and alter its behavior. After engaging with the business, the investors then decide if they will (a) keep threatening to divest because their demands were not sufficiently achieved, (b) no longer do new investments but keep the ones they already have, (c) divest (gradually or all at once), or (d) stop pressuring and continue with business as usual. The engagement can obviously happen without the threat to divest, but according to a sustainability manager at a Brazilian agribusiness association (C1), divestment intimidation sends a more convincing signal that the investors' demands are meaningful, and the companies should take them seriously.

Institutional investors can act in partnership with each other to increase their bargaining power, which was the case when 34 international financial institutions that manage US\$4.5 trillion in assets sent letters to Brazilian embassies in seven countries calling for meetings and expressing concern that Brazil was rolling back environmental protections.⁶⁸ Besides that, one coordinator of a transnational environmental coalition (A2) argued that institutional investors can create backlists for excluded companies operating in a certain country, with the objective of affecting that country's reputation abroad and making capital flows scarcer for it. Related to this, four interviewees (A5, A6, B1, C4) mentioned that shareholders and investors can put so much pressure on companies operating in a certain country that these own enterprises might start to pressure the government themselves to change its public policies and mitigate risks so that they no longer have to deal with investors' threats.

All in all, the interviews provided evidence that institutional investors' motivations for threatening to divest were a mix of financial and reputational risks. Moreover, in terms of their strategies, participants mentioned that divestment threats can be considered part of an engagement approach since they send a signal about how serious institutional investors' demands are.

DIFFERENT GOVERNMENTAL REACTIONS

National governments are constantly confronted with criticism, and although they are not expected to concede to all critiques, responding at least diplomatically can mitigate further conflict while maintaining mutual respect. Such responses can therefore be divided into concrete actions to address the external comments and the tone or style chosen, e.g., a more diplomatic tone or a more adversarial tone. During 2019 and 2021, representatives from foreign countries, civil society, and institutional investors publicly criticized the Brazilian government concerning the Amazon wildfires, each one of them with a different strategy and motivated by distinct reasons, as shown previously. In order to answer the question whether Bolsonaro's government varied its reactions to external criticism, this section will present each governmental reaction along with explanations from the interviews and political analysis of the Brazilian executive branch, a heterogeneous group with sometimes converging, sometimes conflicting interests.

First, concerning NGOs, the media, and celebrities, Bolsonaro was elected with an anti-civil society platform. He adopted the narrative that he would no longer accept the interference of international and domestic non-state players in the Brazilian environment, maintaining a hostile approach towards NGOs and indigenous communities operating and living in the Amazon rainforest since his campaign.² An example of this was when he made a statement right after the first round of voting that said, "Let's put an end to all activism in Brazil."⁶⁹ According to him, these groups only serve to obstruct the potential of exploring forest resources on behalf of foreign countries who benefit from a diminished Brazilian international competitive capacity. He made this clear in his 2020 speech to the UN General Assembly when he spoke about the disinformation campaigns his government allegedly suffered from civil society: "The Brazilian Amazon is known to be extremely rich. This explains the support of international institutions for this campaign, supported by shady interests that are united with Brazilian associations, profiteering and unpatriotic, with the aim of damaging the government and Brazil itself."⁷⁰

When asked about civil society, a senior member of Bolsonaro's government (B3) repeated the same idea, arguing that many NGOs represent foreign countries' interests that benefit from damaging Brazil's environmental reputation. The person stressed that the country was not this pariah that was being sold at the international level, and that it was hypocritical for these organizations to criticize Brazil but not say a word about other countries with high rates of forest fires, such as Australia, thus making the relationship between the federal government and civil society "more complicated" (B3). This mindset was also reproduced by Ricardo Salles, the former environmental minister who worked for Bolsonaro between 2019 and 2021. During his term, he pursued to limit NGOs' influence within public policy decision making and implementation,² besides facilitating natural resources extraction in the region and promoting the private sector expansion into the Amazon by attracting private capital.⁷¹

As for Bolsonaro's reaction to the criticism of the Amazon rainforest wildfires by NGOs and celebrities, the majority of respondents (A1, A4, A5, A6, B2, C1, C2, C3, C4) described them as aggressive, threatening, and hateful, with the aim of delegitimizing and defaming them. Since after his election, the leader cultivated anger against such groups by intimidating the media, threatening NGOs (by trying to criminalize their activities and describing them as cancer, for example),⁷² and pursuing the dismantling of a series of institutional protection frameworks for indigenous communities.² An example regarding his reactions to this category was when he blamed NGOs and indigenous communities to be the ones to have started the wildfires in the Amazon so they could take photos and criticize the government,⁷³ while being financed by the actor Leonardo DiCaprio.⁷⁴ In most of these cases, Bolsonaro first dismissed the criticisms as true and then cast doubt on the intentions of these players, as if none of the involved NGOs and celebrities were truly preoccupied about the Amazon rainforest or Brazil itself but had clandestine interests.

The reaction to criticism from foreign countries was partly based on the "Common but differentiated responsibilities" principle, which defends the idea that developing countries have the right to engage with less ambitious environmental protection commitments than developed countries, since these have already enjoyed the benefits of an industrialized development that did not care for environmental protection. During one conversation with foreign journalists, Bolsonaro said "We preserve more [rainforest] than anyone. No country in the world has the moral right to talk about the Amazon. You destroyed your own ecosystems."⁷⁵ Two other statements of his that illustrate this characteristic are: "Let's use the riches that God gave us for the wellbeing of our population, you won't get any trouble from the Environment Ministry, nor the Mines and Energy Ministry nor any other."⁷⁶ and "It is now our mission to make progress in harmonizing environmental preservation and biodiversity, with much-needed economic development. One should not, of course, emphasize one more than the other."⁷⁴ In this context, two respondents from civil society (A1, A3) argued that Bolsonaro's government responded aggressively to criticism from abroad and tried to establish the narrative that those countries and groups that feel threatened by Brazil's economic growth are the ones

falsely saying that the Amazon was being destroyed. Therefore, these two participants stated that Bolsonaro was selling himself as the defender of Brazil's international commercial competitiveness with this confrontational approach.

In addition, parts of Bolsonaro's government have also resorted to beliefs related to the "Amazon Paranoia", an exaggerated notion that the Amazon resources are under constant threat of being stolen by foreign players, mainly from the global north.⁶⁶ Backed by his foreign relations Minister Ernesto Araújo and his accusations against globalism and ideology in the international relations,⁷⁷ Bolsonaro pursued to defend Brazil's sovereignty when responding to other governments' criticism of the Amazon rainforest fires. In his 2019 address to the U.N. General Assembly, he said "Using and resorting to these fallacies, certain countries, instead of helping... behaved in a disrespectful manner and with a colonialist spirit, they even called into question that which we hold as a most sacred value, our sovereignty."⁷⁸ Interviewees expressed different perspectives on this issue: one portfolio manager at an investment fund that threatened to divest (C2) mentioned that even though different foreign governments had different reasons to criticize Brazil's handling of the Amazon rainforest wildfires, Bolsonaro's government generalized all criticisms as attacks on Brazilian sovereignty, which made his reactions even more aggressive. Two other civil society participants (A4, A6) emphasized that while more respect and diplomacy had been expected, the aggressive and sovereignty-focused responses showed that Bolsonaro's confrontational approach was intended to gain electoral support with his domestic base.

Some examples of reactions to criticism from foreign governments were when Bolsonaro responded to German Prime Minister Angela Merkel and advised her to use the funds frozen by Germany for Amazon projects to reforest Germany itself,⁷⁹ or when he acknowledged Norway as the country that kills whales and explores oil as a reaction to the Norwegian decision to also freeze the aid to the Amazon Fund.⁸⁰ Ricardo Salles constantly reinforced this position arguing that Brazil would be open to accept foreign aid to the Amazon if the Brazilian government remained in charge to decide how to use those resources, no longer accepting external conditionalities.^{81, 82} Another illustration was when Bolsonaro directly attacked the wife of France's President Emmanuel Macron,⁸³ demonstrating once again the level of hostility adopted by the government. Paulo Guedes, the Minister of Economy, echoed this when he said during an event in the United States that "France, Holland, and Belgium use environmental excuses to block Brazil in the OECD. It is like accusing France of burning Gothic cathedrals, it was an accident."⁸⁴ Nevertheless, two interviewees, one science director at a research institute focused on the Amazon and one member at the Bolsonaro's Brazilian executive power sphere (A7, B3), mentioned that there were some more serious reactions, such as the initiative led by Vice-President Mourão to take ambassadors to visit the Amazon rainforest to convince them that the forest was not on fire.⁸⁵

Finally, regarding reactions toward institutional investors, the majority of respondents from civil society and the private sector (A1, A3, A4, A5, A6, A7, C1, C3, C4) indicated that the Bolsonaro government reacted in a more conciliatory and cognizant manner. According to them, while the government responded aggressively, challenging, delegitimizing, ironically, and sarcastically to the pressure coming from the civil society and foreign governments, the tone toward the financial sector was much more serious, and the demands of institutional investors were heard and considered, indicating that Bolsonaro's government perceived the financial sector as a more relevant factor in this context. After receiving the divestment pressure from this category, the government took a series of measures to convince the private sector that Bolsonaro's administration was committed to fighting the wildfires.

It emerged from almost all interviews (A1, A2, A3, A4, A5, A6, A7, B1, B2, B3, C1, C3, C4) that the creation of the Amazon Council (which already existed since Fernando Henrique Cardoso's presidency in 1995, but it had been left out of use until Bolsonaro decided to utilize it once again), a coordination council to organize conjunctural actions between ministries regarding the Amazon rainforest and to be a focal point for related issues, was one of the Bolsonaro government's main reactions to divestment pressures. Two members of Bolsonaro government's sphere (B2, B3) emphasized that the council should not only ensure coordination between ministries, but also act as a dialogue mechanism with external actors to show what was "really" happening in the Amazon rainforest and what efforts the government was making to reduce deforestation and forest fires. Led by General Hamilton Mourão, the Vice President of Brazil, the Council arranged meetings with international institutional investors to hear their demands and create a channel for dialogue,⁸⁶ dispatched and organized Brazilian troops to fight Amazon rainforest fires in a number of different operations, such as Green Brazil Operation 2,⁸⁷ announced federal decrees forbidding fires for farming or other purposes in the Amazon,⁸⁷ and conducted the aforementioned trips with foreign ambassadors,⁸⁵ among other activities. A portfolio manager at an asset management firm that threatened to divest (C4) and participated in some of these meetings promoted by the Amazon Council emphasized that they included companies, representatives from other ministries, such as the ministries of environment and agriculture, and executives from the Central Bank of Brazil. In this regard, one science director at a research institute focused on the Amazon (A7) mentioned that the Ministry of Agriculture also worked with the financial sector and international institutional investors to maintain good relations with them.

On the other hand, almost all the interviewees also criticized the effectiveness of such measures in addressing the environmental problems they were supposed to fix. Several respondents (A4, A6, A7, B1, C2, C3) said that the council was a marketing and greenwashing strategy of the government, which did not serve to solve environmental problems, but only to improve its reputation and public relations. Four of them (A4, A6, A7, B1) even used the same idiomatic expression to characterize the Amazon Council, “para inglês ver,” which means “just for show.” Three interviewees (A1, A2, C2) argued that if the government was really committed to addressing environmental problems, it would have used the institutions that already existed, such as IBAMA and ICMBio, instead of creating a new branch. In addition, five respondents (A1, A3, A5, A7, B1) felt that the efforts and actions promoted by the Council were too costly and provided insufficient results, partly due to the lack of capacity of the Brazilian Army and partly due to limited participation and coordination with civil society.

One coordinator at an international foundation and professor at a Brazilian university (A5) and one senior member of Bolsonaro’s executive government (B3) highlighted that Bolsonaro’s elevation of Mourão to a leadership position in the Amazon Council removed some of Salles’ power and brought in a new person to deal with external criticism. This in itself was another reaction to the divestment pressures, since Salles’ reputation was already eroding as many civil society actors were also blaming his policies for the destruction in the Amazon,² and Mourão was recognized as someone with a good knowledge of the dynamics in the region, turning him into an experienced character to deal with this sensitive issue (B3). Thus, the dispute within the executive branch over who should take care of the situation in the Amazon, Mourão or Salles, shows that Bolsonaro did not ignore pressure from institutional investors, as he tried to select a better prepared person to handle the criticism.

As for Salles himself, one chief of environment at a Brazilian federal bureau (B2) mentioned that two programs he launched were also responses to divestment pressures. One was the “Adopt-a-park” project, which gives the opportunity to private domestic and foreign companies to invest in specific national parks in the Amazon to guarantee their conservation with full transparency.⁸⁸ According to the ex-minister, “In the face of criticism and pressure, we open an opportunity for Brazilians and foreigners to participate in solving the problem. This is an important change from the government. If there was a criticism that the government was not open to outside help, this criticism no longer makes sense.”⁸⁹ In addition, another program launched by Salles in response to external demands was “Forest+”, with the objective to “create, promote, and consolidate the environmental services market, recognizing and valuing environmental activities carried out and encouraging their monetary and non-monetary retribution.”⁹⁰

Moreover, one interviewee from each sector (A3, B2, C4) argued that changes were made to the Brazilian financial and banking system in response to the divestment pressures. They emphasized that the Central Bank of Brazil (BC), a Brazilian autarchy directly related to the government, adopted changes to their financial rules as a reaction to the institutional investors’ pressure. The president of the branch during the studied period, Roberto Campos Neto, who participated in some of the meetings of the Amazon Council with institutional investors,⁹¹ included the theme of sustainability in the bank’s agenda.⁹² As a result, a series of changes related to environmental protection were added not only for the bank’s guidelines itself, but also for the whole National Financial System. The new policies are focused on credit, supervision, and regulation rules, with the inclusion of the “climate risk” concept to stress tests and regulation protocols, for example.⁹³ Another change was to offer a 20% higher rural credit for those groups and individuals who complied with specific environmental standards,⁹⁴ and also to intensify cooperation with the Climate Bonds Initiative (CBI) through new investment plans.⁹⁵ Besides that, the BC signaled its intention to include sustainability criteria for the selection of new investments and for the selection of companies that would manage international reserves.⁹³ In addition, the bank committed to preparing annual reports on socio-economic risks, implementing the recommendations of the Task Force on Climate-Related Financial Disclosures (TCFD), and adopting everyday environmentally friendly measures at its facilities, such as promoting the use of bicycles and reducing plastic consumption.⁹²

One chief of environment at a Brazilian federal bureau (B2) cited perhaps the only confrontational response from a member of Bolsonaro’s government directed at private institutional investors. The Economy Minister Paulo Guedes told investors, businessmen, diplomats, and academics at an event in Washington, “We understand the concern of you, because you have cleared your forests. You want to spare us from clearing our forest, as you have cleared yours. We know that you had civil wars, you also had slavery, and we just ask you to be as kind as we are kind. You killed your Indians, you didn’t miscegenate. The military is saying, thank you for your concern, but this is our land. We don’t need to deforest the Amazon to produce agricultural products.”⁸⁴ Although it was a confrontational response, the interviewee (B2) also said that it was an isolated incident and that Guedes soon changed his attitude towards institutional investors.

It is not the goal of this paper to assess whether the Brazilian government’s responses to institutional investors’ pressure have been effective in addressing the Amazon wildfires problem. However, the interviewees’ positions on this issue contribute to a general understanding of the divestment dynamic and also to their own positionalities in this context. A member at the Bolsonaro’s Brazilian executive power sphere (B3) considered that the increasing export figures and the low number of institutional investors that have actually divested indicate that the political and media pressure from foreign countries and NGOs

was not sufficient to weaken the credibility of Bolsonaro's government. Furthermore, four respondents from civil society (A1, A2, A4, A5) felt that divestment pressure had indeed prompted the government to act, but that the measures were not enough to address the environmental problems in the Amazon rainforest. They pointed, for example, to the ongoing deforestation, forest fires, lack of impunity for those responsible for the crimes, the new laws that encourage the dismantling of regulatory agencies, and the tightening of land laws. In addition, six interviewees from different backgrounds (A3, A7, B1, C1, C2, C3) agreed that while government responses to divestment pressures were insufficient, the pressures succeeded in raising the visibility of the issue in public debate and creating more incentives for the private sector in Brazil to adopt new and more concrete environmental standards and policies, while also demanding more actions from the government. Moreover, one chief of environment at a Brazilian federal bureau (B2) believed that the pressure was successful in bringing about positive changes in the Bolsonaro government, citing the new financial regulations adopted by the BC as evidence of this.

Regarding the limits of divestment strategies, four participants (A2, B2, C4, C5) emphasized that after one institutional investor divests, another can buy up the sold part, showing that these movements need to take place on a large scale to overcome the challenges of collective action, as the literature suggests. It was highlighted, including by two professionals from investment organizations that threatened to divest (C4, C5), that because of this constraint, institutional investors often prefer to use their voices by engaging with the companies and governments in which they invest rather than opting to exit them and losing the opportunity to help these companies make the necessary transition to more investor-friendly operations. Therefore, it could be argued that the pressure to divest was exerted as a bargaining strategy: not necessarily to divest, but to gain more leverage and increase incentives for companies and the government to do more about the Amazon rainforest situation.

The interviews provided ample evidence that the Brazilian government under Bolsonaro's leadership has varied its reactions to external criticism of the Amazon rainforest wildfires. Almost all the interviewees (A1, A3, A4, A5, A6, A7, C1, C2, C3, C4) agreed that the government did indeed take different approaches to dealing with criticism from civil society, foreign governments, and institutional investors. Overall, no aggressive messages or reactions were sent to institutional investors by Bolsonaro or his government officials, especially when compared to the tone used to answer criticisms from civil society and foreign countries. Furthermore, more concrete actions were taken to respond to the divestment pressures from institutional investors. This demonstrates how the international private sector played a more important role for Bolsonaro's government than the other two categories (only two of the interviewees had a different opinion in this regard: an advisor for a Brazilian senator part of the opposition against Bolsonaro (B1) argued that the government was aggressive and intransigent in responding to all criticisms; and a member at the Bolsonaro's Brazilian executive power sphere (B3) defended that there was no different policy for each actor). This paper argues that the divestment pressures from institutional investors were affecting the president's winning coalition, besides aggravating the capital inflow to the country. Therefore, adopting a more conciliatory and serious stand in front of their demands was a strategic decision.

THE LEVERAGE OF THE DIVESTMENT THREATS

This paper assesses the hypothesis that governments are more responsive to institutional investors' pressure in comparison to foreign governments and NGOs when the first plays a major role in the incumbent winning coalition and when financial capital is scarce. In his selectorate theory, Bueno de Mesquita⁹⁶ defines a winning coalition as the group without whose support a leader cannot remain in office. In Bolsonaro's case, the subsets that compose such categories are the military, the agribusiness, the evangelical church, and right-wing ideological enthusiasts. This section will argue that the divestment pressures have affected most of them in a way that foreign countries and civil society's criticisms have not, creating incentives to Bolsonaro to react to institutional investors in a more respectful and cognizant way in order to maintain his winning coalition's loyalty. Besides that, the risk of divestment put additional weight on dealing with institutional investors properly because Brazil is not a capital-intensive economy,⁹⁷ Bolsonaro's economic strategy relied on increasing incoming capital flows, and COVID-19 aggravated even more the international capital supply.

One reason Bolsonaro reacted to institutional investors' pressure in a more solemn way was his electoral preoccupation. Taking the assumption that every leader's main objective is to stay in power, the Brazilian president could be worried that by challenging the international financial sector, some of his supporters would disapprove this action and no longer support him for reelection. Such a dynamic did not happen with NGOs, since his electorate voted for him even after his aggressive statements during the campaign. It was also not the case for foreign countries, who were easily countered with the nationalistic and patriotic discourse used by Bolsonaro to defend his actions, as already explained. However, in the case of the institutional investors, one of Bolsonaro's strongest electoral promises was to adopt more liberal economic measures after being elected. Among the promised projects are the privatization of state-owned bureaus and subsidiaries, the attraction of more foreign capital into Brazil, implementing budget cuts on administrative and pensions systems, and less intervention in the economy.⁹⁸ The announcement that Paulo Guedes would be his economy minister was made even before the end of the presidential election, proving that Bolsonaro planned on raising support by portraying himself as a supporter of the "market" and the private sector, since Guedes

was a well-known figure within the business community (one chief of environment at a Brazilian federal bureau (B2) even mentioned that Guedes was pressured by institutional investors during the Davos 2020 summit regarding environmental issues). As a result, two interviewees (A1, C3) stated that antagonizing the institutional investors, who are part of the private sector and can be associated with economic liberal agendas, on the issue of the Amazon wildfires would create a contradiction with one of Bolsonaro's main electoral agendas, possibly making him lose public support.

The divestment pressures from institutional investors were not only focused on the government, but also on a series of national and multinational companies of the agribusiness sector operating in the Amazon region. In order to maintain their investments safe and therefore protect their businesses, such companies have adopted two strategies: Three participants (A6, C1, C4) argued that the first one was to put into practice corrective measures, such as improving their supply chains' traceability capacity and other ESG-related moves. This, in turn, would provide them with results to present to investors to prove they are committed to meeting their demands and thus retain their access to capital. The second one was to request the Brazilian government to improve its relationship with institutional investors. Investment decisions are made based on a series of factors besides the ones related to a specific company, and the political, economic, and environmental context of a country also are considered by financiers. Therefore, in order to avoid the ripple effect of negative reputational contagion from disengaged firms and producers, as presented by the director of sustainable investing at an asset management firm that threatened to divest (C5), affected businesses have pressured the government to take actions capable of convincing the investors of the country's stability.⁹⁹ According to a portfolio manager at an asset management firm that threatened to divest (C4), this pressure was applied in the form of public letters, formal statements to the press, and meetings with members of the government, congress, and civil society. One science director at a research institute focused on the Amazon (A7) mentioned that some agribusinesses even attended the COP meetings to defend their reputation through alternative strategies.

In Brazil, the bull bench ("bancada do boi") is the group of deputies and senators in the legislative power that represent the interests of the agribusiness sector. Bolsonaro relies on the support of this group, among others, to enable his government to pass laws and fight for its interests in the House of Representatives and in the Senate. As Bolsonaro's policies facilitated mining, agricultural, and hunting activities in the Amazon rainforest,^{76, 100} and distributed amnesties for illegal deforestation,¹⁰¹ these players had incentives to continue to be part of his winning coalition.² According to the head of the Centre for Sustainability Studies at a Brazilian university (A6), when the agribusiness companies started to get pressured with divestment threats by institutional investors, they looked for these bull bench representatives in the legislative for help to their sectors, since many of these members have received and still receive some kind of political and economic support from these businesses to be (re)elected. In turn, these deputies demanded the executive power to alter its behavior to alleviate the pressure from the agribusiness affected businesses.^{102, 103} As a result, Bolsonaro's government adopted a conciliatory tone to the institutional investors' demand as a way to safeguard his own winning coalition support.

However, three interviewees (A7, C1, C4) emphasized that it is important to recognize that the agribusiness sector is not a homogeneous group either: While some agribusiness companies supporting Bolsonaro's aggressiveness towards foreign players have their operations focused on the domestic markets, other organizations are more export-orientated, meaning that they are more reliable on good diplomatic and cooperative Brazilian relations abroad to diminish commerce barriers and bring greater stability to trade agreements, besides being more vulnerable to external demands since many of them are multinationals (affiliates) who have to respond to their corporate headquarters abroad. For this group, for example, the obstruction of the EU-Mercosur agreement represents a setback on their agenda, since it would bring a great deal of new commerce opportunities for them, as one grassroots environmental activist pointed out (A3). As a result, these two groups often have conflicting interests and seek to influence the Agribusiness Ministry and legislative representatives to prioritize each of their visions (C1).

Finally, one must consider that one of the biggest leverage institutional investors have is their capital. Several interviewees, many of whom are from the financial sector (A4, C1, C3, C4), emphasized that institutional investors represent money and that their decisions could have a direct impact on the Brazilian economy, and therefore the Brazilian government has responded better to their criticism. One associate portfolio manager at an investment fund that threatened to divest (C3) explained that many governments rely on foreign capital to administer their national debts and handle their exchange-rate balance. Added to that, the COVID-19 pandemic increased governments' need for foreign capital as national incomes decreased with the urgency to apply quarantine measures. Relatedly, foreign capital supply diminished as many investors reallocated their capital to safer countries in a "flight to quality" movement.¹⁰⁴ As a result, the decisions of investors became more relevant for companies and states as the health crisis advanced.

In Brazil, foreign investors withdrew \$50.9 billion from the Brazilian stock and bond market between June 2019 and June 2020, considered one of the worst historical trends in the country's history.¹⁰⁴ Related to this, Roberto Campos Neto, president of the BC, stated in June 2020 that the country had lost more investments during the pandemic in comparison with the world average,

and that the federal environmental handling contributed to it.¹⁰⁵ With a high public debt to operate and economic plans based on attracting foreign capital to carry out key privatizations and tax adjustments, one chief of environment at a Brazilian federal bureau (B2) indicated that Paulo Guedes was another proponent of the idea that the demands of institutional investors should be considered. Besides him, another participant of the financial sector (C4) added that the own private financial system in Brazil, represented by major private banks, such as Bradesco and Itaú, became uncertain about the whole financial system balance and demanded a better response to institutional investors.

This section has argued that the reason Bolsonaro’s government has been more conciliatory and responsive to institutional investor criticism is related to Bolsonaro’s winning coalition and the need for foreign capital. While the confrontational responses toward civil society and foreign states can be explained by the more right-wing ideological groups and the Brazilian army in his government, the reactions toward institutional investors can be explained by the fact that Bolsonaro was elected on the basis of liberal economic promises and governed with strong support from agribusiness companies. Therefore, he tried to maintain the liberal coherence promised during the election while responding to the demands of parts of the agribusiness sector. In addition, the need for investments and a stable flow of capital, especially during the COVID-19 pandemic, provided extra leverage for the institutional investors’ pressures. As a result, institutional investors’ demands regarding the Amazon rainforest fires were met with a more professional tone and with costly signals from the government.

DISCUSSION

Bolsonaro has not been the only Brazilian leader to deal with external criticism due to environmental concerns. Since re-democratization in Brazil, all presidents up to 2008 recorded higher annual deforestation rates in the Amazon during their time in office than in the last three years under Bolsonaro. Thereafter, there was a steep decline in deforestation rates between 2004 and 2012, followed by relative stability, which reversed under Bolsonaro’s administration, as shown in the following graph (Data retrieved from the Brazilian National Institute for Spatial Research (INPE) website)¹⁰⁶ (Burnt areas do not enter into the calculation of deforestation here, only clear-cutting removal of primary forest vegetation).

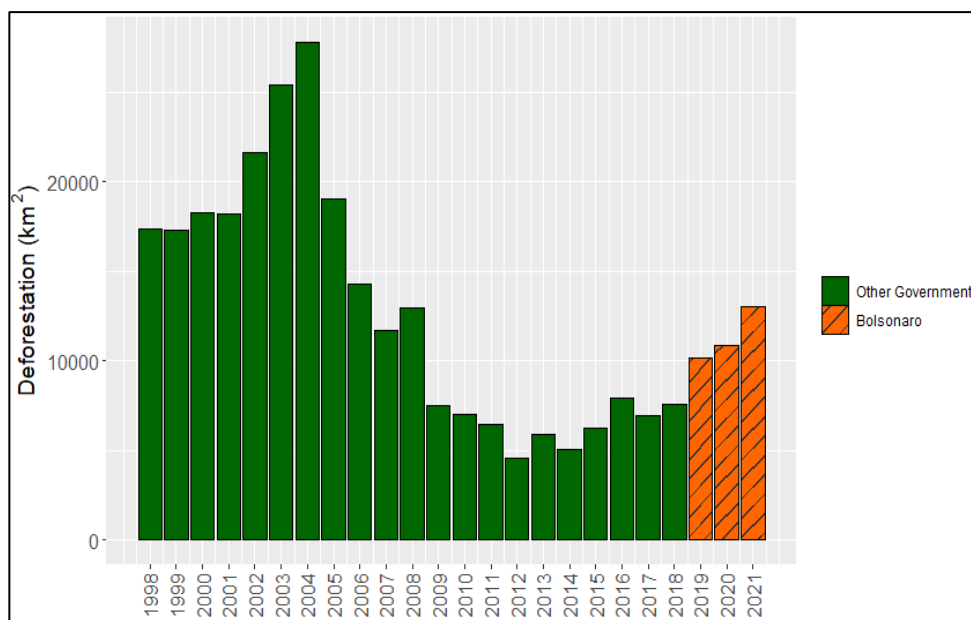


Figure 3. Deforestation in the Brazilian Amazon.

Although it is not this paper’s objective to review investor-government relations in Brazil since re-democratization, one could argue that in addition to the growing Amazonian deforestation rates, Bolsonaro’s government has broken a tradition shared by all his antecessors since 1985: keeping up with the myth of the Brazilian environmental commitment and international climate leadership. According to Viola and Franchini¹⁰⁷, each country possesses a self-image regarding its own level of agency and achievements in the climate arena, being important not only for its own national identity, but also for foreign policy discourse. However, when there is a gap between the self-image discourse and what is done in reality, like credible commitments to stabilize the climate system and climate leadership, the self-image gets distorted into a climate myth.¹⁰⁷ The authors argue that since re-democratization, all Brazilian leaders contributed to the continuous existence of this myth that laid on the fact that, although presidents tried to portray the role of Brazil as a climate leader, there was a gap between their discourse and their real commitments.^{107, 108} Nevertheless, even taking into consideration these contradictions, the myth of a Brazilian commitment to the

environment paved the way for a more inclusive and cooperative environmental governance to exist, beneficial for the country due to the gain of resources (through the Amazon Fund, for example) and international recognition.¹⁰⁸

Bolsonaro was the first president since the re-democratization to give up with the Brazilian myth, as shown in this paper.¹⁰⁷ His decisions and behavior, at least in the first two years of his mandate, signaled to the world that his government would no longer try to portray Brazil as a climate protagonist, but rather abdicate from this position. Among these signals, some that stood out were: being elected on an anti-environment platform with statements against harsh environmental fees for farmers;¹⁰⁹ indicating that he would withdraw Brazil from the Paris Agreement;³⁰ withdrawing the Brazilian candidature to host the 2019 COP;¹¹⁰ engaging in a series of diplomatic animosities with other countries regarding his decisions on the environment, such as Norway and Germany;^{111, 112} and defunding and undermining main Brazilian environmental regulatory agencies, such as IBAMA.^{5, 113} All this evidence proves that Bolsonaro's path of action not only pursued to weaken the country's environmental protection framework, but also disregarded how the world was seeing all these events unfold. They also show how Bolsonaro retreated from maintaining the climate myth alive by no longer bearing the costs of signaling to the international community of the Brazilian climate leadership.¹⁰⁷

As already explained, a country's self-image concerns its own reputation, and trying to keep a credible self-image on environmental issues was a way that past Brazilian presidents demonstrated that Brazil could be a climate leader. Bolsonaro not only rejected that deforestation and climate change were problems, but also encouraged their aggravation with multiple decisions to curb enforcement and surveillance agencies.^{5, 114-118} As signals to the international community regarding Brazil's commitments to environmental protection and climate leadership were substituted by a hostile and apathetic diplomacy, in addition to a series of criticized domestic environmental public policies, Bolsonaro's reputation started to deteriorate, which in turn made it easier for the reputation of companies operating in the country and the institutional investors who invested in those companies to be called into question as well. The media and civil society began to, besides denouncing the federal government itself, shed light on the companies and sectors related to the Amazon wildfires, thus condemning their operations and affecting their reputations. As a result, clients concerned about the environment commenced to pressure the institutional investors to take a stand on the issue. These same investors, motivated by their customers' demands and preoccupied about their own reputations, established strategies to mitigate further deterioration of the situation, including pressuring to divest.

Furthermore, the findings of this article suggest that the international private and financial sectors have increasing influence on national governments with neoliberal agendas and pro-market discourses, especially in a globalized world and in circumstances with limited capital supply. Another contribution of this study to the literature is the finding that the threat of divestment can be used as a bargaining strategy by institutional investors: Since the act of divestment remains a non-preferential decision for them, they may choose to use the threat of divestment to accommodate pressure from their clients and other stakeholders, and continue to do business with firms and governments by seeking constructive engagement with them.

CONCLUSION

This article has examined the Brazilian divestment case, its main dynamics, and complexities. The main contributions of this study are twofold: first, the main motivations and strategies of foreign governments, civil society, and institutional investors were analyzed, highlighting how they differ, with a particular focus on the aspect that institutional investors are mainly concerned about reputational and financial risks in their decision to threaten divestment. Second, through the analysis of in-depth interviews, this paper examined the Bolsonaro government's responses to criticism, showing how different responses were applied to different groups and the reasoning behind such decisions, as well as the leverage of institutional investors in threatening to divest. It was argued that the Brazilian government was more responsive to pressure from institutional investors compared to foreign governments and NGOs, as the former played a key role in the stability of Bolsonaro's winning coalition and his electoral aspirations, and Brazilian financial capital was scarce due to the COVID-19 pandemic.

The study of divestment movements provides us with useful insights into how governmental decision-makers can be influenced, especially when it comes to environmental issues. As the climate crisis continues to worsen, scientists, activists, entrepreneurs, and citizens will face the challenge of pressuring governments to take action to mitigate and adapt to extreme weather events and other climate impacts. In addition, assessing the effects that the new ESG phenomenon is going to produce in the way that private authority is exercised in the international realm is also a vital understanding to the studies of public policies, private governance, and transnational relations. The Brazilian case is a clear example of how a government that is not committed to environmental protection and does not listen to neighboring countries and civil society can be influenced by the financial sector to take more concrete environmental action, especially under the conditions that the winning coalition is dependent on foreign investment and financial capital is scarce. It also shows us how the private sector itself, in this case pressured by investors, can be a driving force for more sustainable businesses, often calling on the government to improve its public policies as well. Further research is needed to examine whether the actions taken by the Bolsonaro government in response to institutional investor

demands were truly effective in dealing with the Amazon wildfires, and whether the entire divestment case in Brazil had any impact on the 2022 Brazilian presidential election.

ACKNOWLEDGEMENTS

The author thanks Prof. Carolina Moehlecke of the International Relations Department of the Getulio Vargas Foundation for her support and supervision of this research. The author also gratefully acknowledges financial support from PIBIC, the Institutional Program of Scientific Initiation Scholarships run by the Brazilian National Council for Scientific and Technological Development (CNPq). In addition, the author would like to thank the interviewees for their willingness to participate in this research.

REFERENCES

1. Aguiar, D. (2019) Bolsonaro's Christmas gift to perpetrators of illegal deforestation. Greenpeace. <https://www.greenpeace.org/international/story/27962/bolsonaros-gift-to-perpetrators-of-illegal-deforestation/> (accessed Feb 2022)
2. Branford, S., Borges, T., Torres, M. (2018) Bolsonaro shapes administration: Amazon, indigenous and landless at risk. Mongabay. <https://news.mongabay.com/2018/12/bolsonaro-shapes-administration-amazon-indigenous-and-landless-at-risk/> (accessed February 19, 2022)
3. Mendes, K. (2019) Future of Amazon deforestation data in doubt as research head sacked. Mongabay. <https://news.mongabay.com/2019/08/future-of-amazon-deforestation-data-in-doubt-as-research-head-sacked/> (accessed Feb 2022)
4. Sauer, N. (2019) Brazil's natural resources open for business, says Bolsonaro. Climate Home News. <https://www.climatechangenews.com/2019/01/22/brazils-natural-resources-open-business-bolsonaro-says/> (accessed Feb 2022)
5. Spring, J., Eisenhammer, S. (2019) Exclusive: As fires race through Amazon, Brazil's Bolsonaro weakens environment agency. Reuters. <https://www.reuters.com/article/us-brazil-environment-ibama-exclusive-idUSKCN1V114I> (accessed Feb 2022)
6. The Telegraph (2019) Amazon deforestation increases by 278% in a year, institute warns climate skeptic president Bolsonaro. <https://www.telegraph.co.uk/news/2019/08/07/amazon-deforestation-increases-278-year-institute-warns-climate/> (accessed Feb 2022)
7. Braungardt, S., Bergh, J., Dunlop, T. (2019) Fossil fuel divestment and climate change: Reviewing contested arguments. *Energy Research & Social Science*, 50, 191–200. <http://dx.doi.org/10.1016/j.erss.2018.12.004>
8. Hunt, C., Weber, O., Dordi, T. (2017) A comparative analysis of the anti-Apartheid and fossil fuel divestment campaigns. *Journal of Sustainable Finance & Investment*, 7(1), 64–81. <https://doi.org/10.1080/20430795.2016.1202641>
9. Soederberg, S. (2009) The Marketisation of Social Justice: The Case of the Sudan Divestment Campaign. *New Political Economy*, 14(2), 211–229. <https://doi.org/10.1080/13563460902825999>
10. Ayling, J., Gunningham, N. (2015) Non-state governance and climate policy: the fossil fuel divestment movement. *Climate Policy*, 17(2), 131–149. <http://dx.doi.org/10.1080/14693062.2015.1094729>
11. Curran, G. (2020) Divestment, energy incumbency and the global political economy of energy transition: the case of Adani's Carmichael mine in Australia. *Climate Policy*, 20(8), 949–962. <https://doi.org/10.1080/14693062.2020.1756731>
12. Nasiritousi, N. (2017) Fossil fuel emitters and climate change: unpacking the governance activities of large oil and gas companies. *Environmental Politics* 26(4), 621–647. <https://doi.org/10.1080/09644016.2017.1320832>
13. Schueth, S. (2003) Socially Responsible Investing in the United States. *Journal of Business Ethics*, 43, 189–194. <https://doi.org/10.1023/A:1022981828869>
14. Shank, T., Manullang, D., Hill, R. (2005) Is it Better to be Naughty or Nice? *The Journal of Investing*, 14(3), 82–88. <https://doi.org/10.3905/joi.2005.580553>
15. Wander, N., Malone, R. E. (2004) Selling Off or Selling Out? Medical Schools and Ethical Leadership in Tobacco Stock Divestment. *Academic Medicine*, 79(11), 1017–1026. <https://doi.org/10.1097/00001888-200411000-00002>
16. Westermann-Behaylo, M. (2010) Institutionalizing Peace through Commerce: Engagement or Divestment in South Africa and Sudan. *Journal of Business Ethics*, 89, 417–434. <https://doi.org/10.1007/s10551-010-0398-0>
17. Arnold, P., Hammond, T. (1994) The Role of Accounting in Ideological Conflict: Lessons from the South African Divestment Movement. *Accounting, Organizations and Society*, 19(2), 111–126. [https://doi.org/10.1016/0361-3682\(94\)90014-0](https://doi.org/10.1016/0361-3682(94)90014-0)
18. Patey, L. A. (2009) Against the Asian Tide: the Sudan divestment campaign. *The Journal of Modern African Studies*, 47(4), 551–573. <http://www.jstor.org/stable/40538335>
19. White, J. A. (2004) Globalisation, Divestment and Human Rights in Burma. *The Journal of Corporate Citizenship*, 14, 47–65. <http://www.jstor.org/stable/jcorpcti.14.47>
20. Bergman, N. (2018) Impacts of the Fossil Fuels Divestment Movement: Effects on Finance, Policy and Public Discourse. *Sustainability*, 10(7), 1–18. <https://doi.org/10.3390/su10072529>
21. Ayling, J. (2017) A Contest for Legitimacy: The Divestment Movement and the Fossil Fuel Industry. *Law & Policy*, 39(4), 349–371. <https://doi.org/10.1111/lapo.12087>
22. Christophers, B. (2019) Environmental Beta or How Institutional Investors Think about Climate Change and Fossil Fuel Risk. *Annals of the American Association of Geographers*, 109(3), 754–774. <https://doi.org/10.1080/24694452.2018.1489213>
23. Apfel, D. C. (2015) Exploring Divestment as a Strategy for Change: An Evaluation of the History, Success, and Challenges of Fossil Fuel Divestment. *Social Research*, 82(4), 913–37. <http://www.jstor.org/stable/44282147>

24. UNPRI (2020) An Introduction to Responsible Investment: Screening. <https://www.unpri.org/an-introduction-to-responsible-investment/an-introduction-to-responsible-investment-screening/5834.article#:~:text=specific%20ESG%20issues,What%20is%20screening%3F,investor's%20preferences%2C%20values%20and%20ethics> (accessed Feb 2022)
25. Trencher, G., Downie, C., Hasegawa, K., Asuka, J. (2020) Divestment trends in Japan's international coal businesses. *Renewable and Sustainable Energy Reviews*, 124, 1–14. <https://doi.org/10.1016/j.rser.2020.109779>
26. Broccardo, E., Hart, O., Zingales, L. (2022) Exit vs. Voice. *Journal of Political Economy*, 130(11). <https://doi.org/10.1086/720516>
27. Grossman, B. R., Sharpe, W. F. (1986) Financial Implications of South African Divestment." *Financial Analysts Journal*, 42(4), 15–29. <https://doi.org/10.2469/faj.v42.n4.15>
28. Wander, N., Malone, R. E. (2006) Fiscal versus social responsibility: how Philip Morris shaped the public funds divestment debate. *Tobacco Control*, 15, 231–241. <https://doi.org/10.1136/tc.2005.015321>
29. Abbott, K., Green, J. F., Keohane, R. O. (2016) Organizational Ecology and Institutional Change in Global Governance. *International Organization*, 70(2), 247–277. doi:10.1017/S0020818315000338
30. Darby, M. (2018) Brazil: Bolsonaro threatens to quit Paris climate deal. Climate Home News. <https://www.climatechangenews.com/2018/08/14/brazils-bolsonaro-threatens-quit-paris-climate-deal/> (accessed Feb 2022)
31. Watts, J. (2018) Fears for Amazon as Bolsonaro plans to merge environment and agriculture ministries. The Guardian. <https://www.theguardian.com/world/2018/nov/01/bolsonaro-environment-agriculture-ministries-amazon> (accessed Feb 2022)
32. Borges, T., Branford, S. (2019) Former Brazilian enviro ministers blast Bolsonaro environmental assaults. Mongabay. <https://news.mongabay.com/2019/05/former-brazilian-enviro-ministers-blast-bolsonaro-environmental-assaults/> (accessed Feb 2022)
33. Dantas, C. (2019) Queimadas aumentam 82% em relação ao mesmo período de 2018. G1. <https://g1.globo.com/natureza/noticia/2019/08/19/queimadas-aumentam-82percent-em-relacao-ao-mesmo-periodo-de-2018.ghtml> (accessed Feb 2022)
34. Eisenhammer, S. (2019) 'Day of Fire': Blazes ignite suspicion in Amazon town. Reuters. <https://www.reuters.com/article/us-brazil-environment-wildfire-investiga-idUSKCN1V1MK> (accessed Feb 2022)
35. McCoy, T. (2019) Smoke plunges Sao Paulo into sudden darkness, baffling the Western Hemisphere's largest city. The Washington Post. <https://www.washingtonpost.com/world/2019/08/20/sudden-darkness-befalls-sao-paulo-western-hemispheres-largest-city-baffling-thousands/> (accessed Feb 2022)
36. Weston, P. (2019) Amazon fires: Brazil sends in 44,000 troops to tackle blazes as Bolsonaro is accused of ignoring illegal deforestation. Independent. <https://www.independent.co.uk/climate-change/news/amazon-rainforest-fires-brazil-bolsonaro-environmental-protection-army-a9078216.html> (accessed Feb 2022)
37. Murakawa, F. (2020) Fogo na Amazônia será proibido por 120 dias. Valor. <https://valor.globo.com/brasil/noticia/2020/07/08/fogo-na-amazonia-sera-proibido-por-120-dias.ghtml> (accessed Feb 2022)
38. Valente, R. (2020) Mourão forma Conselho da Amazônia com 19 militares e sem Ibama e Funai. UOL Notícias. <https://noticias.uol.com.br/colunas/rubens-valente/2020/04/18/conselho-amazonia-mourao.htm> (accessed Feb 2022)
39. Investor statement on deforestation (2019) Investor statement on deforestation and forest fires in the Amazon. https://d8g8t13e9nj2o.cloudfront.net/Uploads/r/q/s/investorstatementondeforestationandforestfiresintheamazon_29_oct_2019_665598.pdf (accessed Feb 2022)
40. Phillips, T. (2020) Trillion-dollar investors warn Brazil over 'dismantling' of environmental policies. The Guardian. <https://www.theguardian.com/environment/2020/jun/23/trillion-dollar-investors-warn-brazil-over-dismantling-of-environmental-policies> (accessed Feb 2022)
41. Holger, D., Trevisani, P. (2020) Nordea Asset Management Drops JBS Over Deforestation, Corruption, Worker Health. The Wall Street Journal. <https://www.wsj.com/articles/nordea-asset-management-drops-jbs-over-deforestation-corruption-worker-health-11595963107> (accessed Feb 2022)
42. Fouche, G. (2019) Nordea Asset Management suspends Brazilian government bond purchases due to Amazon fires. Reuters. <https://www.reuters.com/article/us-brazil-environment-investors-idUSKCN1VK1S0> (accessed Feb 2022)
43. Carter, N., Bryant-Lukosius, D., DiCenso, A., Blythe, J., Neville, A. J. (2014) The use of triangulation in qualitative research. *Oncol Nurs Forum*, 41(5), 545–547. doi: 10.1188/14.ONF.545-547. PMID: 25158659
44. Mosley, L. (2013) *Interview Research in Political Science*. Cornell University Press. <http://www.jstor.org/stable/10.7591/j.ctt1xx5ng>
45. APIB (2019) Declaração de Organizações da Sociedade Civil sobre a Crise do Desmatamento e Queimadas na Amazônia Brasileira. <https://apiboficial.org/2019/08/26/declaracao-de-organizacoes-da-sociedade-civil-sobre-a-crise-do-desmatamento-e-queimadas-na-amazonia-brasileira/> (accessed Feb 2022)
46. DiCaprio, L. (2019) The lungs of the Earth are in flames. Instagram. <https://www.instagram.com/p/B1eBsWDJfF1/> (accessed Feb 2022)
47. Gonzaga, D. (2020) Fires are raging in the Amazon—again. Greenpeace. <https://www.greenpeace.org/international/story/44159/fires-brazil-bolsonaro-amazon-deforestation-2020/> (accessed Feb 2022)
48. MoneyTimes (2019) Bolsonaro é denunciado ao Tribunal Penal Internacional. <https://www.moneytimes.com.br/bolsonaro-e-denunciado-ao-tribunal-penal-internacional/> (accessed Feb 2022)

49. Ronaldo, C. (2019) The Amazon Rainforest produces more than 20% of the world's oxygen and its been burning for the past 3 weeks. Instagram. <https://www.instagram.com/p/B1eXVHMA9AT/> (accessed Feb 2022)
50. WWF (2019) WWF statement on devastating forest fires in the Amazon. https://wwf.panda.org/wwf_news/?351955/WWF-statement-on-devastating-forest-fires-in-the-Amazon (accessed Feb 2022)
51. APIB (2019) Comitativa de lideranças indígenas vai à Europa denunciar violações no Brasil. <https://cimi.org.br/2019/10/comitativa-de-liderancas-indigenas-vai-a-europa-denunciar-violacoes-no-brasil/> (accessed Feb 2022)
52. Amazon Watch (2019) Em Paris, líderes indígenas brasileiros denunciam o papel dos financiadores franceses na destruição da Amazônia. <https://amazonwatch.org/pt/news/2019/1112-in-paris-brazilian-indigenous-leaders-denounce-the-role-of-financiers-in-amazon-destruction> (accessed Feb 2022)
53. Catraca Livre (2020) Sonia Guajajara: 'Não é uma luta de índio, mas pelo planeta'. <https://catracalivre.com.br/cidania/sonia-guajajara-nao-e-uma-luta-de-indio-mas-pelo-planeta/> (accessed Feb 2022)
54. DefundBolsonaro (2021) Defund Bolsonaro. Instagram. <https://www.instagram.com/defundbolsonaro/> (accessed Feb 2022)
55. BR US Embassy (2019) U.S. Government Provides Technical Assistance in Wake of Wildfires in Brazil. <https://br.usembassy.gov/u-s-government-provides-technical-assistance-in-wake-of-wildfires-in-brazil/> (accessed Feb 2022)
56. The Times of Israel (2019) Netanyahu offers Brazil help in fighting devastating Amazon fires. <https://www.timesofisrael.com/netanyahu-offers-brazil-help-in-fighting-devastating-amazon-fires/> (accessed Feb 2022)
57. Boffey, D. (2019) Norway halts Amazon fund donation in dispute with Brazil. The Guardian. <https://www.theguardian.com/world/2019/aug/16/norway-halts-amazon-fund-donation-dispute-brazil-deforestation-jair-bolsonaro> (accessed Feb 2022)
58. Phillips, T. (2019) Merkel backs Macron's call for G7 talks on Amazon fires. The Guardian. <https://www.theguardian.com/world/2019/aug/23/amazon-rainforest-fires-macron-calls-for-international-crisis-to-lead-g7-discussions> (accessed Feb 2022)
59. Reuters (2019) France's Macron says real 'ecocide' going on in Amazon. <https://www.reuters.com/article/us-g7-summit-amazon-idUSKCN1VD2AM> (accessed Feb 2022)
60. Avissar, R., Werth, D. (2005) Global Hydroclimatological Teleconnections Resulting from Tropical Deforestation. *Journal of Hydrometeorology*, 6(2), 134–145. https://journals.ametsoc.org/view/journals/hydr/6/2/jhm406_1.xml
61. McFall-Johnsen, M. (2019) Earth is a spaceship, and the Amazon is a crucial part of our life-support system, creating up to 20% of our oxygen. Here's why we need the world's largest rainforest. Business Insider. <https://www.businessinsider.com/why-amazon-rainforest-is-important-life-support-is-burning-2019-8> (accessed Feb 2022)
62. Abnett, K., Jessop, S. (2022) Explainer: What is the EU's sustainable finance taxonomy? Reuters. <https://www.reuters.com/business/sustainable-business/what-is-eus-sustainable-finance-taxonomy-2022-02-03/#:~:text=The%20EU%20taxonomy%20is%20a,be%20marketed%20as%20sustainable%20investments.&text=It%20includes%20economic%20activities%20as,to%20earn%20a%20green%20label> (accessed Feb 2022)
63. UNPRI (2019) 230 Investors with USD \$16.2 trillion in AUM Call for Corporate Action on Deforestation, Signaling Support for the Amazon. <https://www.unpri.org/news-and-press/230-investors-with-usd-162-trillion-in-aum-call-for-corporate-action-on-deforestation-signaling-support-for-the-amazon/4867.article> (accessed Feb 2022)
64. IPCC (2021) Climate change widespread, rapid, and intensifying – IPCC. <https://www.ipcc.ch/2021/08/09/ar6-wg1-20210809-pr/> (accessed Feb 2022)
65. Pérez, L., Hunt, D. V., Samandari, H., Nuttall, R., Biniak, K. (2022) Does ESG really matter—and why? McKinsey. <https://www.mckinsey.com/capabilities/sustainability/our-insights/does-esg-really-matter-and-why> (accessed Feb 2022)
66. Spangler, T. (2021) The ESG Financing Revolution Is On: How Entrepreneurs Can Ride The Wave. Forbes. <https://www.forbes.com/sites/forbesbusinesscouncil/2021/12/15/the-esg-financing-revolution-is-on-how-entrepreneurs-can-ride-the-wave/?sh=1beb35d87961> (accessed Feb 2022)
67. Amigo, I. (2020) When will the Amazon hit a tipping point? Nature. <https://www.nature.com/articles/d41586-020-00508-4> (accessed Feb 2022)
68. Spring, J. (2020) Global investors demand to meet Brazil diplomats over deforestation. Nasdaq. <https://www.nasdaq.com/articles/global-investors-demand-to-meet-brazil-diplomats-over-deforestation-2020-06-23-1> (accessed Feb 2022)
69. Folha de São Paulo (2018) Organizações repudiam fala de Bolsonaro contra ativismos. <https://www1.folha.uol.com.br/poder/2018/10/organizacoes-repudiam-fala-de-bolsonaro-contra-ativismos.shtml> (accessed Feb 2022)
70. Gimenes, E. (2020) Bolsonaro culpa indígenas, imprensa e ONGs por queimadas e consequências da covid. Brasil de Fato. <https://www.brasildefato.com.br/2020/09/22/bolsonaro-culpa-indios-caboclos-midia-e-ongs-por-queimadas-e-consequencias-da-covid> (accessed Feb 2022)
71. Schipani, A., Harris, B. (2019) Brazil minister calls for the Amazon to be monetised. Financial Times. <https://www.ft.com/content/f791bbc6-c2c3-11e9-a8e9-296ca66511c9> (accessed Feb 2022)
72. SBS News (2020) Brazil's Jair Bolsonaro calls environmental NGOs a 'cancer' amid pressure to better protect the Amazon. <https://www.sbs.com.au/news/article/brazils-jair-bolsonaro-calls-environmental-ngos-a-cancer-amid-pressure-to-better-protect-the-amazon/nmkhvg9g5> (accessed Feb 2022)

73. Watts, J. (2019) Jair Bolsonaro claims NGOs behind Amazon forest fire surge – but provides no evidence. *The Guardian*. <https://www.theguardian.com/world/2019/aug/21/jair-bolsonaro-accuses-ngos-setting-fire-amazon-rainforest> (accessed Feb 2022)
74. Simões, E., Teixeira, M. (2019) Brazil's president accuses actor DiCaprio of paying to burn the Amazon. *Reuters*. <https://www.reuters.com/article/uk-brazil-environment-dicaprio-idUKKBN1Y32H9> (accessed Feb 2022)
75. Phillips, D. (2019) Bolsonaro declares 'the Amazon is ours' and calls deforestation data 'lies'. *The Guardian*. <https://www.theguardian.com/world/2019/jul/19/jair-bolsonaro-brazil-amazon-rainforest-deforestation> (accessed Feb 2022)
76. Fonseca, P., Spring, J. (2019) Bolsonaro says Brazil rainforest reserve may be opened to mining. *Reuters*. <https://www.reuters.com/article/us-brazil-amazon-mining-idUSKCN1RO29H> (accessed Feb 2022)
77. Araújo, E. H. F. (2017) Trump e o Ocidente. *Cadernos de Política Exterior*, 3(6). <https://funag.gov.br/loja/download/CADERNOS-DO-IPRI-N-6.pdf> (accessed Feb 2022)
78. BBC (2019) Amazon rainforest belongs to Brazil, says Jair Bolsonaro. <https://www.bbc.com/news/world-latin-america-49815731> (accessed Feb 2022)
79. Amaral, L. (2019) Bolsonaro manda Merkel reflorestar Alemanha com dinheiro suspenso. *UOL Notícias*. <https://noticias.uol.com.br/meio-ambiente/ultimas-noticias/redacao/2019/08/14/bolsonaro-manda-merkel-reflorestar-alemanha-com-dinheiro-suspenso.htm> (accessed Feb 2022)
80. O GLOBO (2019) Bolsonaro posta vídeo 'na Noruega', mas cenas de caça de baleias são na Dinamarca. <https://oglobo.globo.com/brasil/bolsonaro-posta-video-na-noruega-mas-cenas-de-caca-de-baleias-sao-na-dinamarca-23886703> (accessed Feb 2022)
81. Salerno, D. (2019) Salles diz que regras do Fundo Amazônia estão em discussão e não se surpreende com suspensão de repasse da Noruega. *G1*. <https://g1.globo.com/sp/sao-paulo/noticia/2019/08/15/salles-diz-que-regras-do-fundo-amazonia-estao-em-discussao-e-nao-se-surpreende-com-suspensao-de-repasse-da-noruega.ghtml> (accessed Feb 2022)
82. Senra, R. (2019) Principal doadora, Noruega diz que Bolsonaro não pode alterar fundo bilionário da Amazônia 'sem consentimento'. *BBC Brasil*. <https://www.bbc.com/portuguese/brasil-48875532> (accessed Feb 2022)
83. VEJA (2019) Bolsonaro zomba da esposa de Macron e é acusado de sexismo. <https://veja.abril.com.br/mundo/bolsonaro-zomba-da-esposa-de-macron-e-e-acusado-de-sexismo/> (accessed Feb 2022)
84. InfoMoney (2020) Guedes responde a críticas ambientais dizendo que os EUA "mataram índios." <https://www.infomoney.com.br/economia/guedes-responde-a-criticas-ambientais-dizendo-que-os-eua-mataram-indios/> (accessed Feb 2022)
85. Costa, M. (2021) Para mostrar "real problema", Mourão viaja à Amazônia com 11 embaixadores. *Metrópoles*. <https://www.metropoles.com/brasil/politica-brasil/para-mostrar-real-problema-mourao-viaja-a-amazonia-com-11-embaixadores> (accessed Feb 2022)
86. Paraguassu, L., Spring, J. (2020) Brazil bans fires in Amazon rainforest as investors demand results. *Reuters*. <https://www.reuters.com/article/us-brazil-environment-idUSKBN24A2DV> (accessed Feb 2022)
87. Reverdosa, M., Wenzel, F. (2020) Fires are raging in the Amazon, despite a Brazil government ban. The destruction could be worse than last summer. *CNN*. <https://edition.cnn.com/2020/08/07/americas/brazil-bolsonaro-amazon-fires-intl/index.html> (accessed Feb 2022)
88. GOV.BR (n.d.) Adote um Parque. <https://www.gov.br/mma/pt-br/assuntos/areasprotegidasecoturismo/adoteumparque> (accessed Feb 2022)
89. MoneyTimes (2020) Ministro do Meio Ambiente quer que críticos ajudem na Amazônia. <https://www.moneytimes.com.br/ministro-do-meio-ambiente-quer-que-criticos-ajudem-na-amazonia/> (accessed Feb 2022)
90. GOV.BR (n.d.) Floresta+. <https://www.gov.br/mma/pt-br/assuntos/servicosambientais/florestamais> (accessed Feb 2022)
91. Shalders, A. (2020) Investidores estrangeiros não vão ser convencidos só por retórica ambiental do governo, diz pesquisador. *BBC Brasil*. <https://www.bbc.com/portuguese/geral-53358810> (accessed Feb 2022)
92. Vilela, P. R. (2020) Economia Banco Central lança agenda de sustentabilidade ambiental. *Agência Brasil*. <https://agenciabrasil.ebc.com.br/economia/noticia/2020-09/banco-central-lanca-agenda-de-sustentabilidade-ambiental> (accessed Feb 2022)
93. Ayres, M. (2020) BC lança agenda de sustentabilidade e reconhece pressão por ações no tema. *Reuters*. <https://jp.reuters.com/article/bacen-sustentabilidade-agenda-idBRKBN25Z30I-OBRBS> (accessed Feb 2022)
94. Grilli, M. (2020) Sustentabilidade poderá gerar até 20% a mais de crédito para o produtor rural, diz BC. *GLOBORURAL*. <https://globorural.globo.com/Noticias/Economia/noticia/2020/09/sustentabilidade-podera-gerar-ate-20-mais-de-credito-para-o-produtor-rural-diz-bc.html> (accessed Feb 2022)
95. Canal Rural (2020) Governo lança Plano de Investimento para Agricultura Sustentável. <https://www.canalrural.com.br/noticias/agricultura/governo-lanca-plano-de-investimento-para-agricultura-sustentavel/> (accessed Feb 2022)
96. Mesquita, B. B. D. (2014) The Strategic Perspective: When Foreign Policy Collides with Domestic Politics, in *Principles of International Politics*, 5th Edition, 64–95. 55 City Road, London: SAGE Publications Ltd. <https://dx.doi.org/10.4135/9781506374550.n2>
97. Oatley, T. (2018) Chapter 4: A Society-Centered Approach to Trade Politics, in *International Political Economy*, 6th ed, 108–136. Routledge.

98. Oliveira, J. (2018) Plano econômico de Paulo Guedes, guru de Bolsonaro, depende de uma ‘bala de prata’ para funcionar. El País. https://brasil.elepaais.com/brasil/2018/10/02/politica/1538508720_526769.html (accessed Feb 2022)
99. CEBDS (2019) Nota sobre a Amazônia. <https://cebds.org/nota-do-cebds-sobre-a-amazonia/#.Y1cKdHbMJPb> (accessed Feb 2022)
100. Alencar, C., Andrade, H. D. (2022) ‘Mais importante é o agronegócio’, diz Bolsonaro sobre proteção da Amazônia. UOL Notícias. <https://noticias.uol.com.br/eleicoes/2022/08/26/jair-bolsonaro-entrevista-panico-amazonia-agronegocio.htm> (accessed Feb 2022)
101. Poder360 (2021) Governo tem menor número de multas por crimes ambientais em 20 anos. <https://www.poder360.com.br/governo/governo-tem-menor-numero-de-multas-por-crimes-ambientais-em-20-anos/> (accessed Feb 2022)
102. A Lavoura (2020) Agronegócio cobra do governo medidas contra o desmatamento. <https://alavoura.com.br/meio-ambiente/protecao-ambiental/mais-de-200-representantes-do-agronegocio-apresentam-ao-governo-medidas-de-combate-ao-desmatamento/> (accessed Feb 2022)
103. Fellet, J. (2021) ‘Brasil precisa parar de anistiar irregularidades’, diz líder de empresários do agronegócio. BBC News Brasil. <https://www.bbc.com/portuguese/brasil-56938760> (accessed Feb 2022)
104. Barbosa, M. (2020) US\$ 50,9 bilhões saíram do mercado financeiro brasileiro em 12 meses. Correio Braziliense. https://www.correiobraziliense.com.br/app/noticia/economia/2020/06/24/internas_economia,866513/us-50-9-bilhoes-sairam-do-mercado-financeiro-brasileiro-em-12-meses.shtml (accessed Feb 2022)
105. Moura, J. (2020) Risco ambiental faz Brasil receber menos recursos de estrangeiros, diz Campos Neto. Folha de São Paulo. <https://www1.folha.uol.com.br/mercado/2020/10/risco-ambiental-faz-brasil-receber-menos-recursos-de-estrangeiros-diz-campos-neto.shtml> (accessed Feb 2022)
106. TerraBrasilis (n.d.) TerraBrasilis | PRODES (Desmatamento). http://terrabrasilis.dpi.inpe.br/app/dashboard/deforestation/biomes/legal_amazon/rates (accessed Feb 2022)
107. Viola, E., Franchini M. A. (2019) Myths and images in global climate governance, conceptualization and the case of Brazil (1989 - 2019). *Revista Brasileira de Política Internacional*, 62(2), 1–21. <https://doi.org/10.1590/0034-7329201900205>
108. Vieira, M. A. (2013) Brazilian Foreign Policy in the Context of Global Climate Norms. *Foreign Policy Analysis*, 9(4), 369–386. <http://www.jstor.org/stable/24910821>
109. Gilly, L. (2018) Bolsonaro diz que quer acabar com ‘festa’ de multas do Ibama. G1. <https://g1.globo.com/rj/sul-do-rio-costa-verde/noticia/2018/12/01/bolsonaro-participa-de-formatura-de-cadetes-na-academia-militar-das-agulhas-negras.html> (accessed Feb 2022)
110. Londoño, E., Friedman, L. (2018) Brazil Backs Out of Hosting 2019 Climate Change Meeting. The New York Times. <https://www.nytimes.com/2018/11/28/world/americas/brazil-climate-meeting.html> (accessed Feb 2022)
111. DW (2019) Bolsonaro: Germany can learn ‘a lot’ from Brazil about environment. <https://www.dw.com/en/bolsonaro-germany-can-learn-a-lot-from-brazil-about-environment/a-49384095> (accessed Feb 2022)
112. Fernandes, T., Maisonnave, F. (2018) Norway Should Learn With Brazil How To Save The Environment, Says Bolsonaro’s Chief Of Staff. Folha de São Paulo. <https://www1.folha.uol.com.br/internacional/en/brazil/2018/11/norway-should-learn-with-brazil-how-to-save-the-environment-says-bolsonaros-chief-of-staff.shtml> (accessed Feb 2022)
113. The Guardian (2021) Bolsonaro slashes Brazil’s environment budget, day after climate talks pledge. <https://www.theguardian.com/world/2021/apr/24/bolsonaro-slashes-brazils-environment-budget-day-after-climate-talks-pledge> (accessed Feb 2022)
114. Brant, D., Machado, R. (2020) Apesar de incêndios, governo corta orçamento do Ibama e ICMBio em 2021. Folha de São Paulo. <https://www1.folha.uol.com.br/ambiente/2020/09/apesar-de-incendios-governo-corta-orcamento-do-ibama-e-icmbio-em-2021.shtml> (accessed Feb 2022)
115. Camargo, S. (2020) Prosecutors target Brazil’s environment minister over dismantling of protections. Mongabay. <https://news.mongabay.com/2020/07/prosecutors-target-brazils-environment-minister-over-dismantling-of-protections/> (accessed Feb 2022)
116. Daley, J. (2019) Brazil’s Sacked Space Director Speaks Out on Attacks on Science. Scientific American. <https://www.scientificamerican.com/article/brazils-sacked-space-director-speaks-out-on-attacks-on-science/> (accessed Feb 2022)
117. Paes, C. F. (2019) Brazil’s Roraima state at mercy of 2019 wildfires as federal funds dry up. Mongabay. <https://news.mongabay.com/2019/06/brazils-roraima-state-at-mercy-of-2019-wildfires-as-federal-funds-dry-up/> (accessed Feb 2022)
118. Poder360 (2020) Governo corta verba. Ibama e ICMBio podem ficar sem gasolina. <https://www.poder360.com.br/governo/governo-corta-verba-ibama-e-icmbio-podem-ficar-sem-gasolina/> (accessed Feb 2022)

ABOUT STUDENT AUTHOR

Pedro Eymael studied International Relations and Political Science at the Getulio Vargas Foundation, São Paulo, Brazil. He obtained his bachelor’s degree in December 2022 and plans to pursue a graduate degree in the United States.

PRESS SUMMARY

Devastating forest fires in Brazil’s Amazon rainforest have captured the world’s attention in 2019 and 2020. Within this context, institutional investors threatened to divest from companies potentially linked to the wildfires and to sell government bonds, creating a divestment movement. This article shows that the Brazilian president Jair Bolsonaro’s responses varied for each of the groups criticizing the handling of the environmental situation. It argues that the Brazilian government adopted a more conciliatory

tone and took more concrete actions when responding to institutional investors' demands, compared to the responses for foreign governments and NGOs. Based on fifteen interviews conducted during the second half of 2021 with professionals involved in this divestment case, the paper concludes that institutional investors played a key role in Bolsonaro's winning coalition and electoral aspirations. Moreover, the shortage of financial capital due to the COVID-19 pandemic created further incentives for Bolsonaro to avoid conflicts with institutional investors.

Using Coral Color to Indicate Coral Health in Five Caribbean Species

Gabriella Herrera^a, Alexandra M. Good^b, Alexander Hirota^b, Catherine Razak^c, Nicole Gaertner^b, Justin Sefcik^b, Jesse Gilbert^b, & Keisha D. Babr^a

^a Department of Life Sciences, Texas A&M University-Corpus Christi, Corpus Christi, TX 78413

^b Texas State Aquarium, Corpus Christi, TX 78402

^c Cincinnati Zoo and Botanical Garden, Cincinnati, OH 45220

<https://doi.org/10.33697/ajur.2023.077>

Student: gabriellaber831@gmail.com*

Mentor: keisha.babr@tamucc.edu

ABSTRACT

Coral reefs are one of the most biodiverse and productive ecosystems on Earth, and color has been shown to indicate coral health in Australian and Hawaiian reef systems. However, no standardized method exists to quantify coral health for Caribbean corals. Therefore, a health assessment card using coral color was developed for five species of Caribbean corals to monitor coral health non-invasively. To quantify coral health, individual corals of each species were photographed in a controlled environment to develop color profiles. Simultaneously, nondestructive measurements of “health” were quantified by measuring photosynthetic efficiency (F_v/F_m) using pulse amplitude modulation (PAM) fluorometry, which determines how efficiently the symbiotic algae provides energy to the coral host. The results of this work successfully corresponded photosynthetic efficiency to coral color for five dominant species of Caribbean corals to develop a Coral Health Assessment Card for Caribbean reefs. Implementing a standardized assessment of symbiont performance can assist in monitoring changes in coral health, which can consequently be implemented into long-term and widespread monitoring projects to track overall Caribbean reef health.

KEYWORDS

Photosynthetic Efficiency, *Symbiodinium* spp., Coral Bleaching, Pulse-Amplitude Modulated Fluorometry, Health Assessment

INTRODUCTION

Coral reefs are one of the most biodiverse ecosystems in the ocean.¹ Nearly a quarter of all marine life depends on coral reefs at some point in their life cycle for various services, including shelter and food. Moreover, humans rely on reefs for their ecosystem services (e.g., fishing, tourism, coastal protection, economies),² and they also serve as a significant source of protein for more than half a billion people.³ Coral reefs are also natural barriers from waves and effectively protect tropical coasts and reef islands.⁴ However, coral reefs are declining rapidly, threatening marine biodiversity, local and global economies, communities, coastlines, and islands.² Therefore implementing rapid and effective reef management tools is key to the longevity of coral reefs by providing more information regarding the health of reefs and directing management efforts.⁵

Corals and their reefs thrive in oligotrophic waters because of their mutualistic symbiotic relationship with dinoflagellate algae symbionts (i.e., *Symbiodinium* spp.).⁶⁻⁸ *Symbiodinium* spp. reside in the coral tissue, providing color to the coral along with a large portion of their energy requirements (up to 90%), allowing corals to thrive in these nutrient-poor waters.⁹ The symbiotic relationship between corals and their symbionts may be disrupted by environmental changes (e.g., warming waters, eutrophication, acidification, etc.).^{7,10,11} This disruption is often evidenced by a loss of symbionts and, as a result, is accompanied by a loss of color or significant paling in the coral host.^{9,10} This process is known as ‘coral bleaching’ because the coral tissue becomes translucent, revealing the white coral skeleton.¹¹ A prolonged bleaching state can lead to partial or complete coral mortality,^{8,10} reduced or delayed reproduction,^{9,10} reduced calcification,¹¹ and a decreased ability to resist the invasion of competing species and diseases.¹¹ Due to the loss of color in the coral tissue, coral color can be considered a visual indicator of coral stress.^{13,14}

Since the presence of *Symbiodinium* spp. is imperative for coral health, it is important to understand the symbionts’ health and symbiosis with corals. The photosynthetic pigments of algae may decline up to 80% during periods of stress, directly influencing their photosynthetic capacity and efficiency.¹² Pulse-Amplitude Modulation Fluorometry (PAM) is a rapid, effective, and non-invasive way to quantify photosynthetic efficiency, which has been instrumental in understanding *Symbiodinium* spp. and coral holobiont health.¹⁴⁻¹⁸ For example, PAM can be used to generate a saturation pulse quenching analysis, which measures the efficiency of photosystem II,¹⁵ a minimum and maximum fluorescence value from a rapid light curve (RLC) to quantify photosynthetic efficiency from the maximum quantum yield (F_v/F_m),¹⁹ or the electron transport rate (ETR) from

photosynthetically active radiation (PAR).¹⁹ These photosynthetic analyses can be performed non-invasively on live corals and are highly indicative of the overall health and function of photosynthesis, thereby providing a health assessment of corals and their symbionts. For this study, health is defined by the photosynthetic efficiency (F_v/F_m) of the algal symbiont, *Symbiodinium* spp., which provides the coral host approximately 90% of the energy it needs to survive.⁹

Due to the rapid decline of coral reefs globally, it is crucial to understand the health of the coral holobiont for successful intervention. Coral reef health assessments are instrumental for understanding the effects of stressors facing coral reefs,²⁰ for example, over-harvesting, pollution, disease, and climate change.³ However, it is challenging to quantify coral health rapidly and non-invasively.²¹ Ongoing monitoring is often costly and labor-intensive, making traditional methods unsustainable.¹³ Traditional assessment methods, like the coral reef health index in Sangiang Island, Indonesia, require comprehensive data, time, and high levels of scientific experience.²⁰ Additionally, utilizing PAM fluorometry alone to quantify coral health is unrealistic due to the cost and time associated with the measurements.^{5,21} For rapid, accessible assessment to inform management, coral color can be linked with quantitative measurements from PAM fluorometry to provide a visual indicator for coral health.

Color has been linked to PAM fluorometry measurements via symbiont density in previous studies from Australia and Hawai‘i.^{5,13} A color card is a tool designed to track the coral symbionts’ photosynthetic capabilities over time using visual assessments of coral reefs. The color card can be held up to a coral to understand its health. The Coral Watch Chart uses a six-point color scale designed for Indo-Pacific reefs.¹³ The Hawai‘i Ko‘a card uses a 35-point color scale to detect changes in symbiont density in Hawaiian corals.⁵ Both cards have helped guide local management strategies,^{5,13} but coral species differ between regions. Those color cards were developed to track and monitor bleaching in Indo-Pacific and Hawaiian reef systems, but a color card has not been developed for Caribbean species. Coral pigmentation and zooxanthellae characteristics can vary by region due to species composition and water quality differences.⁵ Therefore, a tool designed specifically for Caribbean species and their respective pigmentations is necessary for the success of efforts to manage coral reefs in the region. This card can be used for Caribbean corals in the wild or captivity. The Hawai‘i Ko‘a card and Coral Watch Chart were designed for corals in the wild. However, the Caribbean coral card was designed in collaboration with Texas State Aquarium, monitoring coral wellness in captivity. To support management efforts, a coral color card was developed for five Caribbean species in collaboration with Texas State Aquarium (TSA); the card drew inspiration from Coral Watch Chart and the Hawai‘i Ko‘a card. Implementing the Caribbean color card into management and wellness programs can benefit Caribbean corals and be a valuable educational tool. This tool can also be incorporated into coral monitoring programs, allowing for standardized, rapid, and non-invasive monitoring of coral health in the Caribbean over time. This tool provides valuable information at ease to reverse the effects of local and global climate change in one of the most biodiverse ecosystems in the world.

METHODS AND PROCEDURES

Phase 1: Card Development

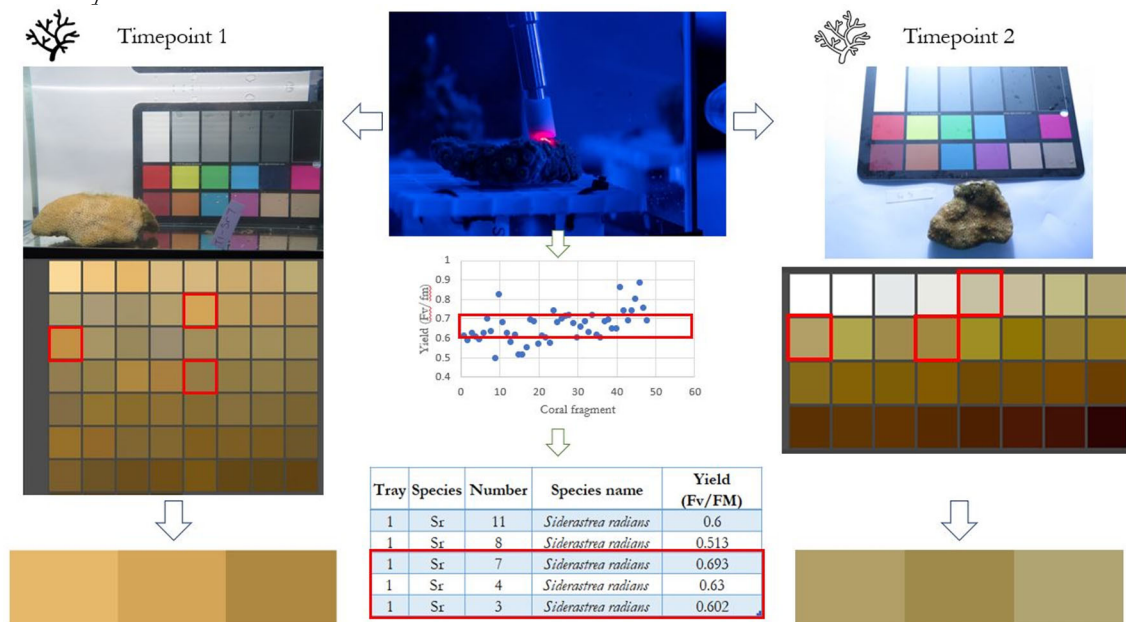


Figure 1. A flow chart showing Phase I of the methods outlined. Phase I was conducted at two time points: Timepoint 1 (Fall 2020) and Timepoint 2 (Fall 2022). Each time point followed the same order: PAM measurements were taken, corals were photographed, and images were processed in Photoshop to produce a color swatch.

Coral Husbandry

The coral species used in this study were *Siderastrea radians*, *Acropora palmata*, *Acropora cervicornis*, *Solenastrea bournoni*, and *Porites* spp. (N=5 species). Most species were acquired from the reefs in the Florida Keys National Marine Sanctuary (FKNMS-2017-041 to Texas State Aquarium).

The data collection was split into two time points: Timepoint 1 (Fall 2020), when the corals appeared healthy, and Timepoint 2 (Fall 2022) when the corals appeared unhealthy with paling coloration. In Fall 2020, corals were kept in stable and optimal growth conditions on a nursery table (318 L). Water parameters were held at optimal conditions for coral growth. The corals received a constant irradiance level (210-120 Watts m⁻²) on a 12 h on-off schedule (Al Hydra 52 LEDs). Raw seawater from Corpus Christi Bay feeds the water table, and water conditions were held at optimal salinity (34 ppt), temperature (25°C), and pH levels (8.0-8.2). However, in the Fall of 2022, a significant amount of algae grew in the nursery table, and corals appeared pale and bleached. Due to inadequate water quality testing at TSA, the water conditions were not recorded; however, it appeared to be unfavorable conditions for coral growth.

Coral Photobiology

The research approach and methodology followed similar methods developed by Siebeck et al.,(2008) and Bahr et al. (2020) for the Coral Watch Chart and Hawai'i Ko'a card, respectively. Rapid light curves (RLC) were conducted on corals using a diving-PAM (V2, Walz GmbH, Effeltrich, Germany) on each coral fragment to measure the photosynthetic efficiency (F_v/F_m) of the symbiotic algae. RLCs measure the effective quantum yield (F_v/F_m) as a function of irradiance.¹⁵ The yield shows the algae reaction to a range of light levels.¹⁵ PAM uses three types of lights: weak measuring light, saturating pulse, and actinic light.¹⁹ The weak measuring light determines the proportion of closed PSII reaction centers and finds the minimum fluorescence; the saturating pulse closes all PSII reaction centers to find the maximum fluorescence.¹⁹ Saturating pulse is used to understand the photosynthetic activity, and actinic light induces photosynthesis.¹⁹ Photosynthetic efficiency can be quantified from the maximum quantum yield (F_v/F_m), which is the minimum and maximum fluorescence value.¹⁹

Selected coral fragments (N=34) were removed from the seawater tables, placed in a small 2-gallon holding tank, and placed in a dark environment for at least a 20-minute acclimation. Dark acclimation allows all chlorophyll reaction centers to close for optimal fluorescence measurements.²² Corals were aerated with battery-powered bubblers during dark acclimation. The diving-PAM was connected to a PC running WinControl software (version 3.25) and was fitted with a red light-emitting probe (470 nm, LED, 0.05 $\mu\text{mol photons m}^{-2}\text{s}^{-1}$, 5 Hz). Rubber surgical tubing was attached to the probe to allow measurements at a consistent distance for each coral and prevent damage to the probe and coral.

Individual corals were separated by a black partition in the acclimation tank for each RLC to prevent photosystems in non-target fragments from reacting to the strong saturating light pulse and the increasing actinic light emitted from the PAM during measurements. RLCs were performed at two unique points and a 90° angle to each coral fragment. The first probe location was selected in the dark, with subsequent locations as far from the previous as possible. This was necessary to avoid photosystem activation in areas adjacent to the probe. The mean value of the two F_v/F_m measurements was used for analysis. The change in F_v/F_m between the two time points for each species was analyzed in RStudio 4.2.2 using a paired t-test (Fig. 3).

Coral Color

The color of each coral was documented as photographic images in a controlled environment. Coral fragments were placed in aquaria filled with clean seawater immediately after PAM measurements for photographing. A digital camera (Canon G16) and an external flash mounted on a stationary stand were used to evenly illuminate and photograph each coral specimen while keeping a fixed distance and angle. Camera parameters were manually set and kept consistent across all images. Camera parameters were set at mode: M, aperture: 8, ISO: 80, and white balance: auto. Flash settings were set at mode: M and power: 1/8. A commercial underwater color reference card (DGK Color Tools WDKK Waterproof Color Chart) was placed on the back wall of the aquaria for color balancing in Adobe Photoshop CS5. Three to five images per species were selected for processing in Adobe Photoshop CS5. All images were preserved as raw image files in DNG format to retain the camera sensor's full resolution while minimizing information loss. Preserved DNG raw image files were balanced to white (90% reflectance) and neutral (gray, 18% reflectance) in Adobe Photoshop CS5 using DGK color Tools WDKK Waterproof Color Chart captured in an image as references. The histogram function allowed evaluation of the distribution of RGB values representing white and neutral to maintain constant values while avoiding over-exposure of images. Images were then converted into TIFF format for subsequent processes of color indexing and selection to establish relationships between the colors of photographs and coral fragments. Each image was white, grey, and black balanced using the curves adjustment. A represented surface area of each coral fragment was outlined, ensuring the selected area did not have shadows, bubbles, or areas of discoloration. A color table was then produced in Adobe Photoshop CS5, and the ten most frequent colors from each area were selected and saved as a color table file with .act extension, which saved

the numerical color values, such as RGB, CMYK, and HSB (hues, saturation, and brightness) (Fig. 2). These methods followed those outlined in Bahr et al., 2020.

A color swatch was produced for each species for each time point (i.e., Fall 2020 and Fall 2022). These colors represent the most frequently observed colors that best represent each fragment of the species (Table 1). A range of healthy colors was chosen to account for morphological and spatial variation in color, as bleaching is not typically a uniform response.¹² The colors from Fall 2020 are considered “healthy” and those from Fall 2022 were considered “unhealthy” colors. The colors were then oriented in a light-to-dark gradient to dark to increase ease of use.


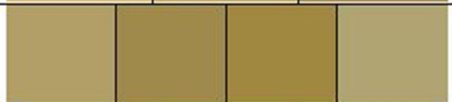
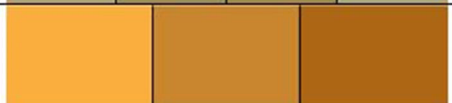


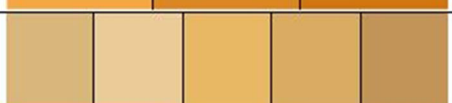
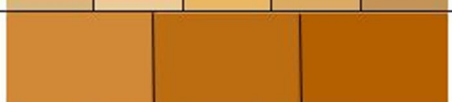
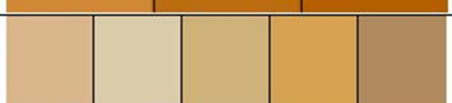
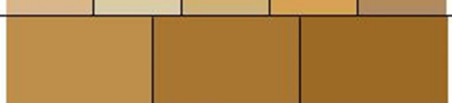
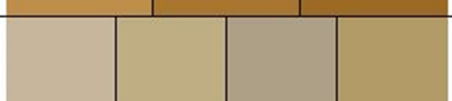
Species	Timepoint	Average F_v/F_m ± SE	Representative Colors
<i>Siderastrea radians</i>	Fall 2020 (N=3)	0.606 ± 0.007	
	Fall 2022 (N=3)	0.577 ± 0.012	
<i>Acropora palmata</i>	Fall 2020 (N=3)	0.455 ± 0.034	
	Fall 2022 (N=3)	0.454 ± 0.029	
<i>Acropora cervicornis</i>	Fall 2020 (N=5)	0.5698 ± 0.04	
	Fall 2022 (N=5)	0.463 ± 0.018	
<i>Solenastrea bournoni</i>	Fall 2020 (N=3)	0.658 ± 0.021	
	Fall 2022 (N=3)	0.582 ± 0.02	
<i>Porites species</i>	Fall 2020 (N=3)	0.527 ± 0.047	
	Fall 2022 (N=3)	0.309 ± 0.019	

Table 1. Detailed information regarding coral species, time point (Fall 2020 or Fall 2022), number of fragments sampled, average quantum yield (F_v/F_m) for all fragments, standard deviation, and the color swatch produced to represent the species.

Phase 2: Card Validation

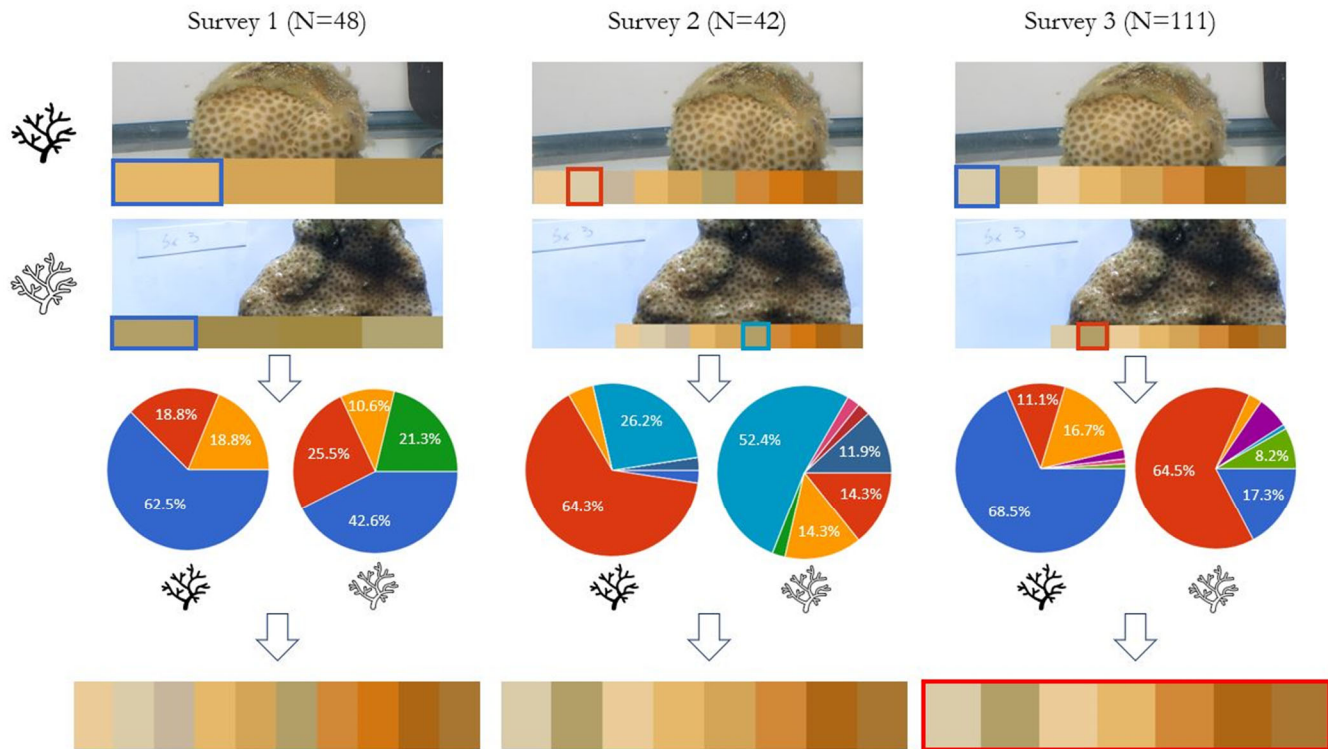


Figure 2. A flowchart showing Phase II methods process for final color card selection following three external surveys. N represents the number of observers for each survey. The pie charts represent the percentage of observers who agreed on a single color for each coral fragment pictured. The highlighted colors show which color was perceived the most for each survey. The results of each survey were used to make the final color swatch.

Quantitative Analysis

The color selection followed a quantitative and qualitative process to represent the five species using a seven-color range. For the quantitative analysis, the PAM measurements from each coral were used to find the mean quantum yield value for each species at both time points (*i.e.*, Fall 2020 and Fall 2022). The F_v/F_m values were compared across all individuals, and the three fragments from each species that best fit the mean quantum yield were selected for color analysis, as they best represented the entire species. A range of 3-5 colors was selected from the color table produced by Adobe Photoshop CS5 (Table 1), and the F_v/F_m values of the selected fragments were correlated to the corresponding color. The color values produced by the images of the coral species from Photoshop were compared with the color values on the card as the expected color values (card) compared to actual color values (coral colors from Photoshop) (Fig. 4).

Qualitative Analysis

The qualitative analysis consisted of four surveys to assess the colors of 31 corals from five species. A photograph of the swatch was placed alongside photographs of each coral on the same computer screen. Each observer independently determined the best representative color for each coral, avoiding the tips and edges of the coral. Other parameters were collected from the observers to help explain variation, including age, gender, coral familiarity, and the highest level of education. Observers were not trained before taking the survey and came from all different backgrounds (*i.e.*, ages, experience levels, educational backgrounds, etc.). The surveys were anonymous, so it is unknown how many repeat observers there were across four surveys. However, each survey was shared and communicated with similar audiences, so we assume there were repeat observers across the surveys.

Survey one (N=48 observers) had 3-5 colors specific to each individual from each species at each time point. The ten colors selected the most were used to make a swatch representing all five species. Survey two (N=42 observers) assessed the ten colors alongside all 30 coral fragments, allowing survey three (N=111 observers) to test eight colors by removing the two least selected colors. The final color swatch used all survey data to produce a 7-color card representing both time points. Survey four (N=26 observers) assessed the final color card with 14 fragments that showed disagreement among all three surveys to ensure the narrowed-down color card accurately represented all variations in pigmentation and observation (Fig. 2).

RESULTS

Quantitative Validation

Coral Photobiology

The PAM measurements show relatively healthy photosynthetic efficiency (F_v/F_m) with a low standard deviation. Table 1 shows all the individuals across the five species tested at each time point. At Timepoint 1, the average yield across species ranged from 0.52-0.65; and at Timepoint 2, the average yield ranged from 0.30-0.58 (t-test: $p < 0.001$). *Porites* spp. displayed the lowest yield (0.527 ± 0.047 and 0.309 ± 0.019) at both time points, and *S. bournoni* displayed the highest yield at both time points (0.658 ± 0.021 and 0.582 ± 0.02). This analysis of the photosynthetic efficiency by time point was correlated with the colors of the corals at that time point so that each species had a 3-5 color swatch for each time point (Table 1). For further analysis of coral color, five individuals from Timepoint 1 were chosen for analysis, so there was evenness across the time points. All species except *A. palmata* ($p = 0.4877$) significantly declined in photosynthetic efficiency between time points (t-test: *A. cervicornis* $p < 0.05$; *S. radians* $p < 0.01$; *Porites* spp. $p < 0.001$; *S. bournoni* $p < 0.01$) (Fig. 3).

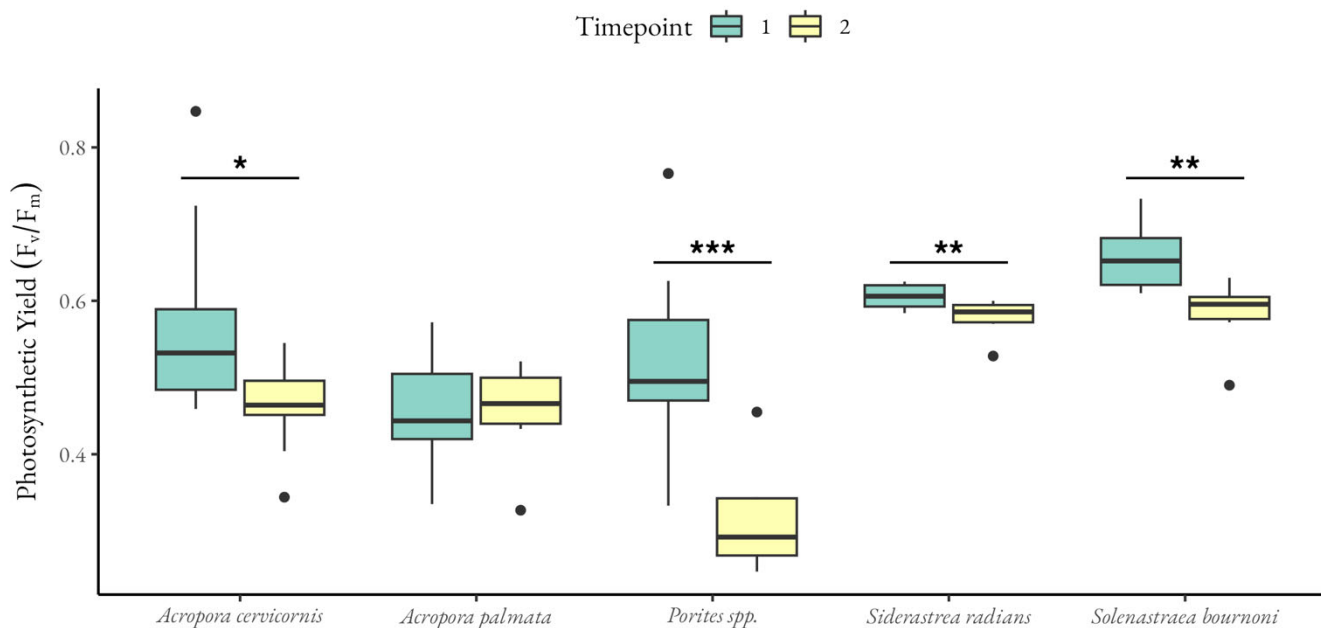


Figure 3. Box plot of the photosynthetic efficiency (F_v/F_m) measured by PAM by species across the two time points (Fall 2020 and Fall 2022). Lower and upper box boundaries represent the 25th and 75th percentiles, the line inside the box represents the median, and the lower and upper error lines represent the 10th and 90th percentiles. The filled circles represent data falling outside the 10th and 90th percentiles. Asterisks represent significance from paired t-tests using RStudio 4.2.2

Coral Color

The final seven colors in the card were correlated to the subset of 31 individuals tested. Photosynthetic yield (F_v/F_m) strongly correlated to color with reasonable variation. High variation was observed in color 1 because unhealthy *Porites* spp. and healthy *S. radians* well represent this color. In this case, this color health metric is species-specific, and the card should be further developed with a morphological key to determine which species is being measured. Photosynthetic yield also correlated with color, with darker colors generally having higher yield (Fig. 4A).

Following this, the color from the image of the coral extracted from Photoshop correlated to the color on the color card. Red, Green, and Blue (RGB) values and hue, saturation, and brightness (HSB) values were calculated for the colors on the card, and the five most representative colors from the corals were generated in Photoshop (Fig. 1). Colors 2, 4, 6, and 7 matched most closely for both the RGB and HSB values, while 1, 3, and 5 had slightly lower values from the images as compared to the card; however, all image values trended towards the card values. For example, colors 6 and 7 had the lowest RGB values for the images and the card (Fig. 4B) and lower brightness with higher saturation for both the images and the card (Fig. 4C).

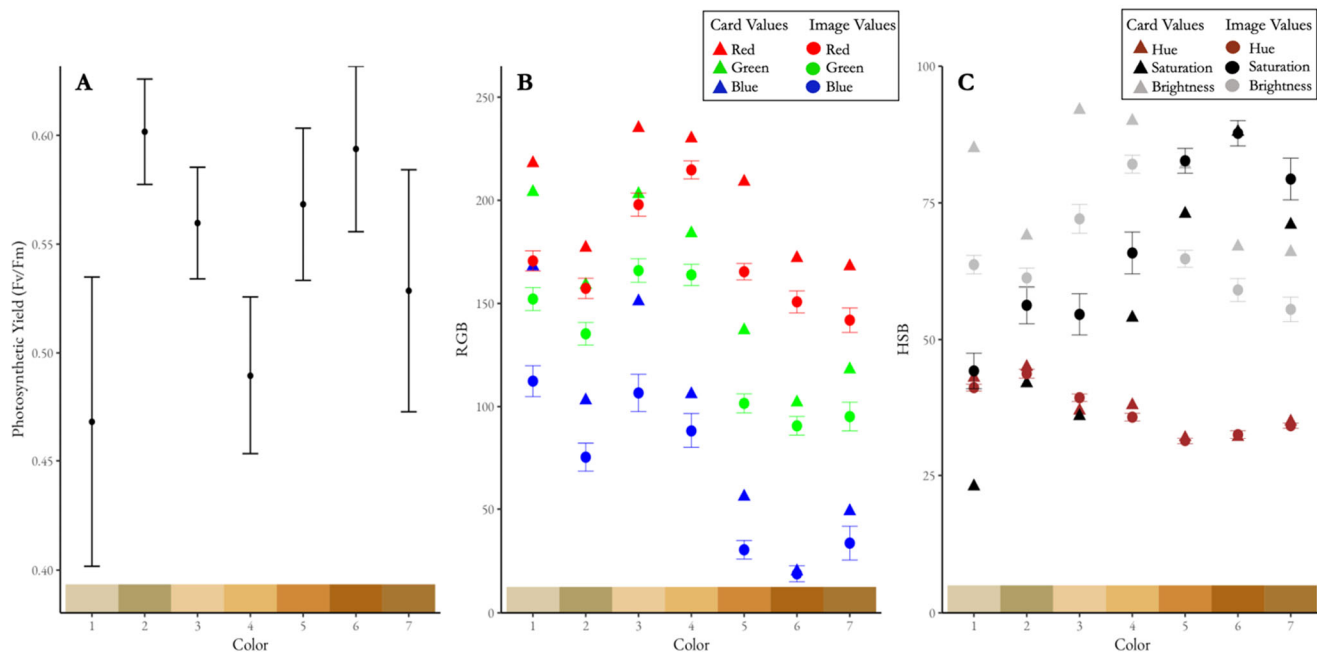


Figure 4. The seven colors (1 (n=6), 2 (n=6), 3 (n=5), 4 (n=5), 5 (n=8), 6 (n=6), 7 (n=5)) (n=number of individuals) of the final color card correlated to the corresponding coral’s photosynthetic yield (A), red, green, blues (RGB) values (B), and hue, saturation, and brightness (HSB) values (C). The triangles represent the actual RGB and HSB values, and the circles represent the mean coral RGB and HSB values with standard error (SE) depicted with error bars.

Qualitative Validation

Four successive surveys were developed to validate the colors for the color card and quantify observer variation. A photograph of the color card was placed alongside photographs of each coral, and the observer independently determined the best representative color for each coral. Observers for each survey ranged from ages 18 to 64, representing diverse education and coral experience levels. Survey one had 48 participants observe between three to five colors specific to each species (n=3) at each time point (Table 1). The results of this survey narrowed down which colors were well-represented the most for each species. Results showed >50% observer agreement on a representative color for 23 of 31 corals. These results were used to develop a 10-color-swatch for the second survey. There was >50% agreement on a single color for 64.5% of fragments. Five fragments had a close split between two colors, and the other six showed no agreement, leading to a reassessment of colors. For survey three, two colors were removed because these colors were shown not to be well represented by the corals in survey 2. The colors were re-oriented to maximize differences in pigmentation between colors for ease of use. If colors 1 and 3 were often selected together for a fragment, they were placed next to each other to show the differences in pigmentation. This survey showed general agreement between over 100 participants, with a few exceptions. Survey two showed 83.9% of corals received >40% agreement, and 64.5% received >50% agreement for a single color. Survey three showed 87.1% of corals received >40% agreement, and 54.8% received >50% agreement from all observers. Therefore, it was observed that removing two colors from survey three did not change the agreement between observers and made the final card more accurate. It is assumed that for some species like *S. radians* and *A. palmata*, high observer variation was caused by a difference in the coloration between the conosarc and polyps. For those two species, differences in color across the individual caused observer variations in the surveys. However, other species like *A. cervicornis* and *Porites* spp. did not have observer variation (>50% agreement), as the individuals had uniform coloration. The final 7-color card was created from the results of surveys two and three. Survey four tested the final color card, but only the 14 corals that showed the most observer variation were used. Survey four justified 85.7% of corals received >40% agreement, and 57.1% received >50% agreement. This final survey was conducted to clarify any discrepancies in color agreement. The corals that already had >50% agreement were omitted. The results of each survey showed that agreement among observers stayed the same as colors were removed.

DISCUSSION

This study successfully created a 7-color card for five key Caribbean coral species. As evidenced by the data in this study, there was a visual decline in photosynthetic yield (F_v/F_m), which correlated with a notable color change. Lighter colors primarily represented lower F_v/F_m; however, some colors, like 1 and 7, represented more extensive F_v/F_m ranges because of numerous species matching with that color (Fig. 4A). The colors on the card also successfully matched the RGB (Fig. 4B) and HSB (Fig. 4C)

values of the coral photos. These correlations between photosynthetic efficiency and color scales help to validate the method used to develop the color card.

With further development, this card could be used for coral health monitoring surveys in the Caribbean, from large-scale remote sensing²³ to smaller-scale citizen science projects.⁵ During this study, we noted some limitations and biases with the experimental method; one such limitation was having too few replicates in our samples. To overcome this, future studies should have a larger sample size with more replicates to avoid the discrepancies seen in this study. The number of corals indicated by our card was limited by the number of coral species available at the Texas State Aquarium (TSA). Another limitation is the subjectivity of color. Color as an indicator of health is subjective as people perceive color differently, which should be considered when using the card for data collection.

The color card should not be used as a stand-alone tool but in collaboration with other health assessment techniques. Nevertheless, the Caribbean color card developed in this study currently only represents five species, and more species should be added to reflect Caribbean coral reef assemblages. Similar to the Hawaiian Ko'a card, a key should be included to decipher the different morphologies among species. A key could sufficiently help users determine the meaning of the color based on the species since one color may represent the health of various species differently. For example, high variation was observed in color 1 because unhealthy *Porites* spp. and healthy *S. radians* represent this color well, and having a morphology key would clarify which species the color is associated with. Additionally, this study could not perform any experimental tests for chlorophyll or symbiont extractions because of the Association of Zoos and Aquariums (AZA) animal wellness expectations to maintain coral health, limiting the extent of the study. Since experimental data could not be collected, the card does not show the stages of bleaching. However, studies have shown that PAM fluorometry measurements capture damage to photosystem II and the underlying physiological collapse of the symbiont regardless of bleaching.¹⁷ Regarding the PAM measurements, two rapid light curves were conducted for each coral fragment and averaged to extrapolate the health of the coral from a point-based measurement. There may be some limitations and biases in two points reflecting the individual's overall health. Subsequent studies should include more experimental data to better understand physiology and how environmental changes affect coral health in aquaria and the field. Aside from coral reef health assessments in the field, color cards could also be used in the zoo and aquaria trade. For example, the AZA carefully evaluates zoos and aquariums to ensure they meet animal welfare, care, and management standards.²⁴ Animal care is defined as excellent animal husbandry procedures that ensure excellent animal health and welfare.²⁴ The color card could supplement existing or new AZA-accredited zoos and aquariums standard practices by implementing a way to diagnose, manage, and track coral health in captivity. The card could also be used as an interactive educational tool for public engagement to illustrate the effects of coral bleaching and how climate change affects marine ecosystems. Existing education tools and resources have been designed to cover a wide range of topics related to coral reefs, such as the many lesson plans available for K-12 classrooms.²⁵⁻²⁷ But there has been an effort to make coral educational tools more interactive and hands-on through 3D Coral Polyp Models and art projects.²⁵⁻²⁸ Therefore, implementing this color card in aquariums and zoos could feasibly provide an engaging and educational coral exhibit for the general public.

CONCLUSION

Understanding coral health is critical for the success of coral reefs under our changing climate. Coral reefs are one of the most biodiverse ecosystems on Earth, supporting roughly 25% of all marine life and billions of humans through food, income, and coastal protection. However, corals are in decline due to human-induced environmental change. Therefore, it is essential to monitor coral health to conserve a valuable marine ecosystem and protect marine biodiversity. Coral reefs in the Caribbean face the synergistic threat of climate change and disease (*e.g.*, stony coral tissue loss disease, white band disease).²⁹⁻³¹ The 7-color card created in this study provides an objective tool to monitor and assess the coral health of 5 key coral species in this region non-invasively. This tool was created by correlating changes in photosynthetic efficiency (F_v/F_m) to changes in coral color. A color card, such as the one created in this study, can be an effective way to implement a visual assessment of the health of corals in captivity. Developing an objective, science-based tool also helps support local and global efforts to monitor the effects of climate change and disease on coral reefs. Individual color cards should be developed as place-based tools to support global efforts since coral species and *Symbiodinium* clades differ between regions.

The next steps for this study are to assess more healthy corals to represent species diversity in the Caribbean and more non-healthy corals to expand the color card to monitor bleaching events. The best way to do this would be through experimental data in the lab that would represent a greater variation of health for the species on the color card. Ultimately, more corals must be assessed to fully understand the Caribbean species' coral color health metric. The color health metric is species-specific, so a morphological key must be added to determine what a given color means for each species. For the card to be used as a monitoring tool in the field, field studies would have to be conducted to validate that the data represents corals in their natural environment.

ACKNOWLEDGMENTS

This research was supported by the National Science Foundation Award No. HRD-1911375 and the Texas A&M University Division of Research and Innovation. We would like to thank the Texas State Aquarium for access to corals. A special thank you to Dr. Angela Richards Dona and Todd Kana for equipment support and guidance. We would also like to thank members of the Bahr Marine Ecology Lab (Kate Gomez-Rangel, David Armstrong, and Caleb Ramos) for their assistance and the coral reef community for providing feedback on selected colors during observer surveys. Additionally, we want to thank all anonymous survey participants. Finally, we would like to thank two anonymous reviewers for their valuable time and for providing feedback on this manuscript.

REFERENCES

1. Knowlton, N., Brainard, R.E., Fisher, R., Moews, M., Plaisance, L., and Cailey M.J. (2010) Coral reef biodiversity, in: *Life in the World's Oceans: Diversity, Distribution, and Abundance* (McIntyre, A., Ed.) 65–76, Blackwell Publishing Ltd.
2. Castro, P., and Huber, M.E. (2010) Marine Biology, P. Castro and M. E. Huber, Marine Biology (8th eds). McGraw Hill Comp., NY, 2010.
3. Bellwood, D.R., Hughes, T.P., Folke, C., and Nystrom, M. (2004) Confronting the coral reef crisis. *Nature* 429, 827–833. <https://doi.org/10.1038/nature02691>
4. Harris, D.L., Rovere, A., Casella, E., Power, H., Canavesio, R., Collin, A., Pomeroy, A., Webster, J.M., and Parravicini, V. (2018) Coral reef structural complexity provides important coastal protection from waves under rising sea levels. *Sci Adv* 4(2). <https://doi.org/10.1126/sciadv.aao4350>. NOAA, Coral reef ecosystems. National oceanic and atmospheric administration, <https://www.noaa.gov/education/resource-collections/marine-life/coral-reef-ecosystems> (accessed Dec 2022)
5. Bahr, K., Severino S., Tsang, A., Han, J., Dona, A., Stender, Y., Weible, R., Graham, A., McGowan, A.E., and Rodgers, K.S. (2020) The Hawaiian Ko'a Card: coral health and bleaching assessment color reference card for Hawaiian corals. *SN Appl. Sci.* 2, 1–15. <https://doi.org/10.1007/s42452-020-03487-3>
6. Muscatine, L., and Porter, J.W. (1977) Reef corals: mutualistic symbioses adapted to nutrient-poor environments. *Bioscience*, 27(7), 454–460. <https://doi.org/10.2307/1297526>
7. Polovina, J.J. (1984) Model of a coral reef ecosystem. *Coral Reefs* 3, 1–11. <https://doi.org/10.1007/BF00306135>
8. Jokiel, P.L. (2004) Temperature stress and coral bleaching, in: *Coral Health and Disease* (Rosenberg, E. and Loya, Y., Ed.) 401–425, Springer, Berlin, Heidelberg. https://doi.org/10.1007/978-3-662-06414-6_23
9. Allemand, D., and Furla, P. (2018) How does an animal behave like a plant? Physiological and molecular adaptations of zooxanthellae and their hosts to symbiosis. *C. R. Biol* 341, 276–280. <https://doi.org/10.1016/j.crv.2018.03.007>
10. Hughes, T.P., Baird, A.H., Bellwood, D.R., Card, M., Connolly, S.R., Folke, C., Grosberg, R., Hoegh-Guldberg, O., Jackson, J.B.C., Kleypas, J., Lough, J.M., Marshall, P., Nyström, M., Palumbi, S.R., Pandolfi, J.M., Rosen, B., and Roughgarden, J. (2003) Climate change, human impacts, and the resilience of coral reefs. *Science* 301, 929–933. <https://doi.org/10.1126/science.1085046>
11. Baird, A.H., Bhagooli, R., Ralph, P.J., and Takahashi, S. (2009) Coral bleaching: the role of the host. *Trends in Ecology and Evolution. Cell Press* 24(1), 16–20. <https://doi.org/10.1016/j.tree.2008.09.005>
12. Glynn, P.W. (1996) Coral reef bleaching: facts, hypotheses, implications. *GCB* 2(6), 495–509. <https://doi.org/10.1111/j.1365-2486.1996.tb00063.x>
13. Siebeck UE, Logan D, and Marshall NJ. (2010) CoralWatch – a flexible coral bleaching monitoring tool for you and your group. Coral Reefs. Proceedings of the 11th International Coral Reef Symposium; 7–11 Jul 2008; Ft Lauderdale, FL. Dania Beach, FL: National Coral Reef Institute.
14. Warner, M.E., Lesser, M.P., and Ralph, P.J. (2010) Chlorophyll fluorescence in reef building corals, in: *Chlorophyll a Fluorescence in Aquatic Sciences: Methods and Applications. Developments in Applied Phycology, vol 4.* (Suggett, D., Prášil, O., Borowitzka, M., Ed.) 209–222, Springer, Dordrecht. https://doi.org/10.1007/978-90-481-9268-7_10
15. Ralph, P.J., Schreiber, U., Gademann, R., Kuhl, M., and Larkum, A. (2006) Coral photobiology studied with a new imaging pulse amplitude modulated fluorometer. *Phycological Society of America* 41(2), 335–342. <https://doi.org/10.1111/j.1529-8817.2005.04034.x>
16. Warner, M.E., Fritt, W.K., Schmidt, G.W. (1999) Damage to photosystem II in symbiotic dinoflagellates: a determinant of coral bleaching. *PNAS* 96(14), 8007–8012. <https://doi.org/10.1073/pnas.96.14.8007>
17. Warner, M.E., Berry-Lowe, S. (2006) Differential xanthophyll cycling and photochemical activity in symbiotic dinoflagellates in multiple locations of three species of Caribbean coral. *Journal of experimental marine biology and ecology* 339(1), 86–95. <https://doi.org/10.1016/j.jembe.2006.07.011>
18. Dellisanti, W., Chung, J.T.H., Chow, C.F.Y., Wu, J., Wells, M.L., Chan, L.L. (2021) Experimental techniques to assess coral physiology in situ under global and local stressors: current approaches and novel insights. *Front Physiol* 594(12). <https://doi.org/10.3389/fphys.2021.656562>
19. Ralph, P.J. and Gademann, R. (2005) Rapid light curves: a powerful tool to assess photosynthetic activity. *Aquatic botany* 82(3), 222–237. <https://doi.org/10.1016/j.aquabot.2005.02.006>

20. Idris, Putri A.R., Adiwijaya, C., Gilang, M., Santoso, P., Prabowo, B., Muhammad, F., Andriyani, W., Lestari, D.F., Setyaningsih, W.A. and Zamani, N.P. (2020) Assessment of coral reefs health in nature recreation park (TWA = taman wisata alam) Sangiang Island, Banten. *IOP Conf Ser: Earth Environ Sci* 429: 012020. <https://doi.org/10.1088/1755-1315/429/1/012020>
21. Miller, I., and Müller, R. (1999) Validity and reproducibility of benthic cover estimates made during broadscale surveys of coral reefs by manta tow. *Coral Reefs* 18, 353–356. <https://doi.org/10.1007/s003380050212>
22. Kautsky, H., and Hirsch, A. (1931) Neue Versuche zur Kohlensäureassimilation. *Naturwissenschaften*, 19, 964. <https://doi.org/10.1007/BF01516164>
23. Leiper, I.A., Siebeck, U.E., Marshall, N.J., Phinn, S.R. (2009) Coral health monitoring: linking coral color and remote sensing techniques. *Canadian Journal of Remote Sensing* 35(3), 276-286. <https://doi.org/10.5589/m09-016>
24. AZA, Animal management. Association of Zoos & Aquariums, <https://www.aza.org/animal-management> (accessed Dec 2022)
25. Living Oceans Foundation, Coral reef ecology curriculum. Khaled bin Sultan Living Oceans Foundation Coral Reef Ecology Curriculum, <https://livingoceansfoundation.org> (accessed Dec 2022)
26. NOAA, Background information. Coral reef information system, <https://www.coris.noaa.gov/activities/oa/welcome.html> (accessed Dec 2022)
27. National Geographic, Coral reefs, <https://education.nationalgeographic.org/resource/coral-reefs> (accessed Dec 2022)
28. NOAA, 3D printed model brings coral education to life. Coral reef conservation program, <https://coralreef.noaa.gov/education/polypmodel.html> (accessed Dec 2022)
29. Aronson, R.B., and Precht, W.F. (2001) White-band disease and the changing face of Caribbean coral reefs. *Hydrobiologia* 460, 25–38. <https://doi.org/10.1023/A:1013103928980>
30. Precht, W.F., Gintert, B.E., Robbart, M.L., Fura, R., van Woosik, R. (2016) Unprecedented disease-related coral mortality in Southeastern Florida. *Sci Rep* 6(31374). <https://doi.org/10.1038/srep31374>
31. AGRRA, Coral disease outbreak. Atlantic and Gulf Rapid Reef Assessment, <https://www.agrra.org/coral-disease-outbreak/> (accessed Dec 2022)

ABOUT STUDENT AUTHOR

Gabriella Herrera is an undergraduate student at Texas A&M University – Corpus Christi. She graduated with a Bachelor of Science in Biology in Fall of 2022.

PRESS SUMMARY

Coral reefs are one of the most biodiverse and productive ecosystems on Earth, and color has been shown as an indicator of health in Australian and Hawaiian reef systems. But there is no standardized method to quantify coral health for Caribbean corals. Therefore, a health assessment card using coral color to non-invasively monitor coral health was developed for five species of Caribbean corals. Nondestructive measurements of “health” were correlated with coral color pigmentation to develop a rapid, non-invasive tool for coral health monitoring. The results of this work successfully corresponded photosynthetic efficiency to coral color for five species of dominant Caribbean corals to develop a Coral Health Assessment Card for Caribbean reefs. By implementing a standardized assessment of coral health, long-term and widespread monitoring projects can be implemented to track overall Caribbean reef health. Consequently, the results of this work support global efforts to conserve marine ecosystems and protect biodiversity.

Synthesis and Palladium-Catalyzed Cross-Coupling of an Alkyl-Substituted Alkenylboronic Acid Pinacol Ester with Aryl Bromides

Shoma Mukai & Nathan S. Werner

Department of Physical Science, Southern Utah University, 351 W University Blvd, Cedar City, UT 84720, USA

<https://doi.org/10.33697/ajur.2023.078>

Student: moltegrazie22@gmail.com

Mentor: nathanwerner@suu.edu

ABSTRACT

The palladium-catalyzed cross-coupling reaction of alkyl-substituted alkenylboron reagents with aryl halides is a versatile method to introduce a hydrophobic hydrocarbon chain onto organic compounds of interest. The application of the cross-coupling reaction is enabled by synthetic methods for the preparation of alkenylboron reagents. The geometrically pure, alkyl-substituted alkenylboron reagent, (*E*)-octenylboronic acid pinacol ester, was prepared by 9-BBN-catalyzed hydroboration reaction of 1-octene with pinacolborane in refluxing 1 M THF solution. This reagent was then evaluated in palladium-catalyzed cross-coupling reactions with aryl bromides. The highest yield of the (*E*)-1-phenyloctene was obtained when SPhos was used as the ligand, K₂CO₃ was used as the base, and DMF was used as the reaction solvent. Other electron-rich, electron-poor, sterically hindered, and heteroaromatic substrates produced the corresponding (*E*)-1-phenyloctene derivatives in moderate to good yield.

KEYWORDS

Organic synthesis; Aryl alkene synthesis; Palladium-catalyzed cross-coupling; Suzuki-Miyaura reaction; Stereocontrolled alkene preparation; Hydroboration; 9-Borobicyclo[3.3.1]nonane; Reaction optimization

INTRODUCTION

Palladium-catalyzed cross-coupling reaction of alkenylboron reagents with aryl halides is a powerful method for the synthesis of stereodefined, organic alkenes.¹⁻⁴ It allows for the C-C bond formation between an alkenylboron group with an sp²-hybridized halide under mildly basic reaction conditions in the presence of a metal catalyst. The low toxicity of alkenylboron groups, the site-selective and stereocontrolled reaction outcomes, and broad functional group tolerance have allowed for ample applications in a variety of synthetic fields.⁵ In particular, the cross-coupling reactions of (*E*)-octenylboronic acids and their ester derivatives have drawn considerable attention as efficient methods to introduce a hydrophobic hydrocarbon chain onto organic compounds of interest. For example, Fairlamb *et al.* reported promising antimicrobial activity of 2-pyrone heterocycles substituted with octenyl hydrocarbon chains by cross-coupling reaction of an (*E*)-octenylboronic acid or (*E*)-octenylboronic acid catechol ester.⁶ More recently, Suzuki *et al.* evaluated fluorogenic probes bearing (*E*)-octenyl chains introduced by cross-coupling reaction of an (*E*)-octenylboronic acid pinacol ester ((*E*)-**3**).⁷ The cross-coupling product was only characterized by high-resolution mass spectrometry, and no optimization of the reaction conditions were reported.

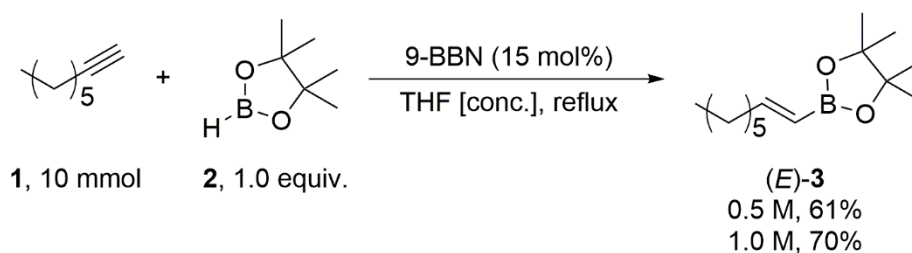
The abundant application of the coupling reaction is enabled by the ease of preparation of alkenylboron reagents.⁵ A common preparation method is via hydroboration reaction of an alkyne; the *syn* addition of a boron and hydrogen atom to the carbon-carbon triple bond of an alkyne. Recently, there has been substantial progress in the development of the hydroboration reactions of 1-octyne with pinacolborane catalyzed by transition metal-catalysts⁸⁻¹³, non-transition metal-catalysts¹⁴⁻¹⁶ and organoboron-catalysts^{3,17-19} to prepare the octenylboronic acid pinacol ester. Hoshi *et al.* first reported the synthesis of (*E*)-octenylboronic acid pinacol ester by Cy₂BH catalyzed hydroboration of 1-octyne with pinacolborane in 2004.²⁰ Thomas and Lloyd-Jones *et al.* elucidated the mechanism of the R₂BH-catalyzed alkyne hydroboration reaction through computational and kinetic approaches.²¹

However, to the best of our knowledge, the preparation of (*E*)-octenylboronic acid pinacol ester by 9-borobicyclo[3.3.1]nonane (9-BBN) catalyzed hydroboration reaction of 1-octyne with pinacolborane has not been reported.

In 2018, we reported the 9-BBN-catalyzed hydroboration reaction of phenylacetylene with pinacolborane.³ Subsequently, we described the 9-BBN-catalyzed hydroboration reaction of other *para*-substituted, terminal, aryl alkynes with pinacolborane.²² Our interest in the generality of this reaction led us to the study of alkyl-substituted alkynes in the 9-BBN-catalyzed hydroboration reaction, and the reactivity of the alkenylboronic acid pinacol ester product in subsequent cross-coupling reactions. Here we report the synthesis of (*E*)-octenylboronic acid pinacol ester by 9-BBN-catalyzed hydroboration reaction and its evaluation in palladium-catalyzed cross-coupling reactions with aryl bromides.

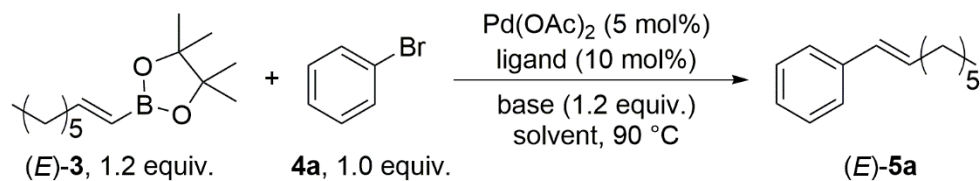
RESULTS AND DISCUSSION

This study began with the preparation of (*E*)-octenylboronic acid pinacol ester by 9-BBN-catalyzed hydroboration reaction of 1-octyne (**1**) with pinacolborane (**2**). Reaction conditions previously used for the 9-BBN-catalyzed hydroboration reaction of phenylacetylene with **2** were initially evaluated with a catalyst loading of 15 mol% and a reaction concentration of 0.5 M.³ Thus, **1** (10 mmol), **2** (1.0 equiv.), and 9-BBN (15 mol%) were combined and refluxed in 0.5 M THF solution under an atmosphere of argon gas (Scheme 1). The hydroboration reaction of **1** under these conditions produced (*E*)-**3** in 61% yield after purification by aqueous workup and column chromatography. The yield of (*E*)-**3** could be increased to 70% by increasing the reaction concentration from 0.5 M to 1.0 M.



Scheme 1. Synthesis of (*E*)-**3** by 9-BBN-catalyzed hydroboration of 1-octene with pinacolborane.

The evaluation of the reaction conditions for the palladium-catalyzed cross-coupling reaction of (*E*)-**3** with bromobenzene **4a** was then investigated (Table 1). These experiments began with the use of reaction conditions previously published for the palladium-catalyzed cross-coupling reaction of (*E*)-2-phenylethenylboronic acid pinacol ester with aryl bromides.³ Thus, (*E*)-**3** (1.2 equiv.), **2** (1.0 equiv.), Pd(OAc)₂ (5 mol%), *t*-Bu₃PhBF₄ (10 mol%), K₂CO₃ (1.2 equiv.), and DMF were combined and heated to 90 °C under an atmosphere of argon gas. These conditions produced (*E*)-**5a** in 52% isolated yield. The ligands JohnPhos, DPPF, Ph₃P, and SPhos were then evaluated in efforts to increase the yield of (*E*)-**5a** (entries 1-5). Of these ligands, the use of the SPhos ligand produced (*E*)-**5a** in the highest yield (entry 5). Dioxane was evaluated as the reaction solvent in reactions that employed both Ph₃P and SPhos as ligands (entries 6 and 7). The use of DMF as the solvent was found to provide a better yield in both of these reactions. A lower yield of (*E*)-**5a** was observed when *t*-BuOK or NaOH were used as the base instead of K₂CO₃ (entries 5, 8 and 9).



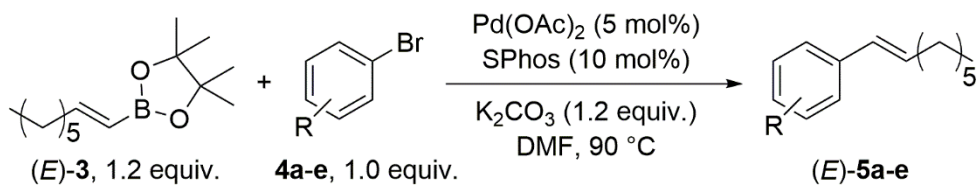
Entry	Ligand	Base	Solvent	Yield, ^b %
1	<i>t</i> -Bu ₃ PhBF ₄	K ₂ CO ₃	DMF	52
2	JohnPhos	K ₂ CO ₃	DMF	69
3	DPPF	K ₂ CO ₃	DMF	73
4	Ph ₃ P	K ₂ CO ₃	DMF	71
5	SPhos	K ₂ CO ₃	DMF	77
6	Ph ₃ P	K ₂ CO ₃	Dioxane	73
7	SPhos	K ₂ CO ₃	Dioxane	65
8	SPhos	<i>t</i> -BuOK	DMF	61
9	SPhos	NaOH	DMF	59

^aReactions were performed on >0.5 mmol scale.

^bYield of isolated, purified product.

Table 1. Optimization of the palladium-catalyzed cross-coupling reaction of *(E)*-3 and 4a.^a

The optimized reaction conditions of *(E)*-3 (1.2 equiv), aryl bromide (1.0 equiv.), Pd(OAc)₂ (5 mol%), SPhos (10 mol%), K₂CO₃ (1.2 equiv), DMF at 90 °C were then used to evaluate the scope of compatible aryl bromides (Table 2). The electronically neutral substrate bromobenzene (**4a**) provided the product *(E)*-5a in the highest isolated yield (entry 1). The substrate 1-bromo-4-nitrobenzene (**4b**) that bears an electron-withdrawing group provided a good yield of the product *(E)*-5b. The substrate 4-bromotoluene (**4c**) that bears an electron-donating group provided the lowest yield of the product *(E)*-5c (entry 3). Interestingly, the sterically hindered *o*-substituted aryl bromide 2-bromotoluene (**4d**) provided the product *(E)*-5d in a higher yield than the less sterically hindered *p*-substituted aryl bromide (entries 3 and 4). This is noteworthy because sterically hindered substrates are typically challenging substrates in palladium-catalyzed cross-coupling reactions.^{23,24} The heterocyclic aryl bromide 3-bromoquinoline (**4e**) that bears a Lewis basic nitrogen atom provided the product *(E)*-5e in a good yield (entry 5).



Entry	Product	Yield, ^b %
1	 (E)-5a	77
2	 (E)-5b	62
3	 (E)-5c	36
4	 (E)-5d	68
5	 (E)-5e	60

^aReactions were performed in duplicate on >0.5 mmol scale.

^bYield of isolated, purified product.

Table 2. Aryl bromides evaluated in the synthesis of 1-phenyloctene derivatives by palladium-catalyzed cross-coupling reaction.^a

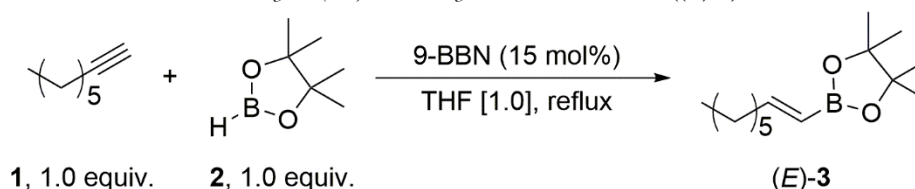
METHODS AND PROCEDURES

General Hydroboration Procedure: An oven-dried, round-bottom flask, containing a magnetic stir-bar, equipped with an oven-dried Liebig condenser was sealed with high-vacuum grease. The reflux apparatus was capped with a septum and purged with argon under a balloon of argon. The followings were added sequentially by syringe: the solvent, 1-octyne, pinacolborane, 9-BBN, and an additional volume of solvent to wash all of the reagents into the flask. The reaction solution was refluxed in a preheated oil bath at 65 °C. Reaction aliquots were analyzed by thin-layer chromatography (TLC) to monitor the progress of the reaction. When the reaction was determined to be complete, it was cooled to room temperature, extracted with ethyl acetate, washed with water, brine, dried with sodium sulfate, filtered and concentrated by rotary evaporation (50 °C, 70 torr). The crude product was purified by flash chromatography on silica. The amount of silica used in the chromatography was approximately 50 times the mass of the concentrated crude product. The composition of the eluent began at 97.5:2.5, hexane/ethyl acetate and the polarity of

the eluent was gradually increased to 90:10, hexane/ethyl acetate until the product was completely eluted. The product was concentrated *in vacuo* (2 torr) to afford the desired product.

General Cross-Coupling Procedure: To an oven-dried, round-bottom flask, containing a magnetic stir-bar was added (*E*)-**3a**, aryl bromide, base, ligand, and Pd(OAc)₂. The flask was capped with a septum and purged with argon under a balloon of argon. The solvent was then added by syringe. The reaction solution was stirred under a balloon of argon in a preheated oil bath at 90 °C. Reaction aliquots were analyzed by TLC to monitor the progress of the reaction. When the reaction was determined to be complete, it was cooled to room temperature, extracted with ethyl acetate, washed with water, brine, dried with sodium sulfate, filtered and concentrated by rotary evaporation (50 °C, 70 torr). The crude product was purified by flash chromatography on silica. The amount of silica used in the chromatography was approximately 50 times the mass of the concentrated crude product. Elution began with hexane and the polarity of the eluent was gradually increased to 95:5, hexane/ethyl acetate until the product was completely eluted. The product was concentrated in *vacuo* (2 torr) to afford the desired product.

Procedure for the synthesis of 4,4,5,5-Tetramethyl-2-(1*E*)-1-octen-1-yl-1,3,2-dioxaborolane ((*E*)-**3**)



Scheme 2. Synthesis of (*E*)-**3** by 9-BBN-catalyzed hydroboration of **1** with **2**.

Following the General Hydroboration Reaction Procedure, 1-octyne (1.54 mL, 10 mmol, 1.0 equiv), pinacolborane (1.45 mL, 10 mmol, 1.0 equiv), 9-BBN (3.0 mL, [0.5], 1.5 mmol, 0.1 equiv.), and THF (10 mL) were combined and heated to 65 °C for 1.25 h. Purification by aqueous workup and flash chromatography afforded 1.678 g (70%) of (*E*)-**3** as a clear, colorless oil.²⁵

Data for 4,4,5,5-Tetramethyl-2-(1*E*)-1-octen-1-yl-1,3,2-dioxaborolane ((*E*)-**3**)

¹H NMR: (400 MHz, CDCl₃)
6.63 (dt, *J* = 17.9 & 7.4 Hz, 1H), 5.42 (dt, *J* = 17.9 & 1.6 Hz, 1H), 2.17-2.11 (m, 2H), 1.43-1.37 (m, 2H), 1.27-1.24 (m, 18H), 0.89-0.85 (m, 3H).

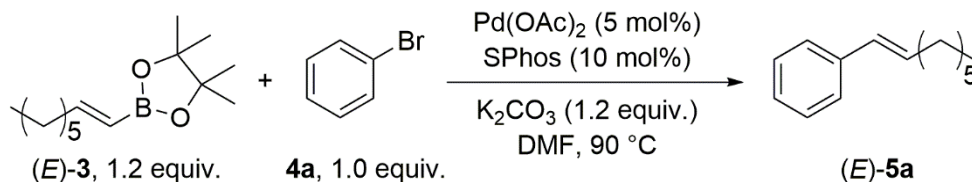
¹³C NMR: (101 MHz, CDCl₃)
154.8, 83.0, 35.8, 31.7, 28.9, 28.2, 24.8, 22.6, 14.10.

IR: (neat)
2977 (w), 2924 (m), 2855 (w), 2179 (w), 1743 (w), 1638 (m), 1467 (w), 1398 (w), 1360 (m), 1388 (s), 1316 (s), 1269 (w), 1215 (w), 1145 (s), 1047 (w), 997 (m), 970 (m), 900 (w), 849 (m), 724 (w), 646 (w), 577 (w), 522 (w).

MS: (EI, 70 eV)
238 ([M]⁺, 1), 223 ([M-CH₃]⁺, 28), 222 (7), 181 (7), 168 (5), 154 (21), 153 (100), 152 (47), 140 (14), 139 (66), 138 (26), 137 (8), 125 (10), 124 (8), 123 (9), 112 (9), 111 (38), 110 (48), 109 (27), 101 (34), 98 (5), 97 (20), 96 (33), 95 (42), 94 (7), 87 (5), 86 (6), 85 (77), 84 (60), 83 (61), 82 (36), 81 (45), 80 (7), 79 (9), 71 (10), 70 (10), 69 (67), 68 (73), 67 (55), 66 (8), 65 (5), 59 (43), 58 (11), 57 (47), 56 (16), 55 (96), 54 (96), 53 (17).

TLC: R_f 0.63 (hexane/ethyl acetate, 90:10) [silica gel, I₂]

Procedure for the synthesis of (1*E*)-1-Octen-1-ylbenzene ((*E*)-**5a**)



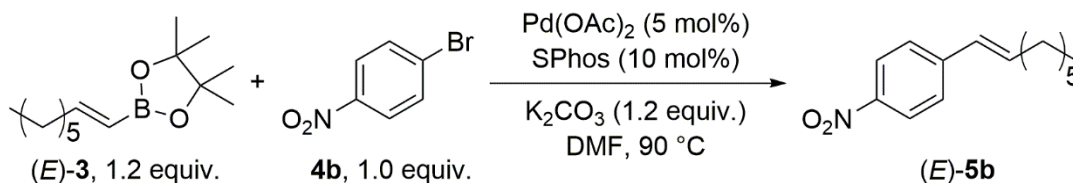
Scheme 3. Synthesis of (*E*)-**5a** by palladium-catalyzed cross-coupling of (*E*)-**3** with **4a**.

Following the General Cross-Coupling Procedure, (*E*)-**3** (190 mg, 0.8 mmol, 1.2 equiv.), bromobenzene (70 μ l, 0.67 mmol, 1.0 equiv), K_2CO_3 (110 mg, 0.80 mmol, 1.2 equiv.), $Pd(OAc)_2$ (7.4 mg, 0.033 mmol, 0.05 equiv.), SPhos (27 mg, 0.067 mmol, 0.1 equiv), and DMF (3.3 mL) were combined and heated to 90°C for 3 h. Purification by aqueous workup and flash chromatography afforded 96 mg (77 %) of (*E*)-**5a** as a clear oil.²⁶

Data for (*E*)-1-Octen-1-ylbenzene ((*E*)-**5a**)

- ¹H NMR:** (400 MHz, $CDCl_3$)
7.36-7.26 (m, 4H), 7.21-7.16 (m, 1H), 6.37 (appd, $J = 15.8$ Hz, 1H), 6.23 (dt, $J = 15.8$ & 6.8 Hz, 1H), 2.24-2.17 (m, 2H), 1.51-1.43 (m, 2H), 1.39-1.28 (m, 6H), 0.91-0.88 (m, 3H).
- ¹³C NMR:** (101 MHz, $CDCl_3$)
138.0, 131.3, 129.6, 128.4, 126.7, 125.9, 33.0, 31.8, 29.3, 28.9, 22.6, 14.1.
- IR:** (neat)
3023 (w), 2953 (w), 2922 (m), 2851 (m), 2190 (w), 1994 (w), 1917 (w), 1737 (s), 1596 (w), 1492 (w), 1447 (m), 1365(m), 1228 (m), 1216 (m), 1070 (w), 1028 (w), 961 (m), 907(w), 740 (w), 690 (m), 527 (w).
- MS:** (EI, 70 eV)
188 ($[M]^+$, 32), 129 (6), 118 (14), 117 ($[M-(CH_2)_4CH_3]^+$, 100), 116 (12), 115 (41), 105 (9), 104 (92), 91 (31).
- TLC:** R_f 0.80 (hexane/ethyl acetate, 90:10) [silica gel, UV light and I_2]

Procedure for the synthesis of 1-Nitro-4-(*E*)-1-octen-1-ylbenzene ((*E*)-**5b**)



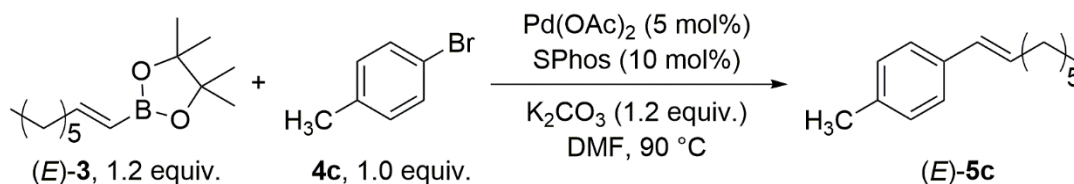
Scheme 4. Synthesis of (*E*)-**5b** by palladium-catalyzed cross-coupling of (*E*)-**3** with **4b**.

Following the General Cross-Coupling Procedure, (*E*)-**3** (213 mg, 0.89 mmol, 1.2 equiv.), 1-bromo-4-nitrobenzene (149 mg, 0.74 mmol, 1.0 equiv), K_2CO_3 (123 mg, 0.89 mmol, 1.2 equiv.), $Pd(OAc)_2$ (8.2 mg, 0.047 mmol, 0.05 equiv.), SPhos (30 mg, 0.074 mmol, 0.1 equiv), and DMF (3.7 mL) were combined and heated to 90°C for 3.5h. Purification by aqueous workup and flash chromatography afforded 107 mg (62%) of (*E*)-**5b** as a yellow oil.²⁷

Data for 1-Nitro-4-(*E*)-1-octen-1-ylbenzene ((*E*)-**5b**)

- ¹H NMR:** (400 MHz, $CDCl_3$)
8.17-8.14 (m, 2H), 7.47-7.43 (m, 2H), 6.45-6.43 (m, 2H), 2.29-2.24 (m, 2H), 1.53-1.46 (m, 2H), 1.39-1.28 (m, 6H), 0.91-0.88 (m, 3H).
- ¹³C NMR:** (101 MHz, $CDCl_3$)
146.4, 144.5, 136.7, 128.1, 126.3, 124.0, 33.2, 31.7, 28.94, 28.90, 22.6, 14.1.
- IR:** (neat)
2968 (w), 2953 (m), 2924 (m), 2189 (w), 2163 (w), 2117 (w), 2018 (w), 1737 (m), 1647 (w), 1594 (m), 1512 (s), 1455 (w), 1374 (w), 1339 (s), 1228 (m), 1216 (m), 1205 (m), 1180 (w), 1108 (m), 1010 (w), 966 (m), 954 (m), 859 (m), 822 (w), 743 (m), 689 (w), 665 (w), 630 (w), 537 (w), 527 (w).
- MS:** (EI, 70 eV)
233 ($[M]^+$, 13), 150 (17), 149 (100), 137 (14), 129 (7), 128 (10), 119 (14), 117 (11), 116 (57), 115 (48), 103 (7), 91 (9), 55 (12).
- TLC:** R_f 0.74 (hexane/ethyl acetate, 90:10) [silica gel, UV light and I_2]

Procedure for the synthesis of 1-Methyl-4-(1E)-1-octen-1-ylbenzene ((E)-5c)



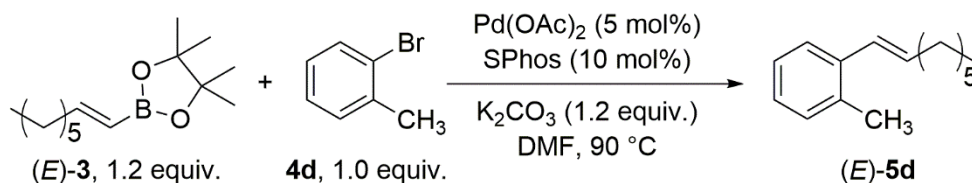
Scheme 5. Synthesis of (E)-5c by palladium-catalyzed cross-coupling of (E)-3 with 4c.

Following the General Cross-Coupling Procedure, (E)-3 (180 mg, 0.76 mmol, 1.2 equiv.), 4-bromotoluene (77 μ l, 0.63 mmol, 1.0 equiv.), K_2CO_3 (104 mg, 0.76 mmol, 1.2 equiv.), $Pd(OAc)_2$ (7.0 mg, 0.032 mmol, 0.05 equiv.), SPhos (26 mg, 0.063 mmol, 0.1 equiv.), and DMF (3.2 mL) were combined and heated to 90 $^\circ C$ for 17 hr. Purification by aqueous workup and flash chromatography afforded 46 mg (36 %) of (E)-5c as a clear oil.²⁸

Data for 1-Methyl-4-(1E)-1-octen-1-ylbenzene ((E)-5c)

- ¹H NMR:** (400 MHz, $CDCl_3$)
7.24-7.23 (m, 2H), 7.11-7.09 (m, 2H), 6.34 (appd, $J = 15.8$ Hz, 1H), 6.17 (dt, $J = 15.8$ & 6.9 Hz, 1H), 2.32 (s, 3H), 2.22-2.16 (m, 2H), 1.49-1.42 (m, 2H), 1.37-1.27 (m, 6H), 0.91-0.87 (m, 3H).
- ¹³C NMR:** (101 MHz, $CDCl_3$)
136.4, 135.2, 130.2, 129.5, 129.1, 125.8, 33.0, 31.7, 29.4, 28.9, 22.6, 21.1, 14.1.
- IR:** (neat)
3020 (w), 2954 (m), 2921 (m), 2852 (m), 2293 (w), 1987 (w), 1844 (w), 1690 (w), 1628 (w), 1511 (m), 1455 (m), 1376 (w), 1229 (w), 1204 (w), 1197 (w), 1105 (w), 1101 (w), 962 (s), 837 (m), 787 (m), 723 (m), 516 (w), 502 (w).
- MS:** (EI, 70 eV)
202 ($[M]^+$, 28), 132 (11), 131 ($[M-(CH_2)_4CH_3]^+$, 100), 129 (13), 128 (9), 118 (43), 117 (12), 116 (14), 115 (17), 111 (6), 105 (13), 97 (9), 91 (16), 85 (100, 83 (9), 71 (15), 70 (7), 69 (10), 57 (20), 55(12).
- TLC:** R_f 0.82 (hexane/ethyl acetate, 90:10) [silica gel, UV light and I_2]

Procedure for the synthesis of 1-Methyl-2-(1E)-1-octen-1-ylbenzene ((E)-5d)



Scheme 6. Synthesis of (E)-5d by palladium-catalyzed cross-coupling of (E)-3 with 4d.

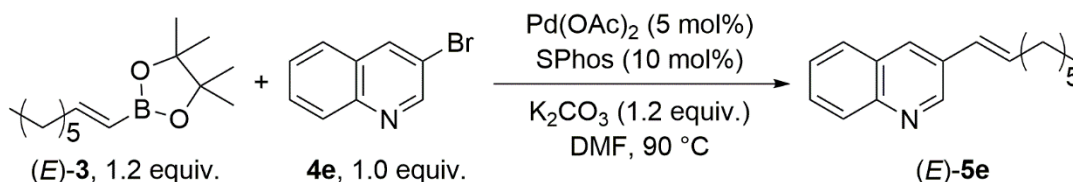
Following the General Cross-Coupling Procedure, (E)-3 (172 mg, 0.72 mmol, 1.2 equiv.), 2-bromotoluene (72 μ l, 0.60 mmol, 1.0 equiv.), K_2CO_3 (99 mg, 0.72 mmol, 1.2 equiv.), $Pd(OAc)_2$ (6.7 mg, 0.030 mmol, 0.05 equiv.), SPhos (25 mg, 0.060 mmol, 0.1 equiv.), and DMF (3.0 mL) were combined and heated to 90 $^\circ C$ for 17.5 hr. Purification by aqueous workup and flash chromatography afforded 83 mg (68 %) of (E)-5d as a clear oil.²⁷

Data for 1-Methyl-2-(1E)-1-octen-1-ylbenzene ((E)-5d)

- ¹H NMR:** (400 MHz, $CDCl_3$)
7.43-7.41 (m, 1H), 7.18-7.11 (m, 3H), 6.58 (appd, $J = 15.6$ Hz, 1H), 6.10 (dt, $J = 15.6$ & 7.0 Hz, 1H), 2.34 (s, 3H), 2.27-2.21 (m, 2H), 1.54-1.45 (m, 2H), 1.41-1.30 (m, 6H), 0.93-0.89 (m, 3H).
- ¹³C NMR:** (101 MHz, $CDCl_3$)
137.1, 134.8, 132.6, 130.1, 127.5, 126.7, 126.0, 125.4, 33.3, 31.7, 29.4, 28.9, 22.6, 19.8, 14.1.
- IR:** (neat)
3016 (w), 2953 (w), 2922 (m), 2852 (w), 2015 (w), 2007 (w), 1954 (w), 1887 (w), 1737 (m), 1647 (w), 1600 (w), 1483 (w), 1457 (m), 1376 (m), 1228 (m), 1216 (m), 1032 (w), 963 (m), 742 (m), 527 (w).

- MS:** (EI, 70 eV)
202 ($[M]^+$, 33), 132 (13), 131 ($[M-(CH_2)_4CH_3]^+$, 100), 129 (16), 128 (12), 119 (8), 118 (57), 117 (24), 116 (20), 115 (25), 111 (7), 105 (19), 97 (11), 91 (22), 85 (12), 83 (10), 71 (17).
- TLC:** R_f 0.81 (hexane/ethyl acetate, 90:10) [silica gel, UV light, and I_2]

Procedure for the synthesis of 3-(1*E*)-1-Octen-1-ylquinoline ((*E*)-5e)



Scheme 7. Synthesis of (*E*)-5e by palladium-catalyzed cross-coupling of (*E*)-3 with 4e.

Following the General Cross-Coupling Procedure, (*E*)-3 (211 mg, 0.89 mmol, 1.2 equiv.), 3-bromoquinoline (100 μ l, 0.74 mmol, 1.0 equiv), K_2CO_3 (122 mg, 0.89 mmol, 1.2 equiv.), $Pd(OAc)_2$ (8.3 mg, 0.037 mmol, 0.05 equiv.), SPhos (30 mg, 0.074 mmol, 0.1 equiv), and DMF (3.7 mL) were combined and heated to 90°C for 2 hr. Purification by aqueous workup and flash chromatography afforded 107 mg (60 %) of (*E*)-5e as a clear oil.²⁹

Data for 3-(1*E*)-1-Octen-1-ylquinoline ((*E*)-5e)

- 1H NMR:** (400 MHz, $CDCl_3$)
8.971-8.966 (m, 1H), 8.08-8.06 (m, 1H), 7.997-7.992 (m, 1H), 7.78-7.76 (m, 1H), 7.67-7.62 (m, 1H), 7.53-7.49 (m, 1H), 6.53 (appd, $J = 16.1$ Hz, 1H), 6.50-6.43 (m, 1H), 2.31-2.26 (m, 2H), 1.56-1.48 (m, 2H), 1.41-1.30 (m, 6H) 0.92-0.89 (m, 3H).
- ^{13}C NMR:** (101 MHz, $CDCl_3$)
149.0, 146.7, 134.3, 131.8, 130.8, 128.92, 128.88, 128.2, 127.7, 126.9, 126.4, 33.3, 31.7, 29.1, 28.9, 22.6, 14.1.
- IR:** 3129 (w), 3099 (w), 3078 (w), 2952 (w), 2921 (m), 2851 (m), 2088 (w), 2075 (w), 2052 (w), 1649 (w), 1567 (w), 1490 (m), 1464 (m), 1374 (w), 1339 (w), 1295 (w), 1204 (w), 1189 (w), 1122 (w), 1015 (w), 962 (s), 906 (m), 858 (w), 783 (m), 748 (s), 616 (w).
- MS:** (EI, 70 eV)
240 ($[M+1]^+$, 7), 239 ($[M]^+$, 37), 182 (7), 180 (9), 169 (15), 168 ($[M-(CH_2)_4CH_3]^+$, 100), 167 (61), 166 (8), 157 (9), 156 (21), 155 (50), 154 (8), 143 (15), 142 (7), 115 (8).
- TLC:** R_f 0.31 (hexane/ethyl acetate, 90:10) [silica gel, UV light and I_2]

CONCLUSION

A hydrophobic octenyl chain can be introduced to aromatic bromides by palladium-catalyzed cross-coupling reaction of (*E*)-3 with aryl bromides. The geometrically pure reagent (*E*)-3 can be prepared by the 9-BBN-catalyzed hydroboration reaction of **1** with **2** in refluxing 1 M THF solution. The alkyl-substituted alkenylboronic acid reagent (*E*)-3 undergoes efficient cross-coupling with aryl bromides under palladium catalysis to provide the desired products (*E*)-5a-e in moderate to good yield. The highest reaction yield was obtained when SPhos was used as the ligand, K_2CO_3 was used as the base, and DMF was used as the reaction solvent. We intend to continue to explore the 9-BBN-catalyzed hydroboration reaction and the palladium-catalyzed cross-coupling reaction of the alkenylboronic acid pinacol ester products.

ACKNOWLEDGEMENTS

We are grateful to Organic Syntheses Inc. for a Summer Research at an Undergraduate Institution Grant (N.S.W.), and Southern Utah University for a Walter Maxwell Gibson Research Fellowship (S.M.) and L. S. and Aline W. Skaggs Research Grant (S.M.) to generously support this work. We are grateful to Maddelyn Lunt for providing characterization data for (*E*)-3.

REFERENCES

1. Miyaura, N. (2004) Metal-Catalyzed Cross-Coupling Reactions of Organoboron Compounds with Organic Halides, in *Metal-Catalyzed Cross-Coupling Reactions* (de Meijere, A., Diederich, F., Ed.) 2nd ed., 41–123, Wiley-VCH, New York.
2. Miyaura, N., Suzuki, A. (1995) Palladium-catalyzed cross-coupling reactions of organoboron compounds. *Chem Rev* 95, 2457–2483. <https://doi.org/10.1021/cr00039a007>
3. Rau, H. H., and Werner, N. S. (2018) Stereocontrolled synthesis of (*E*)-stilbene derivatives by palladium-catalyzed Suzuki-Miyaura cross-coupling reaction, *Bioorg Med Chem Lett* 28, 2693–2696. <https://doi.org/10.1016/j.bmcl.2018.04.004>
4. Tobrman, T., and Mrkobrada S. (2022) Palladium-catalyzed cross-coupling reactions of borylated alkenes for the stereoselective synthesis of tetrasubstituted double bond, *Organics* 3, 210–239. <https://doi.org/10.3390/org3030017>
5. Sakamaki, S., Kawanishi, E., Nomura, S., and Ishikawa, T. (2012) Aryl- β -C-glucosidation using glucal boronate: application to the synthesis of tri-*o*-methylnorbergenin, *Tetrahedron* 68, 5744–5753. <https://doi.org/10.1016/j.tet.2012.05.035>
6. Marrison, L. R., Dickinson, J. M., and Fairlamb, I. J. S. (2003) Suzuki cross-coupling approaches to the synthesis of bioactive 3-substituted and 5-substituted-4-methoxy-6-methyl-2-pyrones, *Bioorg Med Chem Lett* 13, 2667–2671. [https://doi.org/10.1016/S0960-894X\(03\)00546-8](https://doi.org/10.1016/S0960-894X(03)00546-8)
7. Kurebayashi, Y., Takahashi, T., Miura, T., Otsubo, T., Minami, A., Fujita, Y., Sakakibara, K., Tanabe, M., Iuchi, A., Ota, R., Ikeda K., and Suzuki, T. (2019) Fluorogenic probes for accurate in situ imaging of viral and mammalian sialidases, *ACS Chem Biol* 14, 1195–1204. <https://doi.org/10.1021/acscmbio.9b00103>
8. Lyu, Y., Toriumi, N., and Iwasawa, N. (2021) (*Z*)-selective hydroboration of terminal alkynes catalyzed by a PSP–pincer rhodium complex, *Org Lett* 23, 9262–9266. <https://doi.org/10.1021/acs.orglett.1c03606>
9. Feng, X., Ji, P., Li, Z., Drake, T., Oliveres, P., Chen, E. Y., Song, Y., Wang, C., and Lin, W. (2019) Aluminum hydroxide secondary building units in a metal-organic framework support earth-abundant metal catalysts for broad scope organic transformations, *ACS Catal* 9, 3327–3337. <https://doi.org/10.1021/acscatal.9b00259>
10. Wang, Y., Guan, R., Sivaguru, P., Cong, X., and Bi, X. (2019) Silver-catalyzed anti-Markovnikov hydroboration of C–C multiple bonds, *Org Lett* 21, 4035–4038. <https://doi.org/10.1021/acs.orglett.9b01217>
11. Jia, J., Wu, T., Fu, Y., Hu, Z., Tang, H., Pan, Y., and Huang, F. (2022) Integrating terminal CoBr_n salts into a 2D cobalt(II) coordination polymer to promote the β -(*E*)-selective hydroboration of alkynes, *Adv Synth Catal* 364, 1873–1878. <https://doi.org/10.1002/adsc.202200056>
12. Garhwal, S., Fridman, N., and Rüter, G. (2020) *Z*-Selective Alkyne Functionalization Catalyzed by a trans-dihydride N-heterocyclic carbene (NHC) iron complex, *Inorg Chem* 59, 13817–13821. <https://doi.org/10.1021/acs.inorgchem.0c02057>
13. Khranov, D. M., Rosen, E. L., Er, J. A. V., Vu, P. D., Lynch, V. M., and Bielawski, C. W. (2008) N-heterocyclic carbenes: deducing σ - and π -contributions in Rh-catalyzed hydroboration and Pd-catalyzed coupling reactions, *Tetrahedron* 64, 6853–6862. <https://doi.org/10.1016/j.tet.2008.04.030>
14. Sarkar, N., Bera, S., and Nembenna, S. (2020) Aluminum-catalyzed selective hydroboration of nitriles and alkynes: a multifunctional catalyst, *J Org Chem* 85, 4999–5009. <https://doi.org/10.1021/acs.joc.0c00234>
15. Bisai, M. K., Yadav, S., Das, T., Vanka, K., and Sen, S. S. (2019) Lithium compounds as single site catalysts for hydroboration of alkenes and alkynes, *Chem Commun* 55, 11711–11714. <https://doi.org/10.1039/C9CC05783H>
16. Guermazi, R., Specklin, D., Gourlaouen, C., Frémont, P., and Dargorne, S. (2022) Two-coordinate NHC-supported ZnII organocations: steric and electronic tunability and use in alkyne hydroboration catalysis, *Eur J Inorg Chem* 2022, e202101002. <https://doi.org/10.1002/ejic.202101002>
17. Maj, A., Pawluc, P., and Zaranek, M. (2022) Hydroboration of alkynes initiated by sodium triethylborohydride, *Polyhedron* 223, 115961–115973. <https://doi.org/10.1016/j.poly.2022.115961>
18. Bismuto, A., Cowley, M., and Thomas, S. (2020) Zwitterion-initiated hydroboration of alkynes and styrene, *Adv Synth Catal* 363, 2382–2385. <https://doi.org/10.1002/adsc.202001323>
19. Lawson, J. R., Wilkins, L. C., and Melen, R. L. (2017) Tris(2,4,6-trifluorophenyl)borane: an efficient hydroboration catalyst, *Chem Eur J* 23, 10997–11000. <https://doi.org/10.1002/chem.201703109>
20. Shirakawa, K., Arase, A., and Hoshi, M. (2004) Preparation of (*E*)-1-alkenylboronic acid pinacol esters via transfer of alkenyl group from boron to boron, *Synthesis* 11, 1814–1820. <https://doi.org/10.1055/s-2004-829165>
21. Nieto-Sepulveda, E., Bage, A. D., Evans, L. A., Hunt, T. A., Leach, A. G., Thomas, S. P., and Lloyd-Jones, G. C. (2019) Kinetics and mechanism of the Arase-Hoshi R₂BH-catalyzed alkyne hydroboration: alkenylboronate generation via B-H/C-B metathesis, *J Am Chem Soc* 141, 18600–18611. <https://doi.org/10.1021/jacs.9b10114>

22. Ruesch, G. L., Rowley, S. L., Mifflin, M. C., and Werner, N. S. (2020) 9-Borobicyclo[3.3.1]nonane-catalyzed hydroboration of terminal aromatic alkynes with pinacolborane, *Am J Undergrad Res* 17, 3–12. <https://doi.org/10.33697/ajur.2020.011>
23. Yin, J., Rainka, M. P., Zhang, X. X., and Buchwald, S. L. (2002) A highly active Suzuki catalyst for the synthesis of sterically hindered biaryls: novel ligand coordination, *J Am Chem Soc* 124, 1162–1163. <https://doi.org/10.1021/ja017082r>
24. Li, C., Xiao, G., Zhao, Q., Liu, H., Wang, T., and Tang, W. (2014) Sterically demanding aryl–alkyl Suzuki–Miyaura coupling, *Org Chem Front* 1, 225–229. <http://doi.org/10.1039/c4qo00024b>
25. Brondani, P. B., de Gonzalo, G., Fraaije, M. W., Andrade, L. H. (2011) Selective Oxidations of Organoboron Compounds Catalyzed by Baeyer-Villiger Monooxygenases. *Adv Synth Catal* 353, 2169–2173. <https://doi.org/10.1002/adsc.201100029>
26. Chen, K., Zhu, H., Li, Y., Peng, Q., Guo, Y., and Wang, X. (2021) Dinuclear cobalt complex-catalyzed stereodivergent semireduction of alkynes: switchable selectivities controlled by H₂O, *ACS Catal* 11, 13696–13705. <https://doi.org/10.1021/acscatal.1c04141>
27. Nakao, H., Imanaka, A., Sahoo, K. A., Yada, A., and Hiyama, T. (2005) Alkenyl- and aryl[2-(hydroxymethyl)phenyl]dimethylsilanes: an entry to tetraorganosilicon reagents for the silicon-based cross-coupling reaction, *J Am Chem Soc* 127, 6952–6953. <https://doi.org/10.1021/ja051281j>
28. Zhang, W., Chen, G., Wang, K., and Xia, R. (2019) Palladium-catalyzed decarboxylative coupling of α,β -unsaturated carboxylic acids with aryl tosylates, *Appl Organomet Chem* 33, e4914. <https://doi.org/10.1002/aoc.4914>
29. Muto, K., Yamaguchi, J., Musaev, G. D., and Itami, K. (2015) Decarbonylative organoboron cross-coupling of esters by nickel catalysis. *Nat Commun* 6, 1–8. <https://doi.org/10.1038/ncomms8508>

ABOUT STUDENT AUTHOR

Shoma Mukai graduated Summa Cum Laude from Southern Utah University in 2022 with a B.S. degree in Biology with a minor in Chemistry. While at SUU, Shoma was the recipient of the Walter Maxwell Gibson Research Fellowship, and the L.S. and Aline W. Skaggs Research Grant. He currently works as Process Research Associate at Wilmington Pharmatech in Newark, Delaware and intends to pursue a graduate degree in synthetic organic chemistry in the fall of 2023.

PRESS SUMMARY

The palladium-catalyzed cross-coupling reaction is a versatile method to introduce a hydrophobic, water-fearing, hydrocarbon chain onto a variety of organic compounds of interest to science and medicine. In this work, a reagent was prepared with a hydrophobic hydrocarbon chain and was shown to undergo a cross-coupling reaction with aryl bromides under palladium-catalysis. The reaction conditions for the carbon-carbon bond forming, cross-coupling reaction were optimized to achieve a high yield of the product. A variety of reaction partners were shown to undergo this site-selective and stereocontrolled chemical reaction.

Spawning Conditions Affect Clutch Probability and Size in Laboratory-Housed Zebrafish (*Danio rerio*)

Sydni Anderson, Elizabeth Sipes, Megan Franke, & Dena R. Hammond-Weinberger*

Department of Biological Sciences, Murray State University, Murray, KY

<https://doi.org/10.33697/ajur.2023.079>

Students: sanderson33@murraystate.edu, esipes@murraystate.edu, mfranke1@murraystate.edu

Mentor: dweinberger@murraystate.edu*

ABSTRACT

Zebrafish are common experimental models used in biological studies that are bred and raised in laboratory settings. Published studies, anecdotal evidence, and industry practices are variable and offer conflicting suggestions on maximizing reproductive success, particularly regarding sex ratios and segregating males and females before spawning. This study identified conditions that promote maximum reproductive success (clutch probability and average clutch size) in zebrafish. Clutch probability was higher when females were seven to ten months old and bred in groups with equal sex ratios and an artificial spawning substrate in the winter or spring. Clutch size was significantly larger when females were seven to ten months old, outnumbered by males, and bred with an artificial spawning substrate. Optional spawning substrates (marbles and plants) improved reproductive success, whereas other parameters had no impact. These data support the implementation of simple steps that reliably maximize reproductive success of laboratory zebrafish.

KEY WORDS Reproduction; Breeding; Seasonality; Behavior; Substrate; Sex Ratios; Captivity; Eggs

INTRODUCTION

Zebrafish (*Danio rerio*) are commonly used experimental models in biological research and biomedicine.^{1,2} Zebrafish are small, tropical freshwater fish that can tolerate a wide variety of environmental conditions and breed in captivity,¹ which contributes to their popularity in the laboratory. Zebrafish mature quickly and can produce thousands of eggs in their lifetime.¹ Reliable generation of large batches of eggs is essential for the success of zebrafish as a model organism. Reproductive success can be measured in several ways, and most often refers to the frequency and size of viable clutches. Several factors affect reproductive success and can be grouped into those related to health and husbandry, social factors, and spawning habitat. Unsurprisingly, parameters that affect fish health³ including water quality,⁴ diet,⁵ and parasite load⁶ all affect reproductive success. This analysis focused on spawning habitat and social factors that are purported to increase reproductive success in otherwise healthy fish, though the parameters tested may also be applicable in compromised populations.

Social factors

Clutch size is affected by the age and size of fish. Laboratory-raised zebrafish reach sexual maturity in 3–6 months,¹ though fish aged 7–18 months lay more eggs than do younger or older fish,⁷ with best reproductive success attained while fish are 6–12 months.³ Young adults may lay poorer quality eggs³ than more mature fish. Fish body size is a factor in reproductive success – larger females lay larger and more frequent clutches.^{8–10} Female size differences may be strictly due to larger females being able to physically produce greater numbers of eggs, though reproductive success also differs by social rank in which territorial females reproduce more successfully than other females in their territory.¹¹ As a shoaling species, social factors influence zebrafish reproductive success. Sex ratios and housing density of zebrafish affect male territoriality, which may affect reproductive success.¹² Females are selective and spawn more frequently when paired with a certain male, but their preferences do not correlate with male dominance.⁹ Wild zebrafish reproduce in pairs,¹³ while laboratory-housed fish are often spawned in groups.^{7, 14, 15} Some have reported that group spawning and pair spawning in laboratory populations are equally successful,^{16, 17} though most sources suggest setting up spawning groups with females outnumbering males to increase the number of eggs generated.^{7, 12, 18}

The suggested practice of some researchers and tank manufacturers is to segregate males and females overnight using clear dividers that are removed when the lights are turned on in the morning^{4, 19, 20} or at the desired breeding time. This is intended to serve two purposes. First, dividers separate sexes to allow for controlled timing of breeding. Second, dividers prevent fish from interacting while allowing them to process olfactory and visual displays as a way to increase spawning behaviors, because zebrafish reproductive behavior is influenced by both olfactory and visual cues.^{21, 22} Ovarian steroid glucuronides serve as sex attractants for

males.²³ Male zebrafish release pheromones that trigger female ovulation and in turn, females release a pheromone that triggers courtship behavior in males.¹ Common practice suggests selecting the most vibrant and colorful males for successful breeding,²² though some evidence suggests that female choice may not depend on appearance, but rather on male personality.²⁴ It is unclear if the use of dividers increases reproductive success related to these displays or is simply a useful mechanism to regulate breeding timing.

Spawning habitat

Laboratory spawning is meant to mimic certain factors that are associated with zebrafish spawning in the wild. Reproduction of both wild-strain and laboratory zebrafish occurs exclusively in the morning for roughly two hours beginning at “dawn” (when the system lights turn on).^{7,13} Wild zebrafish spawn seasonally, and laboratory colonies are maintained at temperatures and light cycles that mimic this breeding season to allow for generation of eggs year-round.⁷ Indeed, light pollution negatively influences reproductive success.²⁵ Seasonal breeding may correlate with diet that changes with the seasons, rather than season per se, as wild-caught zebrafish breed year-round in a controlled setting.¹⁵ In the wild, zebrafish tend to inhabit shallow ponds, ditches, and slow-flowing streams,¹⁵ so laboratory spawning is typically set up in shallow tanks. Spawning in too small volumes (≤ 200 mL) negatively affects reproductive success.^{14,26} Wild zebrafish also spawn around plants¹³ and after heavy downpour,¹⁵ which is mimicked in the lab by changing the water in the spawning tank at dawn (this also serves to clean the water into which eggs are laid). Factors purported to promote large clutch sizes include using a substrate such as marbles in the spawning tank.^{12,17,27} Similarly, incorporating live plants into zebrafish housing may have positive impacts on health and stress,^{28,29} and thus reproduction.

Despite such common use, there is insufficient experimental data to support recommended best practices to increase spawning success in laboratory-housed zebrafish. Though many sources outline factors that are purported to aid in reproductive success contradictions abound. These factors include characteristics of the fish (age, health, size), social factors (number and sex ratio of breeding fish, housing density, social dominance, pheromone cues), and environmental factors (light duration, intensity, temperature, season, substrate, habitat). These experiments consist of retrospective analyses bolstered by controlled spawning to probe for and test correlations in reproductive success to identify variables associated with clutch production and size that can be readily implemented in zebrafish colonies.

METHODS AND PROCEDURES

Animal husbandry

Zebrafish husbandry and all experimental procedures were approved by the Murray State Institutional Animal Care and Use Committee, protocol #2017-024. Adult zebrafish (*Danio rerio*) were raised in house from the AB and EKK strains which were originally purchased from the Zebrafish International Resource Center (Eugene, OR) and Ekkwill Waterlife Resources (Ruskin, FL) respectively. Fish were housed in a recirculating rack system (Aquaneering, San Diego, CA) with a 14:10 h light: dark cycle in tanks of mixed sexes at a density of five fish or fewer per L (though juveniles are stocked at higher densities based on age and size). Water quality was continuously monitored using Neptune APEX (Morgan Hill, CA). The pH ranged between 7.5 and 8 and water temperatures were kept at $27.5^{\circ}\text{C} \pm 1$. The zebrafish were fed twice daily with adult zebrafish diet (Ziegler, East Berlin, PA).

Basic spawning parameters

Ages of spawned fish ranged from 2–25 months old. Individuals were set up to spawn at most twice a week. Fish were set up in 1 L breeding tanks with a slotted liner to segregate eggs from adults (Aquaneering) after the last feeding in the evening (5 pm). Clear plastic dividers were purchased as part of the spawning tank assembly (Aquaneering) and fit into grooves inside the slotted tank liner. A single floating broad-leaf green plastic aquarium plant approximately 7 cm long was used to provide cover to zebrafish. When plants were included together with dividers, females were placed in the plant side of the spawning tank. A single layer of assorted marbles (blue, green, clear, and yellow) per tank was used to mimic rocky substrate. When marbles and dividers were both present, marbles were distributed evenly on each side of the divided tank.

Two locations were used for spawning: the fry incubator and the standard housing room rack system. Both locations were kept on 14:10 h light:dark cycles. The housing room dawn was 9 am, had an illuminance of 60 lux of full-spectrum fluorescent light, and the air temperature fluctuated between 23.5 and 29.5 °C. The incubator dawn was 8 am (to allow earlier egg laying for other experiments), had an illuminance of 2000 lux of full-spectrum fluorescent light, and the air temperature was tightly regulated at 28.5 °C. Because the water temperature was not regulated within the spawning tanks, the room temperature affected the water temperature. Spawning tanks were left undisturbed overnight on a designated vacant shelf of the standard housing rack or the fry incubator. The total information collected for each spawning tank was the set-up date, day of the week, tank ID, number of males and females, spawning room, and presence or absence of each: dividers, plants, and marbles.

In the morning at lights on (dawn), spawning tank water was replaced with fresh system water in tanks without dividers. In the

incubator, fresh system water was pre-filled the night before so the water change would be a consistent temperature. At the same time, dividers were removed from divided tanks and water was not replaced to maintain the pheromone cues. Approximately two hours after dawn, spawning tanks were checked for eggs. Clutches were collected, counted, and recorded. All fish were returned to their home tanks before the first feeding.

Two sets of experiments were conducted: a retrospective analysis of spawning records to identify patterns and controlled breeding events to test those patterns.

Retrospective spawning analytics

Groups of two to seven wild-type fish were set up to spawn from over a span of two years for routine laboratory use. The previous reproductive success of the fish varied from first controlled spawning to experienced breeders and included fish born and raised in-house and fish acquired externally. The variable spawning parameters were at the discretion of whomever of the authors set up the spawning tanks that day. These variable parameters were the spawning location, the number and sex ratio of fish, and tank additions (dividers, marbles, and aquarium plants). The divider was used to separate male and female fish before dawn. Dividers were added at the time of spawning tank set up, before fish were added. Water could flow freely between the two sides of the divided tanks below the level of the slotted tank liner. Ratios of fish were grouped into equal sex, male-dominant, and female-dominant groups. Equal sex groups included groupings of two or four fish. Male-dominant groups included ratios of 2:1, 3:1, 3:2, 4:1, and 4:3 of males to females. Female-dominant groups included ratios of 1:2, 1:3, 1:5, and 2:3 of males to females. Reproductive success as a function of age and of season were also measured. No other persons handled these fish for the duration of these experiments.

These analyses pooled data from several home tanks (“colony” in figures) to assess the aggregate effects of the various parameters. The collected data from a single home tank (“1 tank” in figures) of nine fish (four females, five males; date of birth 3-28-17) from August 2017 to March 2019 was used to assess how these manipulations affect the breeding behavior of the same fish over time. These results were compared to the colony data in some of the analyses as indicated in each section or figure. Because the variables tested occur together and may influence reproductive success in complex ways, individual factors and compound effects were compared. First, each independent variable was collapsed into a binary (presence or absence; group or pair; room or incubator) or three to four variate analyses (age bin, season, group bin) to assess the contribution of each variable on a broad scale. Following the binary analysis, interactions among variables were assessed by grouping between two attributes at a time, such as marbles and room, to generate assessments between four groups: marbles + room; marbles + incubator; no marbles + room; no marbles + incubator.

MONDAY	TUESDAY	WENDESDAY	THURSDAY	FRIDAY
Set up groups 1-3 (1M:3F) No Substrate	Collect 1-3 eggs Set up groups 4-6 (2M:2F) Marbles	Collect 4-6 eggs Set up groups 7-9 (3M:1F) Plants	Collect 7-9 eggs Set up groups 1-3 (1M:3F) Marbles + Plants	Collect 1-3 eggs
Set up groups 4-6 (2M:2F) No Substrate	Collect 4-6 eggs Set up groups 7-9 (3M:1F) Marbles	Collect 7-9 eggs Set up groups 1-3 (1M:3F) Plants	Collect 1-3 eggs Set up groups 4-6 (2M:2F) Marbles + Plants	Collect 4-6 eggs
Set up groups 7-9 (3M:1F) No Substrate	Collect 7-9 eggs Set up groups 1-3 (1M:3F) Marbles	Collect 1-3 eggs Set up groups 4-6 (2M:2F) Plants	Collect 4-6 eggs Set up groups 7-9 (3M:1F) Marbles + Plants	Collect 7-9 eggs

Figure 1. Seasonal spawning rotations. Groups of four sexually mature, laboratory-raised fish from mixed parentage were set up in triplicate (three sex ratios, nine total tanks) with three sex ratios: one male (M) and three females (F) (1M:3F), 2M:2F, or 3M:1F in a rotating cycle. Spawning substrate was consistent to the day of the week. This three-week setup was repeated three consecutive times for a total of twelve breeding events per tank.

Controlled spawning environments

Groups of four sexually mature (three to six months old), in-house raised fish from mixed parentage and a minimum of two generations removed from externally-sourced founder fish were set up in triplicate (three sex ratios, nine total tanks) with different sex ratios (3M:1F, 2M:2F, or 1M:3F). These groups were set up to spawn on a rotating schedule for three months (spanning a season) according to the following rotation: all three tanks from a sex ratio group were set up to spawn rotating through four consecutive days each week (**Figure 1**). Thus, one sex ratio group would spawn on days one and four. The substrate was kept the same each week such that the spawning tanks set up on day one had no substrate, day two had marbles, day three

had plants, and day four tanks had both marbles and plants. Thus, each sex ratio grouping spawned in each substrate condition three times and on each day of the week three times for a total of twelve spawning events during the experiment. This setup was repeated each season with a new batch of fish so that the fish were the same age at the start of each season. Seasons were defined as follows: January 1–March 31 as winter, April 1–June 30 as spring, July 1–September 31 as summer, and October 1–December 31 as fall. These trials were all conducted in the standard fish housing room with no dividers.

Reproductive success

Reproductive success was assessed in two ways: clutch success and the number of eggs per female. Clutch success was defined as the presence of at least one egg in the spawning tank at the time of collection (roughly two hours after dawn) and was scored as either zero (no eggs) or one (eggs), thus generating a probability of egg generation. Egg viability was not assessed. Tanks with multiple females were scored as a single clutch for determining clutch probability as a function of the number of animals in the group. The number of eggs per female is the total number of eggs in the spawning tank divided by the number of females in that tank. This value was counted as multiple, equal sized clutches to assess the average number of eggs per female.

Statistical analyses

Values are expressed as means (M) ± the standard error of the mean (SEM). Unpaired two-tailed t-tests were used to compare means between two groups. Comparisons between observed and expected means were compared using two-tailed one-sample t-tests. Analyses between three or more groups were made using one-way ANOVA with post-hoc Tukey’s multiple comparisons test. Multivariate analyses with two-way ANOVA followed by Tukey’s multiple comparisons tests were used to test variable interactions. P < 0.05 were considered significant. GraphPad Prism 8 software (San Diego, CA) and Microsoft Excel were used for analyses and graphs.

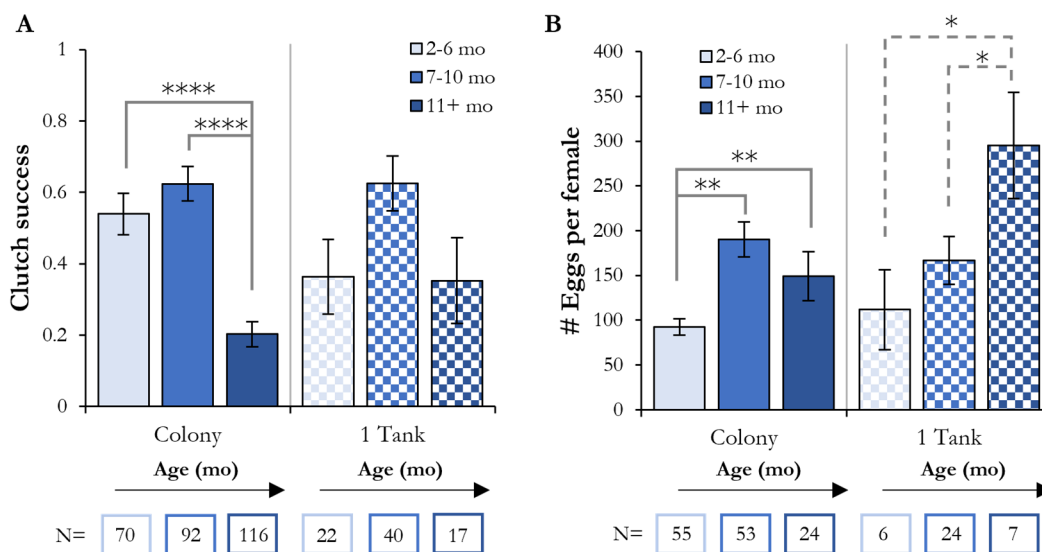


Figure 2. Zebrafish function as an annual species. Spawning success and clutch size declined after 10 months (mo) of age in most of the colony. **A.** Clutch success was similar in young (2–6 mo) versus adult fish (7–10 mo) and was reduced in aged fish (11+ mo). The single tank (checked bars) shows the behavior of the same fish across all ages examined versus the colony. **B.** Adult fish produced the largest clutches in the colony and aging adults produced even larger clutches in the single tank. Values depict mean ± SEM. N = number of spawning events, indicated under each bar. Statistical significance tested by one-way ANOVA with Tukey’s multiple comparisons test. * p < 0.05, ** p < 0.01, **** p < 0.0001.

RESULTS

Age

To test the suggestion that young and aged fish reproduce less successfully than mature adults, the retrospective data was binned into one of three age categories: young (2–6 months), adult (7–10 months), and aged (11+ months). Age had a significant effect on clutch success [F (2, 281) = 29.59, p < 0.0001] (**Figure 2A**) and clutch size [F (2, 129) = 9.578, p = 0.0001] (**Figure 2B**). Aged fish produced significantly fewer clutches (M = 0.16 ± 0.03) than young fish (M = 0.54 ± 0.06) or adults (M = 0.61 ± 0.05). Though clutch success was comparable between young fish and adults, adults produced larger clutches (M = 197.3 ± 21.89, p < 0.0001) than either young (M = 90.00 ± 9.31) or aged fish (M = 135.1 ± 30.75). Analysis of a single tank of fish over the course of one year highlighted the consistency of the pattern of clutch success (**Figure 2A**) and revealed that these experienced breeders who were spawned routinely produced significantly larger clutches (M = 295.1 ± 59.58) as they aged [F (2, 34) = 3.484; p = 0.042] (**Figure 2B**). Peak clutch probability and size occurred at eight months of age (data not shown).

Fish groupings

Clutch probability and size were compared between male-female pairs, female-dominant groups, male-dominant groups, and equal sex groups (Figure 3A). Clutch probability was significantly greater for groups (group M = 0.60 ± 0.05) versus pairs (M = 0.35 ± 0.03; p < 0.0001; Figure 3B). Significant differences in clutch success emerged between male-dominant, equal sex breeding (equal sex groups and pairs combined), and female-dominant groupings [F (2, 269) = 7.366, p = 0.0008]. Male-dominant groups had significantly greater clutch probability (M = 0.66 ± 0.07) than equal sex groups (M = 0.37, ± 0.03; p = 0.0006; Figure 3C). The number of eggs per clutch was comparable between groups and pairs (group M = 149.8 ± 16.57 versus pairs 131.4 ± 14.45, p > 0.05) when controlled for the number of females present (Figure 3D). Clutch sizes by sex ratio followed a similar pattern as clutch success, with the largest clutches occurring in male-dominant groupings [F (2, 135) = 3.512; p = 0.0326] (Figure 3D). Data from the single tank revealed contradictory results. Pairs and groups produced clutches with equal frequency (Figure 3B) while females produced more eggs in a group setting (group M = 319.4 ± 54.33 versus pairs 150.1 ± 22.68, p = 0.0033; Figure 3D). For the colony as a whole, groups of fish with males outnumbering females had the highest reproductive success by both measures of success.

The effect of sex ratios was tested with groups of four (Figure 3A). Clutch success was highest in equal sex groupings (Figure 3C; M = 0.52 ± 0.03) [F (2, 584) = 5.819; p = 0.0295]. Females produced the largest clutches when outnumbered by males (Figure 3E; M = 118.2 ± 13.65) [F (2, 485) = 26.23; p < 0.0001].

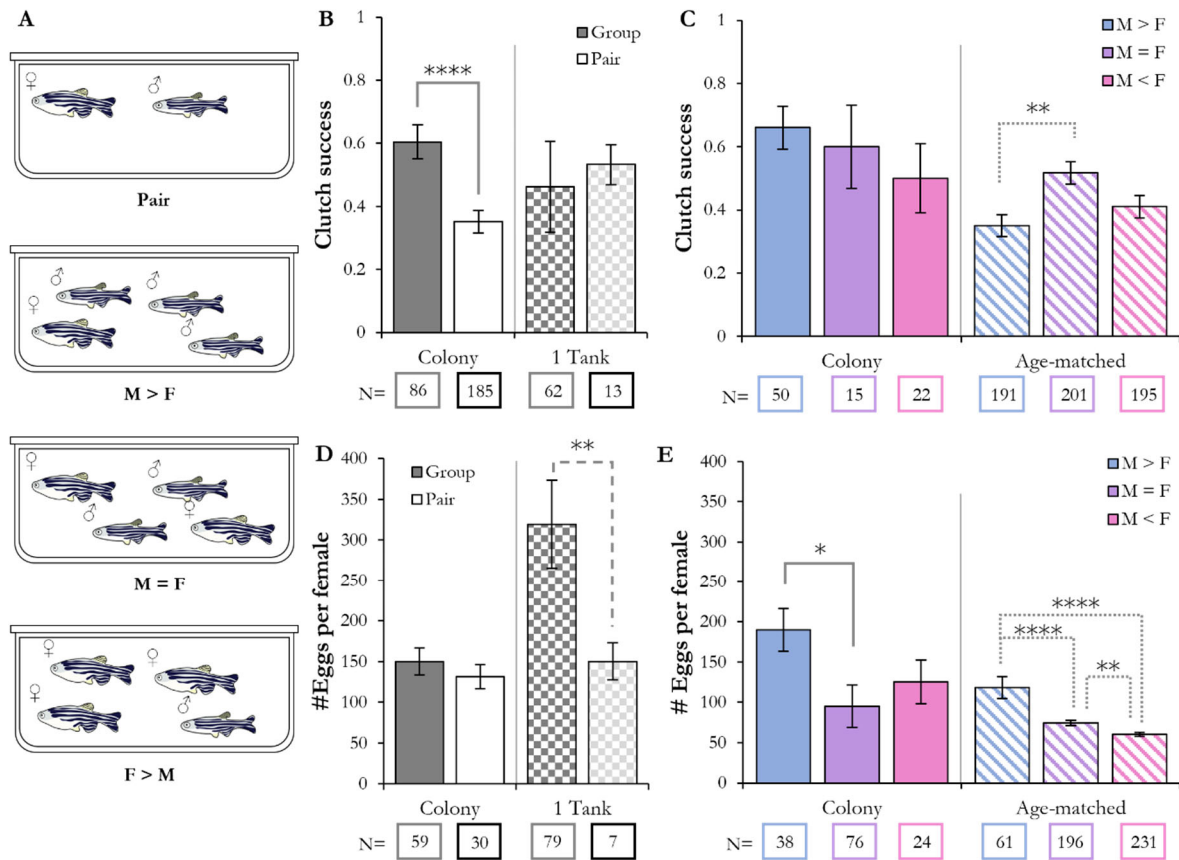


Figure 3. Male-dominant groupings enhance reproductive success. **A.** Pairs, equal sex (M = F), male-dominant (M > F), and female-dominant groupings (M < F) were compared from all fish (colony), a single tank (checkered bars), and age-matched groups (striped bars). **B.** Groups of fish had higher clutch success than pairs. **C.** Equal sex groups had highest clutch success in age-matched fish, but not in the colony as a whole. **D.** For most of the colony, females lay equal numbers of eggs in pair or group settings. However, the fish in this sample tank produced more eggs in group settings. **E.** Females produced larger clutches when outnumbered by males in the colony and in age-matched tanks. Values depict mean ± SEM. N = number of spawning events, indicated under each bar. Statistical significance tested by unpaired t-tests (B/D) or one-way ANOVA with Tukey’s multiple comparisons test (C/E). * p < 0.05, ** p < 0.01, *** p < 0.001, **** p < 0.0001.

Tank additions

Dividers separated the sexes overnight, a single plastic plant was used to provide shelter and hiding places, and marbles were

meant to mimic spawning substrates like rocks (Figure 4A). From the retrospective analysis, the use of dividers did not affect clutch probability or size (Figure 4B). Clutch size and egg probability were compared between tanks with no substrate, or any substrate (a plant, marbles, or both plant and marbles). The clutch probability and size were not significantly different. When comparing each habitat substitute separately, clutch probability and size between these groups were not statistically significant (Figures 4C and 4D). However, the presence of both marbles and plants significantly increased clutch success [$F(3, 305) = 3.701$; $p = 0.0121$].

In age-matched groups, clutch probability was comparable between substrate conditions [$F(3, 865) = 1.173$; $p = 0.3188$, not significantly different, Figure 4C], while the clutch size differed between conditions [$F(3, 479) = 5.674$, $p = 0.0008$]. Fish spawned with both marbles and plants produced the largest clutches (Figure 4D; $M = 87.06 \pm 7.879$) and without any substrate produced the smallest clutches ($M = 58.05 \pm 7.879$). The use of any type of substrate, versus none, was associated with significantly larger clutches ($p = 0.0007$ Figure 4D).

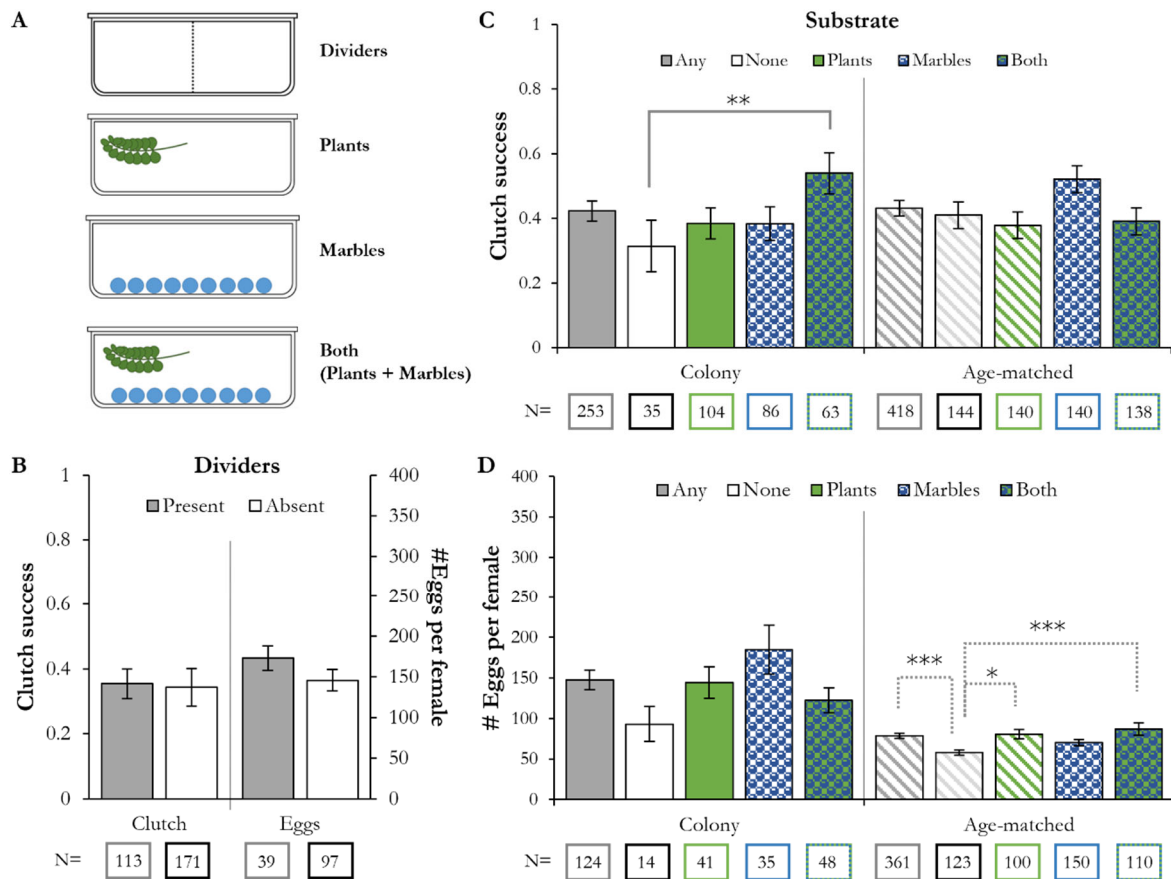


Figure 4. A habitat substitute increases reproductive success. **A.** Tank additions include clear dividers, plants, and marbles. **B.** The use of dividers had no effect on clutch probability or size. **C.** Presence versus absence of any substrate (plants, marbles, or both) did not significantly affect the probability of clutch success. Marbles + plants offered additional benefit to increase clutch success in the colony but not the age-controlled experimental groups (striped bars). **D.** Type of substrate had no significant impact on the number of eggs per female in the colony at large, while age-matched fish produced slightly larger clutches with marbles and/or plants. Values depict mean \pm SEM. N = number of spawning events, indicated under each bar. Statistical significance tested by unpaired t-tests (B) or one-way ANOVA with Tukey’s multiple comparisons test (C/D). * $p < 0.05$, ** $p < 0.01$, *** $p < 0.001$.

Spawning room parameters

Spawning tanks were placed on a shelf in either the standard housing room or the fry incubator (Figure 5A). Egg probability and clutch sizes between groups spawned in the incubator and housing room were not statistically significant, though there was a trend toward larger clutches in the housing room ($p = 0.06$; Figure 5B). While each tank substrate (plants, marbles) independently did not affect spawning success, nor did the spawning location, the room and tank additions mattered depending on the combination of these factors. Fish were more likely to lay eggs in the housing room if plants were present ($M = 0.48 \pm 0.05$) and more likely to spawn in the incubator if plants were absent ($M = 0.46 \pm 0.07$) [$F(1, 276) = 5.49$; $p = 0.0198$] (Figure

5C). Clutches were of comparable size in these conditions. Reproductive success in the presence of marbles did not show this pattern.

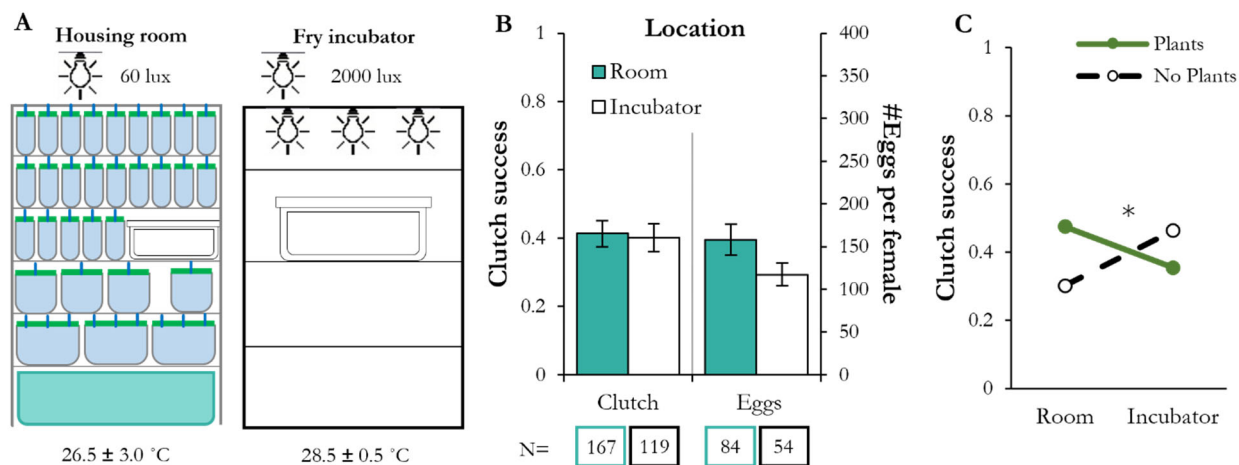


Figure 5. The spawning location does not affect reproductive success. **A.** The standard housing room and fry incubator have different temperature and lighting conditions. **B.** Fish spawned in the room and incubator had equal spawning success and clutch sizes. **C.** Plants best predicted spawning success in the standard housing room. Values depict mean \pm SEM. N = number of spawning events, indicated under each bar. Statistical significance tested by unpaired t-tests (B) and two-way ANOVA with Tukey’s multiple comparisons tests (C). * $p < 0.05$.

Seasonal effect

From the retrospective analysis, there was a significant effect of season on breeding success of laboratory-raised zebrafish [F (3, 289) = 6.297; $p = 0.0004$]. Spawning in the winter (Jan–Mar) or spring (Apr–Jun) was associated with higher clutch probability (winter $M = 0.49 \pm 0.05$; spring $M = 0.65 \pm 0.08$) and summer (Jul–Sep) spawning had the lowest clutch success ($M = 0.31 \pm 0.05$) (Figure 6A). Differences in clutch size followed the same pattern [F (3, 138) = 4.035; $p = 0.0087$] (Figure 6B), with largest clutches in the spring ($M = 186.9 \pm 31.62$). Analysis of the single tank of fish over the course of one year followed similar trends as the larger colony. This particular tank produced significantly more eggs in the spring [F (3,33) = 2.987; $p = 0.0451$], despite being older than ten months at the time. Compared to the clutch probability of fish in this age group, these fish had significantly higher clutch success ($p = 0.04$). Reproductive success was highest when fish were spawned in the spring and poorest in the summer. When controlled for age reproductive success was poorest by both measures in the fall, with fewer ($M = 0.11 \pm 0.03$ [F (3, 576) = 33.52; $p < 0.0001$, Figure 6A] and smaller clutches ($M = 49.72 \pm 4.723$) [F (3, 484) = 8.523; $p < 0.0001$, Figure 6B].

DISCUSSION

Zebrafish gained popularity as an experimental model in part because they breed well in captivity. Even so, zebrafish reproduction is incredibly variable between individual fish, genetic lines and strains, and institutions. Spawning success in zebrafish requires knowledge and some intuition that many fish facility staff or researchers do not have. Because of this, the techniques used at different institutions have created confusion regarding best spawning practices. This set of experiments retrospectively analyzed and subsequently tested published and anecdotal best practices for laboratory-housed zebrafish spawning success through correlative analysis over two years and subsequent manipulations. These results should guide zebrafish users to maximize spawning success. The probability of clutch success (presence or absence of eggs) and the number of eggs per female were compared with the following tracked or manipulated variables: age, sex ratios, groupings, habitat substitutes, dividers, light intensity, temperature fluctuations, and seasons. While some of these results support published recommendations, there are several instances that are in direct contrast to such recommendations.

Previous publications reported that adults between the ages of 7–12 months lay the most eggs^{3,7} Consistent with previous published reports, the probability of clutch success and the size of individual clutches were highest among fish aged seven to ten months, though with an exception: consistent breeders continue to produce frequent, large clutches well beyond ten months. The current study found the most frequent and largest clutches were produced by eight-month-old fish. This coincides with the suggestion that while zebrafish can live and reproduce well beyond one year, in reality they function as an annual species.³⁰ While the benefits of spawning 7–10 month-old fish is clear, it is encouraging that fish as old as 25 months are capable of spawning

successfully because this expands the timeframe that fish may be useful, particularly among transgenic fish that may otherwise be precious and maintained in a colony longer than would their wild-type counterparts. Furthermore, highly fecund fish that are spawned regularly continued to produce large clutches beyond ten months of age, suggesting that consistent breeders, which are known to have greater reproductive success³ need not be retired until fertility declines. One limitation to the interpretation of the current data, particularly with respect to aging, is that the present analysis did not track viability of eggs or survival of larvae. As such, egg quality may indeed vary with the age of the parents as some have previously suggested, at least in young parents.³

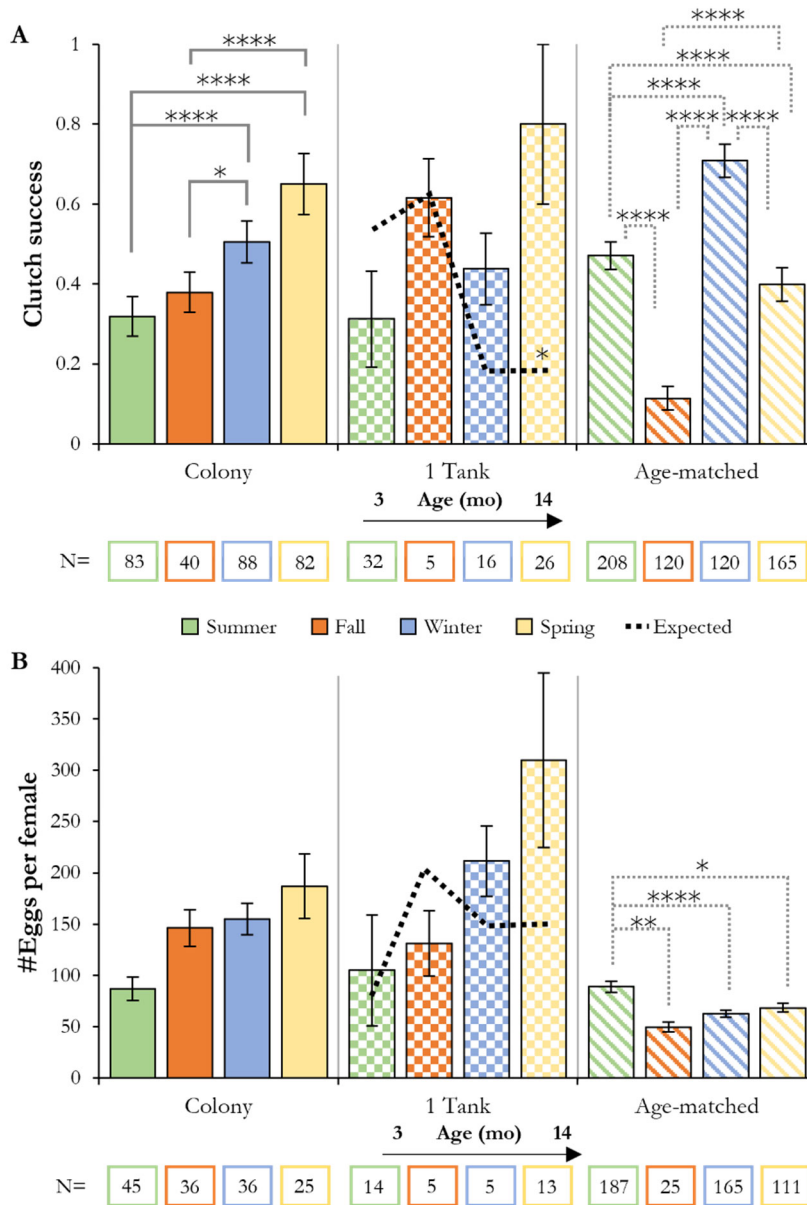


Figure 6. Laboratory-housed zebrafish exhibit seasonal spawning patterns. **A.** Zebrafish clutch success was highest in the spring (April–June, yellow) and lowest in the summer (July–September, green) for both the colony and a single tank (checkered bars). The age-matched controls (striped bars) had higher clutch success in winter (January–March, blue). **B.** Clutch size followed the same pattern, with the largest clutches in spring. A single tank of fish bred over an entire year followed the same trends. These patterns did not match predicted reproductive success based on the age of the single tank (dotted line, * on bar). The age-matched fish produced smaller clutches overall, but with the largest in summer. Values depict mean ± SEM. N = number of spawning events, indicated under each bar. Statistical significance tested by one-way ANOVA with Tukey’s multiple comparisons test. * p < 0.05, ** p < 0.01, **** p < 0.0001.

While the age-related decline in fertility is clear, it is expected that the apparent sharp decline in fertility after ten months is in reality more gradual, as the current dataset did not have spawning data for every month of age after ten months, but rather binned

by ages into young, adult, and aged fish. Fish as young as two months old successfully reproduced. Because the age at which zebrafish reach sexual maturity spans a range of months^{7, 14} size is a better indicator of sexual maturity. Precise assessment of the contribution of size to spawning success can be stressful for the fish because it requires significant handling³¹ and is likely unnecessary for routine spawning. Because size has been previously linked to reproductive success,^{8, 10, 32} the current report assessed raw age independent of size. These data support spawning fish once males and females can be visually distinguished, regardless of the exact age.

Laboratory-raised fish are often spawned in groups.^{7, 14, 15} Previous data suggested highest egg success would be achieved with female-dominant groupings (more females than males).^{7, 12, 18} The present data suggests rather the opposite - females were more likely to lay eggs when outnumbered by males or when not competing with another female. Some groups have reported male-dominant large groups generate more eggs because it ensures all females have access to a mate,²⁰ which the present data supports. Spawning fish in groups, as is common in laboratory settings, led to higher clutch probability, but not larger clutches than pair-spawning. This suggests two possibilities: females may lay fewer eggs in a group setting, or not all females are laying eggs in these groups. Without directly assessing parentage, the latter scenario is likely, given that our data indicate that the clutch size is consistent between all groups of four fish, regardless of sex ratio. The previous reports that females prefer to spawn with a favorite male³² and that wild fish spawn in pairs¹³ suggests the primary benefit of group spawning is an increased likelihood of matching a preferred spawning pair together. Therefore, spawning fish in groups from the same home tank best ensures reproductive success by allowing females to choose their preferred mate, which could also be one reason why clutch success was greater in male-dominant groups - the single female was more likely to be paired with her preferred mate without any same sex competitors. Recommended spawning practice is therefore to set up groups of two males and one female.

The greater success of male-dominant groups also suggests that the presence of multiple females may actually decrease egg production, possibly due to intrasex conflict. This finding is in direct contrast to published recommended spawning practices promoting female-dominant groups^{7, 14, 18} that perhaps did not take female choice preference and female-female competition into account. Males and females both initiate intrasex aggression,^{33, 34} exhibiting such behaviors as chasing, circling, and biting. Because chasing and circling are exhibited during mating displays between males and females,^{35, 36} the present study did not specifically assess these behaviors. Quantifying intrasex competition in spawning tanks may correlate with reproductive success in group spawning. While group spawning was associated with greater clutch probability, it is important to note that pairs laid similar sized clutches as group breeders because laboratory experiments often require controlling for the parental genotype, often necessitating pair breeding. The current results suggest that successful pairs lay equally large clutches as group breeders. Pairs that fail to breed may benefit most from simply trading for a different mate.

Many researchers spawn with clear plastic dividers to segregate males and females overnight in an effort to increase spawning success.^{4, 19, 20} Dividers separate males and females while allowing them to detect pheromones and visual cues (**Figure 4A**). When spawning pairs of zebrafish, some researchers recommended segregating the fish using clear plastic dividers to allow fish to observe visual and olfactory cues prior to mating.^{21, 22} The practice of using dividers in the spawning tank is purported to increase reproductive success⁴ and to allow more controlled timing of egg laying.^{19, 20} The present study found no significant differences in clutch probability or size with the use of dividers. Segregating the sexes within the spawning tank is time-consuming and the current findings are important not only because it suggests segregating fish before dawn offers no benefit in the frequency of spawning events or number of eggs, but also because the use of dividers did not hinder reproductive success. Therefore, the use of dividers that are removed when eggs are desired can allow more controlled timing of breeding without significantly impacting egg production.

Perhaps one of the most varied parameters in zebrafish spawning between institutions and users is the use of habitat substitutes in the spawning tank.^{7, 12, 27, 37} The present results suggest that fish are more likely to spawn in the presence of some sort of habitat substitute, and the use of both plants and marbles maximized clutch size.

At times it is necessary to change the spawning environment. Fish may be transferred to different breeding rooms after quarantine, or may be transferred to a housing system on a shifted light cycle to generate eggs at a different time of day. This experiment used two spawning rooms to estimate the impact these types of scenarios may have on reproductive success. The fry incubator has a higher, more stable temperature, higher daytime luminescence, and fewer sources of potential light pollution than does the standard housing room. The housing room has more potential sources of light pollution (door gaps, monitoring system LEDs) that may negatively affect reproductive success.²⁵ There were no significant differences in clutch probability or size between these two rooms, suggesting that fish have a wide range of tolerance for temperature fluctuations and light intensity, and these factors do not significantly influence spawning success. These results are limited in that it is not possible from the current dataset to distinguish the contributions of each of these variables individually. Air (and therefore tank water) temperature fluctuations during the day or across seasons, as well as light levels, could potentially affect reproductive success independently.

However, the fact that the fish show wide ranges of tolerance for temperature fluctuation, light level, and basic room differences is encouraging because it means that zebrafish can be transferred to different housing rooms or light cycles as is experimentally relevant with minimal impact on reproductive success. The spawning location did affect fish behavior in that fish exhibited a preference for plants when spawning in the standard housing room. While the reason for this preference is unclear, the difference in illumination of the two locations may play a role. Fish behavior may be different in the spawning environments due to stress and differences in social interactions. In the incubator, where light is brighter and the water is warmer, fish may be more vigilant for predators and engage in fewer intraspecific conflicts, while in the housing room, fish are using the plants as hiding places to escape from aggressive mates or as territories to be guarded.³⁸ Further experiments would be necessary to test these possibilities.

Anecdotally, zebrafish researchers often experience a spawning slump during the summer months and this was the impetus for the present study. Laboratory-housed fish are kept year-round on a 14:10 h light:dark cycle to mimic their natural spawning season to generate eggs year-round,^{7, 13} and fed a standard diet, eliminating seasonal differences in prey that have been suggested as a source of seasonal spawning differences.¹⁵ Water quality and temperature are consistent year-round. In spite of these controls, there was a strong effect of season on laboratory-housed zebrafish spawning. Fish produced more frequent, larger clutches in spring. Importantly, this seasonality trend does not appear to be correlated with the ages of the fish. Using age-related spawning data from both previous data^{3, 7} and results from this paper, the expected seasonal output of the single tank of fish was expected to be highest between fall and winter, when these fish were 6–11 months old. Instead, their reproductive output was highest in the spring when they were 12–14 months old (**Figure 6**). Because these lab-raised fish are kept on a consistent light cycle, water temperature, and nutrition source, the fish may be detecting some other factor of seasonality that is not being controlled in the laboratory environment. This raises the question, what are they detecting? One possibility is barometric pressure. Rapid drops in barometric pressure, as occur preceding precipitation events, changes the behavior of wild fish and sharks,^{39–41} which could affect reproductive behavior. Regardless of the underlying cause, this seasonal breeding component should be kept in consideration for experiments requiring frequent clutches. Experiments that require frequent clutches of eggs would be best suited for winter or spring months whenever possible, and setting up extra spawning tanks during the summer and fall may be necessary to generate sufficient eggs.

CONCLUSIONS

Studies researching zebrafish spawning practices in a laboratory setting are important because of the magnitude of zebrafish use in science. It is also important to study spawning in order to maximize spawning events and egg count for research in which zebrafish are used as a model. The optimal conditions were groups of three fish (two males and one female) aged seven to ten months spawned in the spring with both plants and marbles in the spawning tank. These data support the implementation of simple steps that reliably maximize reproductive success of laboratory zebrafish.

ACKNOWLEDGEMENTS

The authors thank the animal care facility workers and KM Dunn for maintaining the facility and JC Weinberger and KM Dunn for thoughtful comments on the manuscript.

This work was supported by the NSF KY EPSCoR under Grant 1355438 (3200000271-023) awarded to DH-W, KY INBRE under NIH 8P20GM103436 awarded to DH-W, and the U.S. Department of Education, McNair Grant #P217A090330 to Murray State University awarded to ES.

REFERENCES

1. Harper, C., and Lawrence, C. (2011) *The laboratory zebrafish*. CRC Press, Boca Raton, FL.
2. Lieschke, G. J., and Currie, P. D. (2007) Animal models of human disease: zebrafish swim into view. *Nat Rev Genet* 8(5), 353–367. <https://doi.org/10.1038/nrg2091>
3. Nasiadka, A., and Clark, M. D. (2012) Zebrafish breeding in the laboratory environment. *ILAR J* 53(2), 161–168. <https://doi.org/10.1093/ilar.53.2.161>
4. Avdesh, A., Chen, M., Martin-Iverson, M. T., Mondal, A., Ong, D., Rainey-Smith, S., Taddei, K., Lardelli, M., Groth, D. M., Verdile, G., and Martins, R. N. (2012) Regular care and maintenance of a zebrafish (*Danio rerio*) laboratory: an introduction. *J Vis Exp* 69, e4196. <https://doi.org/10.3791/4196>
5. Markovich, M. L., Rizzuto, N. V., Brown, P. B. (2007) Diet affects spawning in zebrafish. *Zebrafish* 4(1), 69–74. <https://doi.org/10.1089/zeb.2006.9993>
6. Ramsay, J. M., Watral, V., Schreck, C. B., and Kent, M. L. (2009) Pseudoloma neurophilia infections in zebrafish *Danio rerio*: effects of stress on survival, growth, and reproduction. *Dis Aquat Organ* 88(1), 69–84. <https://doi.org/10.3354/dao02145>
7. Westerfield, M. (2000) *The zebrafish book*. A guide for the laboratory use of zebrafish (*Danio rerio*). University of Oregon Press: Eugene, OR.

8. Paull, G. C., Van Look, K. J., Santos, E. M., Filby, A. L., Gray, D. M., Nash, J. P., and Tyler, C. R. (2008) Variability in measures of reproductive success in laboratory-kept colonies of zebrafish and implications for studies addressing population-level effects of environmental chemicals. *Aquat Toxicol* 87(2), 115–126. <https://doi.org/10.1016/j.aquatox.2008.01.008>
9. Spence, R., and Smith, C. (2006) Mating preference of female zebrafish, *Danio rerio*, in relation to male dominance. *Behav Ecol* 17(5), 779–783. <https://doi.org/10.1093/bebeco/arl016>
10. Uusi-Heikkilä, S., Wolter, C., Meinelt, T., and Arlinghaus, R. (2010) Size-dependent reproductive success of wild zebrafish *Danio rerio* in the laboratory. *J Fish Biol* 77(3), 552–569. <https://doi.org/10.1111/j.1095-8649.2010.02698.x>
11. Gerlach, G. (2006) Pheromonal regulation of reproductive success in female zebrafish: female suppression and male enhancement. *Anim Behav* 72(5), 1119–1124. <https://doi.org/10.1016/j.anbehav.2006.03.009>
12. Spence, R., and Smith, C. (2005) Male territoriality mediates density and sex ratio effects on oviposition in the zebrafish, *Danio rerio*. *Anim Behav* 69(6), 1317–1323. <https://doi.org/10.1016/j.anbehav.2004.10.010>
13. Hutter, S., Penn, D. J., Magee, S., and Zala, S. M. (2010) Reproductive behaviour of wild zebrafish (*Danio rerio*) in large tanks. *Behaviour* 147(5/6), 641–660. <https://www.jstor.org/stable/27822142>
14. Tsang, B., Zahid, H., Ansari, R., Lee, R. C., Partap, A., and Gerlai, R. (2017) Breeding Zebrafish: A Review of Different Methods and a Discussion on Standardization. *Zebrafish* 14(6), 561–573. <https://doi.org/10.1089/zeb.2017.1477>
15. Spence, R., Gerlach, G., Lawrence, C., and Smith, C. (2008) The behaviour and ecology of the zebrafish, *Danio rerio*. *Biol Rev Camb Philos Soc* 83(1), 13–34. <https://doi.org/10.1111/j.1469-185X.2007.00030.x>
16. Eaton, R. C., and Farley, R. D. (1974) Spawning cycle and egg production of zebrafish, *Brachydanio rerio*, in the laboratory. *Copeia* 1, 195–204. <http://jstor.org/stable/1443023>
17. Ruhl, N., McRobert, S. P., and Currie, W. J. (2009) Shoaling preferences and the effects of sex ratio on spawning and aggression in small laboratory populations of zebrafish (*Danio rerio*). *Lab Anim* (NY) 38(8), 264–269. <https://doi.org/10.1038/labani0809-264>
18. Grimaldi C. (2018) Couples Counselling for Zebrafish: How to Optimize Breeding Efficiency. Science Squared Ltd / Bitesize Bio: Gorebridge, Midlothian, UK. <https://bitesizebio.com/41018/couples-counselling-for-zebrafish-how-to-optimize-breeding-efficiency/> (Accessed Mar 2023)
19. Meyers, J.R. (2018) Zebrafish: Development of a Vertebrate Model Organism. *Curr Protoc* (1), e19. <https://doi.org/10.1002/cpet.19>
20. Adatto, I., Lawrence, C., Thompson, M., and Zon, L. I. (2011) A new system for the rapid collection of large numbers of developmentally staged zebrafish embryos. *PLoS One* 6(6), e21715. <https://doi.org/10.1371/journal.pone.0021715>
21. Cavallino, L., Valchi, P., Morandini, L., and Pandolfi, M. (2019) Modulation of behavior in zebrafish, *Danio rerio*, according to female reproductive status and visual and chemical cues. *Mar Freshw Behav Phy* 52(1), 53–66. <https://doi.org/10.1080/10236244.2019.1635886>
22. Hutter, S., Hettzey, A., Penn, D. J., and Zala, S. M. (2012) Ephemeral Sexual Dichromatism in Zebrafish (*Danio rerio*). *Ethology* 118, 1208–1218. <https://doi.org/10.1111/eth.12027>
23. van den Hurk, R. and Lambert, J. G. D. (1983) Ovarian steroid glucuronides function as sex pheromones for male zebrafish, *Brachydanio rerio*. *Can J Zool* 61(11), 2381–2387. <https://doi.org/10.1139/z83-317>
24. Vargas R, Mackenzie S, and Rey S. (2018) 'Love at first sight': The effect of personality and colouration patterns in the reproductive success of zebrafish (*Danio rerio*). *PLoS One* 13(9), e0203320. <https://doi.org/10.1371/journal.pone.0203320>
25. Adatto, I., Krug, L., and Zon, L. I. (2016) The Red Light District and Its Effects on Zebrafish Reproduction. *Zebrafish* 13(3), 226–229. <https://doi.org/10.1089/zeb.2015.1228>
26. Goolish, E. M., Evans, R., Okutake, K., and Max, R. (1998) Chamber Volume Requirements for Reproduction of the Zebrafish *Danio rerio*. *Prog Fish Cult* 60(2), 127–132. [https://doi.org/10.1577/1548-8640\(1998\)060%3C0127:CVRFRO%3E2.0.CO;2](https://doi.org/10.1577/1548-8640(1998)060%3C0127:CVRFRO%3E2.0.CO;2)
27. Spence, R., Ashton, R., and Smith, C. (2007) Oviposition decisions are mediated by spawning site quality in wild and domesticated zebrafish, *Danio rerio*. *Behaviour* 144(8), 953–966. <https://www.jstor.org/stable/4536490>
28. Tsang, B., and Gerlai, R. T. (2022) Common Aquarium Plants as an Enrichment Strategy in Zebrafish Facilities. *Zebrafish* 19(6) 218–223. <https://doi.org/10.1089/zeb.2022.0036>
29. Gerlai, R. (2023) Zebrafish (*Danio rerio*): A Newcomer With Great Promise in Behavioral Neuroscience. *Neurosci Biobehav Rev* e104978. <https://doi.org/10.1016/j.neubioren.2022.104978>
30. Spence, R., Fatema, M. K., Ellis, S., Ahmed, Z. F., and C. Smith (2007) Diet, growth and recruitment of wild zebrafish in Bangladesh. *J Fish Biol* 71, 304–309. <https://doi.org/10.1111/j.1095-8649.2007.01492.x>
31. Ramsay, J. M., Feist, G. W., Varga, Z. M., Westerfield, M., Kent, M. L. and Schreck, C. B. (2009) Whole-body cortisol response of zebrafish to acute net handling stress. *Aquaculture* 297(1–4), 157–162. <https://doi.org/10.1016/j.aquaculture.2009.08.035>
32. Spence, R., Jordan, W. C., and Smith, C. (2006) Genetic analysis of male reproductive success in relation to density in the zebrafish, *Danio rerio*. *Front Zool* 3(5). <https://doi.org/10.1186/1742-9994-3-5>

33. Zabegalov, K. N., Kolesnikova, T. O., Khatsko, S. L., Volgin, A. D., Yakovlev, O. A., Amistislavskaya, T. G., Friend, A. J., Bao, W., Alekseeva, P. A., Lakstygal, A. M., Meshalkina, D. A., Demin, K. A., de Abreu, M. S., Rosemberg, D. S., and Kaleuff, A. V. (2019) Understanding zebrafish aggressive behavior. *Behav Process* 158, 200–210. <https://doi.org/10.1016/j.beproc.2018.11.010>
34. Paull, G. C., Filby, A. L., Giddins, H. G., and Coe, T. S. (2010) Dominance hierarchies in zebrafish (*Danio rerio*) and their relationship with reproductive success. *Zebrafish* 7(1), 109–117. <https://doi.org/10.1089/zeb.2009.0618>
35. Yabuki, Y., Koide, T., Miyasaka, N., Wakisaka, N., Masuda, M., Ohkura, M., Nakai, J., Tsuge, K., Tsuchiya, S., Sugimoto, Y., and Yoshihara, Y. (2016) Olfactory receptor for prostaglandin F2 α mediates male fish courtship behavior. *Nat Neurosci* 19(7), 897–904. <https://doi.org/10.1038/nn.4314>
36. Yong, L., Thet, Z., and Zhu, Y. (2017) Genetic editing of the androgen receptor contributes to impaired male courtship behavior in zebrafish. *J Exp Biol* 220(Pt 17), 3017–3021. <https://doi.org/10.1242/jeb.161596>
37. Ghoshal, A., Daniel, D. K., and Bhat, A. (2019) Temporal patterns and sex differences in dyadic interactions in a wild zebrafish population. *Behav Process* 166, e103896. <https://doi.org/10.1016/j.beproc.2019.103896>
38. Woodward, M. A., Winder, L. A., and Watt, P. J. (2019) Enrichment Increases Aggression in Zebrafish. *Fishes* 4(1), 22. <https://doi.org/10.3390/fishes4010022>
39. Udyawer, V., Chin, A., Knip, D. M., Simpfendorfer, C. A., and Heupel, M. R. (2013) Variable response of coastal sharks to severe tropical storms: environmental cues and changes in space use. *Mar Ecol Prog Ser* 480, 171–183. <https://doi.org/10.3354/meps10244>
40. Heupel, M. R., Simpfendorfer, C. A., and Hueter, R. E. (2003) Running before the storm: blacktip sharks respond to falling barometric pressure associated with Tropical Storm Gabrielle. *J Fish Biol* 63, 1357–1363. <https://doi.org/10.1046/j.1095-8649.2003.00250.x>
41. Sackett, D. K., Able, K. W., and Grothues, T. M. (2007) Dynamics of summer flounder, *Paralichthys dentatus*, seasonal migrations based on ultrasonic telemetry. *Estuar Coast Shelf S* 74(1–2), 119–130. <https://doi.org/10.1016/j.ecss.2007.03.027>

ABOUT STUDENT AUTHORS

Sydni Anderson graduated from Murray State University in 2020 with a degree in biomedical sciences and a minor in chemistry. She began research with Dr. Hammond-Weinberger in 2017. Sydni is currently attending University of Kentucky College of Medicine. Elizabeth Sipes is a member of the Ronald E. McNair Baccalaureate program majoring in mathematics with minors in biology and chemistry. Following her anticipated 2024 graduation, she plans to continue with graduate education in mathematics. Megan Franke will be graduating from Murray State University in 2025 with a degree in the polymer and materials science track, with a minor in physics. She is a part of the governor's scholars program alumni, and worked with Dr. Hammond-Weinberger in 2022. She now works towards her goal of nuclear engineering and free energy production.

PRESS SUMMARY

Zebrafish are common biological model organisms that are bred in laboratory settings. This study identified conditions that promote maximum clutch probability and size in laboratory zebrafish. These data support the implementation of simple steps that reliably maximize reproductive success of laboratory zebrafish while raising some interesting questions about how zebrafish exhibit seasonal behaviors in a climate-controlled environment.

Color Saturation: Upper and Lower Percentage Histogram Manipulation

Kyra Obert^{*1}, Maria Schudt¹, & Ian Bentley^{1,2}

¹Department of Chemistry and Physics, Saint Mary's College, Notre Dame, IN

²Department of Engineering Physics, Florida Polytechnic University, Lakeland, FL

<https://doi.org/10.33697/ajur.2023.080>

Students: kobert01@saintmarys.edu*, mschudt01@saintmarys.edu

Mentor: ibentley@floridapoly.edu

ABSTRACT

There are various color correction techniques that can be applied to digital photographs to account for environmental lighting variations. This manuscript contains a proposed method for such color correction. The method involves saturating an image by a specified percentage of its pixels via upper and lower percentage histogram manipulation using the image's RGB histograms. Variations of this new technique, the white balance (WB) correction method, and a multi-variable fit are used to test its performance against common color correction techniques. The findings demonstrate that the upper and lower percentage histogram manipulation method is not only more applicable to photos because it doesn't require calibration regions to be sampled but it is also more consistent in its correction of photos when there are substantial gray scale features (e.g. a black and white grid or text). Our motivation for testing these techniques is to find the most robust color correction technique that is broadly applicable (not requiring a color checker chart) and is consistent across different lighting.

KEYWORDS

Color Correction; Histogram Manipulation; Saturation; White Balance; Scientific Image Analysis; Color Comparisons; Euclidean Distance; Standard Deviation; Color Difference

INTRODUCTION

The RGB values for each pixel in a digital image range between 0 and 255 and combine to define each pixel's color. Color correction is used in digital imaging to edit an image to achieve a desired effect or remove effects due to environmental factors, such as lighting. Variations in lighting can distort colors and change the RGB values interpreted and stored in by a camera for pixels in an image.

The importance of color correction extends to general photography, film-making, and photo analyses for scientific studies. In particular, the color correction techniques compared and discussed throughout this paper are of interest to be applied to the Scientific Image Analysis (SIA) application.¹ The SIA application is currently being used for biological studies of motion and has also been produced as a standalone tracking application called BatCount² which also relies on the color correction technique described in this manuscript to increase the contrast on images.

Previous work in color correction

Due to its applications in both the scientific and entertainment communities, several color correction techniques have been extensively developed and compared for their intended uses. Some of the alternative correction types consider or focus on one or two specific issues in image production due to limitations in photography, such issues include flares,

illumination settings, and weather.³⁻¹⁰ Although white balance is commonly used in the camera industry, several other methods have been proposed and advocated for in favor over white balance. Nonetheless, white balance is frequently used as the metric to compare proposed techniques against.^{4, 6, 8}

MATLAB was used to test our color correction technique. MATLAB contains a variety of functions for correction methods. One of the correction techniques used in MATLAB is *imadjust*. This function, like the technique studied in this manuscript, adjusts the intensity of image input values so that a percentage of the data is saturated to low and high intensities.¹¹ The default of the correction method with a grayscale image is 1%. One of the variations we make in the analysis described in this manuscript is to change this saturation percentage. When considering the various MATLAB contrast enhancement techniques in grayscale, *imadjust* is also compared to the *histeq* and *adapthisteq* functions. The function *histeq* adjusts the histogram values of the image so that the histogram of the resulting image approximates a specified histogram, with the default setting being a uniform distribution.¹¹ This adjustment is referred to as “histogram equalization.” The other function, *adapthisteq*, applies a similar technique to *histeq* but by analyzing smaller regions across the image to compute and make appropriate adjustments.¹¹ This approach is known as “contrast-limited adaptive histogram equalization” and is used to reduce the amount of noise that may otherwise be amplified through *histeq*.

The variations in these styles is used to address specific image types and issues. The *imadjust* method, in particular, is effective in having a clear effect on images whose histogram distributions are concentrated in the center of the histogram. Images that are more uniformly distributed already have RGB values closer to the ends of the intensity spectrum, reducing the effectiveness of *imadjust* creating contrast in an image.¹¹

Similarly, *histeq* maintains difficulties with adjusting images with both concentrated and uniformly distributed histograms. While this method effectively reveals details hidden in an image, it often also over-saturates areas, especially those that are lighter in the original image.¹¹ The adaptability of *adapthisteq* makes it the most preferable method in most cases of an equally distributed histogram, as it computes for appropriate adjustments across the image while also allowing the user to limit the amount of contrast enhancement in the image.¹¹ The latter of these characteristics is particularly helpful in reducing the over-saturation demonstrated by *histeq*.

These techniques can also be applied to color images. In order to do this, colored (RGB) images are converted to a color space that has luminosity as one of its channels.¹¹ In each of the methods, only the values in the luminosity layer are adjusted before the image is converted back to RGB space. This method allows the pixels colors to be maintained while their intensity is appropriately adjusted.

Methods of white balance used in MATLAB and ones similar to these methods have also formally been tested. One report compared various automatic white balance techniques: the gray world assumption, the perfect reflector algorithm, and a proposed Gaussian distribution technique.¹² The gray world assumption concludes that if there is enough color in an image, then the average values of each R, G, and B tend to be the same. However, if the color in an image does not follow this specification in variety, this method often fails. In the perfect reflector algorithm, the brightest area in the image is considered to be standard white, so the average value of this area is used for cast correction. In this case, this method fails when the brightest point in the image cannot be concluded or the image lacks a white area. The proposed method is to superimpose multiple Gaussian distributions to represent the histogram for an image. This particular method is preferred for nature scenes, as opposed to object scenes. The results of this study demonstrate that this proposed method effectively removes color casts and brings the image closer to what the human eye perceives than the other tested methods because it is able to overcome the limitations described in the other methods.¹²

In addition to the various approaches to white balance techniques, there are also multiple approaches that involve histogram manipulation. One technique focuses on an idea referred to as “histogram matching.”¹³ In this method, one image is adjusted previously using tools such as PhotoShop. This image is intended to act as a reference image so that it is the only image that needs to be corrected using these tools, which can often be time-consuming. Once this is done,

a mapping relation is developed between a source image and the reference image, which results in the images having a similar color characteristic. This is the point where the source image is said to be corrected. The final results showed that the visual effect of the source images were maintained while any color differences between these images and the reference image were effectively removed. However, the process of developing a reference image can be difficult without experience, which may make this method difficult for some users.

Another approach to histogram matching has involved the inclusion of a color matching card.¹⁴ These cards vary in design, but they contain a wide variety of shades and hues of colors. In one demonstration of this method, a color matching card with a hole is placed over a solid colored card. The card is detected in an output image, whose color is changed via histogram matching using a reference image which contains the same matching card and solid colored card. While comparing the solid colors, it was found that this technique effectively visually replicates the solid color between images, but some shadowing due to lighting in the environment is still present in some corrected images. While this approach does not require the labor of a previously corrected image, as this method allows for any color similarities between the images to be detected, it maintains the issue of requiring a color matching card in both images.

Another method of histogram manipulation stretches the actual cumulative distribution function (CDF) of an image to a target CDF.¹⁵ This method is demonstrated to work well with images taken in the dark because it takes the values skewed toward the lower end of the spectrum and stretches them towards higher intensity values, thus lighting the image. The difficulty with this method is determining what type of distribution to use for the target CDF. For the tested image, it was found that using a logistic target CDF worked better than a Cauchy or linear function. The upper values of the logistic function closer matched the original cdf, so it was mostly the lower intensity values that were corrected. This was the desired effect. However, since each of the other functions had their own benefits in the way they adjusted the image (particularly the Cauchy function), it was concluded that no one method fits all images. Thus, it should be up to the person correcting the image to determine which method works best for the particular image that is being processed.¹⁵

Histogram manipulation, as mentioned previously, is also used in MATLAB functions. Some of the automatic techniques using histograms in MATLAB were tested against a Multi-scale Retinex with color restoration (MSRCR) method. One of such histogram manipulation techniques is RGB histogram equalization, which uses histogram equalization for each channel in the RGB space.¹⁶ The other method is the RGB to HSI (Hue-Saturation-Intensity model) method. This technique only uses histogram equalization for the H heft, while leaving S and I unchanged. The aforementioned MSRCR approach uses three sub-images that determines the reflection ability of different waves, calculates the relationship between every two pixels (to determine their colors), and linearly maps from Retinex space to RGB space. This method is demonstrated to maintain the color of an image while strengthening the image's details so that it is the most consistent method in replicating human vision, but it comes at the expense of time. In contrast, RGB histogram equalization takes less time and makes the images more colorful, but some details of the image are less clear. The RGB to HSI method remains between these two methods in both time and its ability to replicate human vision. Ultimately, the difference in run time experienced between the RGB histogram equalization and MSRCR methods was, on average, two seconds.¹⁶ However, this is something to consider with slower processing computers or images with a higher pixel count.

Some methods and comparisons emphasize and compare measured illuminates, rather than the colors in images. One suggestion notes that, under colored illumination, one color channel in an image will have a significantly different standard deviation than at least one other.¹⁷ Using this, the illuminate in an image can be estimated, which can be used to correct the image accordingly. This estimated illumination color can be compared against the ground truth illumination color by finding the root mean squared. While this technique succeeds in some images, the presence of noise and other illuminates negatively affect the accuracy of this method based on the assumptions made (such as that with the standard deviation) in this process.¹⁷

Many of the aforementioned studies of color rely, at least partially, on visual comparisons of colors. However, this method of comparison can be subjective and inconsistent, often taking time to achieve less accuracy.¹⁸ As such, quantitative approaches have been explored to correct this issue. In addition to the methods formally mentioned, colors in images have been compared with methods such as the Euclidean color distance.^{18, 19, 20} While there are multiple approaches to using Euclidean color distance, this work will focus on using the RGB color space as the values for this comparison. This method has been proposed for use in medical fields, including the detection of jaundice in babies. In one instance, the bilirubin levels in babies were detected by comparing images of babies' complexion to color calibration cards.¹⁹ The application of Euclidean approximate distance of RGB values in the digital image processing led to a 90% accuracy in detecting jaundice.¹⁹

Other research involving Euclidean distance and Bayesian methods has been rooted in cloud and sky detection.²⁰ Again, the application and results of Euclidean distance proved successful with a correlation of 97.9% for clouds and 98.4% for sky.²⁰ The application of this method proved to not only be comparable to other cloud detection software, but it also contained additional attributes that stem from the assessment of color attributes in the clouds. This data collection and comparisons also extended to the classification of Rayleigh-scattering patterns.

Despite its uses, other research suggests that there are some limitations in the application of Euclidean color distance. One source notes that a large color distance in one of either the red, green, or blue values and a small distance in the others may skew interpretations of results.²¹ Such differences in the distances between values will lead the increase in the overall distance calculated using the Euclidean method to be less than the difference one can visually perceive. For example, if the distance between the blue values is 70 while the red and green distances are very small, then the calculated color distance will only be around 70. In some cases, if that distance is determined with an even spread across the red, green, and blue values, this distance may be acceptable. However, with this distance being solely concentrated in the blue region of the RGB color space, the visual difference may be more significant. This is an issue that one needs to consider when making image comparisons that may contain significant color differences.

Issues with accuracy have been demonstrated in some studies that use this method of color comparison. In one case where the color of beef to determine its quality was examined, this method proved to have a 60% success rate.¹⁸ While this is argued to be a potential improvement upon visual comparisons, this rate of accuracy is low with the consideration of the purposes of this study. This is particularly important when considering the fact that, like the beef, the images being compared are textured with color variation. As such, a combination of correction comparisons is used to account for the shortcomings of the techniques used in this study.

The work described in this manuscript follows its own quantitative comparisons with the use of standard deviation and Euclidean distance comparisons, both described in more detail in the following subsection and the Methodology section. Like the previous work, this research also compares multiple images and correction techniques, with an emphasis on the white balance technique, to provide a general understanding of how the proposed method performs overall and in relation to the commonly used technique. The proposed method also takes the importance of the histogram distribution in reducing color cast into consideration, as it relies on the stretching of histogram values to correct the image, which is later described in the Methodology.

Color comparisons in this paper

Using computer software, the exact RGB values present in a pixel of an image can be determined. For this reason, it is possible to quantitatively compare images to determine if they match using some of the aforementioned methods. One method by which one could do this is by taking a mean value coincidence of each RGB value of a particular color region in an image as well as the standard deviation of the RGB values of that area and compare that with the same color region in another image. If the colors of the two images match within an chosen number of standard deviations, then they may be considered a true positive. If they do not match and are not supposed to be the same color, then one

would consider that a true negative comparison. Any other result would either result in a false positive, where the colors match and should not, or a false negative, where the colors do not match but should.

The Euclidean distance provides another means of comparison and the idea is to calculate the distance between two different colors. The 3-dimensional Pythagorean theorem is used where the values R, G, and B in place of x, y, and z in the formula. For a source 1, e_1 , and a source 2, e_2 , this is demonstrated in **Equation 1**:²²

$$d_{Euc.}(e_1, e_2) = \sqrt{(R_2 - R_1)^2 + (G_2 - G_1)^2 + (B_2 - B_1)^2}. \tag{Equation 1.}$$

From there, one can determine if this distance falls within an acceptable range for comparisons. Then, the same true-false positive-negative labeling is used as described previously.

An effective way to determine the precision and accuracy of a color correction method is through the use of a color checker chart. A color checker chart is broken into four rows, each with its own variety of colors in a particular color type: grayscale, primary and secondary, miscellaneous, and natural colors.²⁴ Each row has six colors, which all contain their own set of known RGB values, as demonstrated in **Figure 1**.

Dark Skin 115 81 68	Light Skin 194 150 130	Blue Sky 98 122 157	Foliage 87 108 67	Blue Flower 133 128 177	Bluish Green 103 189 170
Orange 214 126 44	Purple Red 80 91 166	Moderate Red 193 90 99	Purple 94 60 108	Yellow Green 157 188 64	Orange Yellow 224 163 46
Blue 56 61 150	Green 70 148 73	Red 175 54 60	Yellow 231 199 31	Magenta 187 86 149	Cyan 8 133 161
White 243 243 242 5%	Neutral 8 200 200 200 26%	Neutral 65 160 160 160 44%	Neutral 5 122 122 121 62%	Neutral 35 85 85 85 75%	Black 52 52 52 86%

Figure 1. Layout of the Color Checker Chart Used with Known RGB Values²⁴. This figure provides the color distribution in the color checker chart used for this research. The values within each square correspond to their measured and accepted red, green, and blue values, defined in that order. From top to bottom, the rows consist of natural tones, miscellaneous colors, primary and secondary colors, and grayscale colors. The color checker chart has fewer colors than the color matching card and often is often larger in size.

Not only does the chart provide several colors that can be cross-compared across images under multiple lightnings to determine the precision of a correction technique using the methods described previously, but it also presents the RGB values that should be present for each square in an image of the chart. Thus, color correction techniques can be checked for accuracy by comparing the corrected image values against the known chart values. This combination makes it possible to determine if a technique is correcting images both consistently and accurately, which would also make the pros and cons of different color correction techniques more visible and quantifiable for a better understanding of the effectiveness of each method.

METHODS AND PROCEDURES

Prior to testing each color correction method, a set of eighteen photos were taken to provide variety for comparisons. All of the photos contained the color checker chart, presented in **Figure 2**, but were taken with three different cameras under six different light bulbs. The three cameras consisted of an iPhone, an Android phone, and an iPad camera. The six lighting's included: a overhead light, a Reveal LED bulb at 50 Watts, a Sylvania bulb at 60 Watts, a Zilotek bulb at 100 Watts, a Hungary soft white bulb at 70 Watts, and a Solar Spectra bulb.

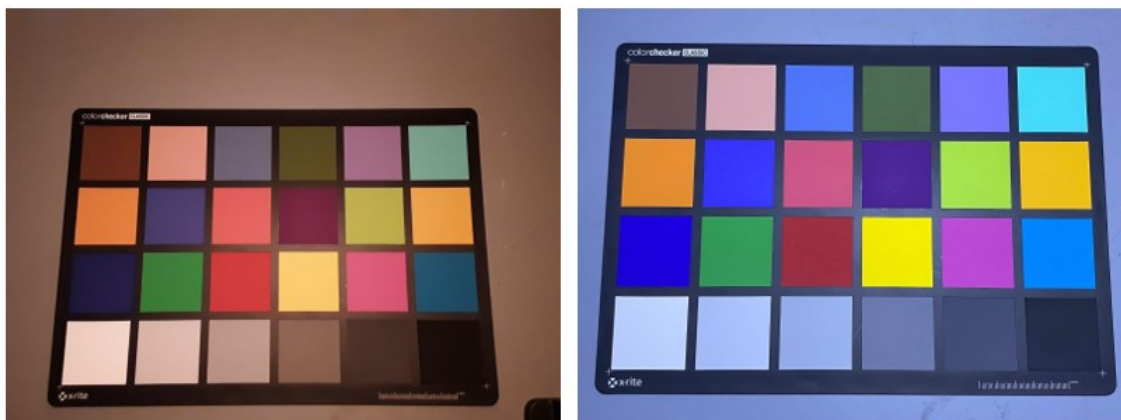


Figure 2. Two Examples of Images Taken and Used for Comparisons. The left image was taken with an Android phone under the Hungary soft white bulb while the right image was taken with an iPhone under the Zilotek bulb. Such variations enabled each of the color corrections to be tested under multiple conditions.

To include a set of real-life photo comparisons, 500 more photos taken in 20 locations with a variety of lightings. Twenty of these photos were taken of a chart created to imitate the color checker chart in its color variety, but each square consisted of a photo of a real-life object. The other 480 photos consist of 20 photos of each individual square from the chart, placed in the scenery without any other squares. These photos were all taken with an iPhone under the natural lighting of the scenery. Examples of each of these are presented in **Figure 3**.



Figure 3. Examples of Photos Taken of the Textured Chart and the Individual Squares. The first photo (left) contains one of the 20 images taken of the textured real-life photos chart. On the right, one of the 20 photos for one of the 24 squares, a zoomed-in image of a fire hydrant, is also shown. These images were used to demonstrate how color correction techniques perform with textured photos containing a single (right) or combination (left) of textured objects.

An additional set of 500 photos also followed the same scheme, but with the addition of a black and white checkered chart or paper with text taking up 20-100% of the background. Half of the colored chart and square photos included the black and white checkered chart and half included the text. Like the previous set, these photos were taken with iPhone camera under the natural lighting of the scenery. Examples of these photos are illustrated in **Figure 4**.

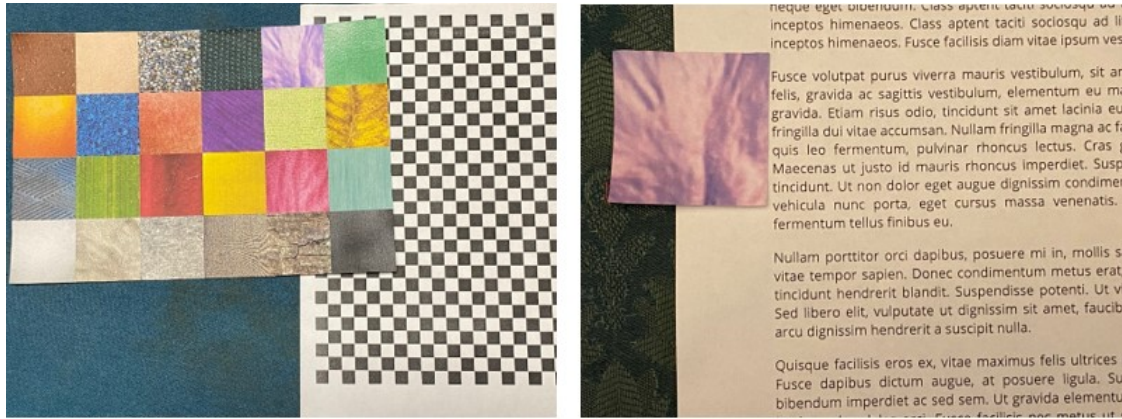


Figure 4. Examples of Textured Photos taken with Black and White Backgrounds. The left image consists of a textured chart photo example taken with a checkered background, while the right one is an individual square photo with a textual background. Both photo sets consist of 50% photos taken with the checkered background and 50% taken with the textual background. In each photo, the percentages of the frame that these black and white backgrounds take up vary.

White balance

The first correction method to be compared is the white balance correction. To achieve the best possible results for this method, a manual white balance method that involved choosing a grayscale was used. For this white balance method, the user is required to select a grayscale portion of the image. This allows the white balance to be automated with fiducial markers, which the code is written to recognize and use to achieve the most accurate results with this correction method.

Using the *drawrectangle* function, an area of the photo can be selected to have the coordinates of that area saved²⁶. Then, using the *imcrop* function and these saved coordinates, the image can be cropped down to this selected area.²⁷ While using the white balance method, an area area of the image is selected and set as the grayscale. Since there are six colors in the grayscale of the color checker, each square is individually selected. Each time the user selects an area, the RGB values for each pixel of the image are saved to be appropriately used.

The average RGB value for each square is found. Then, the average for each red, green, and blue value is found between the six squares. The image is then corrected via white balance using the *chromadapt* function, which takes the average RGB values and the original image as inputs before outputting the white balance image.²⁸ This image is then displayed.

Since the photos of the individual squares in the first set of 500 photos do not include a grayscale for selection, an automatic white balance function, *lin2rgb*, is used to correct the image instead.²⁹ The second set of 500 photos allowed for the selection of a grayscale from the text or checkered chart backgrounds. However, this scale could be selected in one area instead of multiple steps. For this reason, the user only selects an area to gather the RGB values from once before using the *chromeadapt* function. In the case of the chart background, four consecutive squares (two white and two black) were selected at once. For the textual background, a single word was selected.

Multi-variable fit method

In order to determine the standard deviation and Euclidean distance that would be used for comparisons in a 3-dimensional distribution, a “best case scenario” color correction technique is necessary for comparison. This correction technique involves a third order multi-variable fit function, which follows the format demonstrated in **Equation 2**:³⁰

$$R_s = r_0 + r_1R_e + r_2B_e + r_3G_e + r_4R_e^2 + r_5G_e^2 + r_6B_e^2 + r_7R_eG_e + r_8R_eB_e + r_9G_eB_e + r_{10}R_e^2G_e + r_{11}R_e^2B_e + r_{12}G_e^2R_e + r_{13}G_e^2B_e + r_{14}B_e^2R_e + r_{15}B_e^2G_e + r_{16}R_e^3 + r_{17}G_e^3 + r_{18}B_e^3 + r_{19}R_eG_eB_e. \quad \text{Equation 2.}$$

This is just one of the equations generated for the RGB values for a pixel, specifically the red value. Here, any variable with the subscript e is an RGB value collected from the original image for a particular pixel, as described later in this methodology. Each r represents a coefficient in the expression that is calculated using the multi-variable fit function, also described later in this methodology. While these coefficients remain the same for calculating all red values in a single image, they will vary between each red, green, and blue equations. The value calculated out of this particular expression is the “corrected” red value for a single pixel, which is then used to correct that pixel in the image. Apart from the varying coefficient values, the general format of this equation remains the same for each red, green, and blue calculation.

The accuracy of this method was verified through multivariable goodness of fit plots. This was done for each the red, green, and blue corrections by comparing their adjusted values against the true color values for each square in the color checker chart. An example of these plots for the red values of the color checker squares in an image is provided in **Figure 5**.

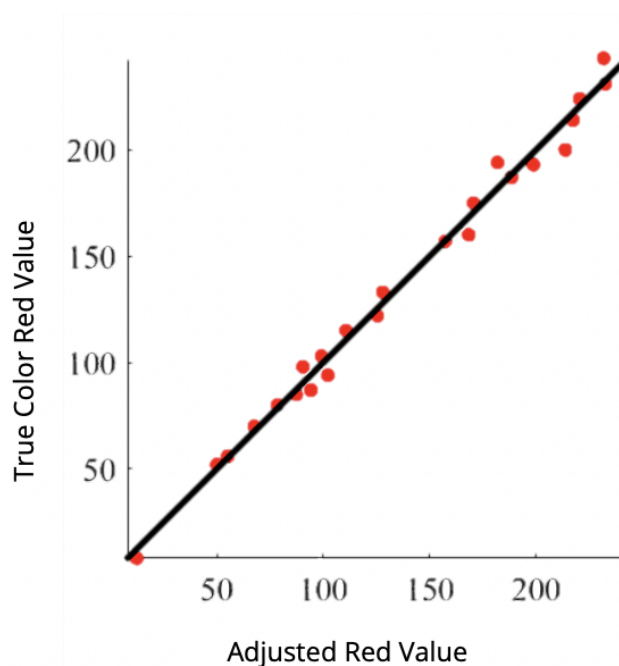


Figure 5. Goodness of Fit Plot for Adjusted Red Values. This figure demonstrates the goodness of fit of the average corrected red values for the pixels of each square in the color checker chart. This information is plotted against the true chart red values, illustrating the close fit of the corrected values to the actual values. Similar plots were developed for both the green and blue values in this and other corrected images.

In order to create this function, both the photographic and actual RGB values for each color checker square need to be known. The actual values are provided by literature, which is demonstrated back in **Figure 1**. The RGB values for each square in the photo, in contrast, needed to be collected from cropping and saving the RGB values for each square. An example of a cropped square and the chart that it belongs to, for comparison, was demonstrated in **Figure 3**.

This data is then used in an outside function, *MultiPolyRegress*.³⁰ Here, the polynomial fit for the red values is found by taking the first column of the experimental values array, the true red values, and and telling the function to make a third order polynomial fit. This is then repeated for both the green and blue polynomial fits with their respective experimentally recorded RGB values.

These polynomial fit functions are then used to correct the RGB values for each pixel. From there, the values for respective pixels are assigned to their appropriate location to make up a new, corrected image. This is then displayed for visual and data-based comparisons, which RGB values are collected for. This function could not be used for either of the sets of 500 photos because none of the true RGB values in those photos were known.

Upper and lower percentage histogram manipulation

Our chosen color correction technique is an upper and lower percentage histogram manipulation method. We will test this technique against the white balance methods.

This method focuses on saturating each the red, green, and blue value histograms by a given percentage. In order to do so, the method finds the first occurrences of pixel intensities in the histogram and continues to adjust those pixel intensities to a value of zero until the desired percentage of pixels in the image are corrected to this point. The same is done starting from the other side of the histogram (with the maximum values), but these values are corrected to the maximum intensity value of 255. This is done for each the red, green, and blue value histograms. The remaining histogram values are then used to fill in the intensity values between these extremities. This new distribution is then used to correct and update the image. Examples of the original and adjusted histograms is provided in **Figure 6**. Again, once the image is corrected, the RGB values of each square are saved for quantitative comparisons.

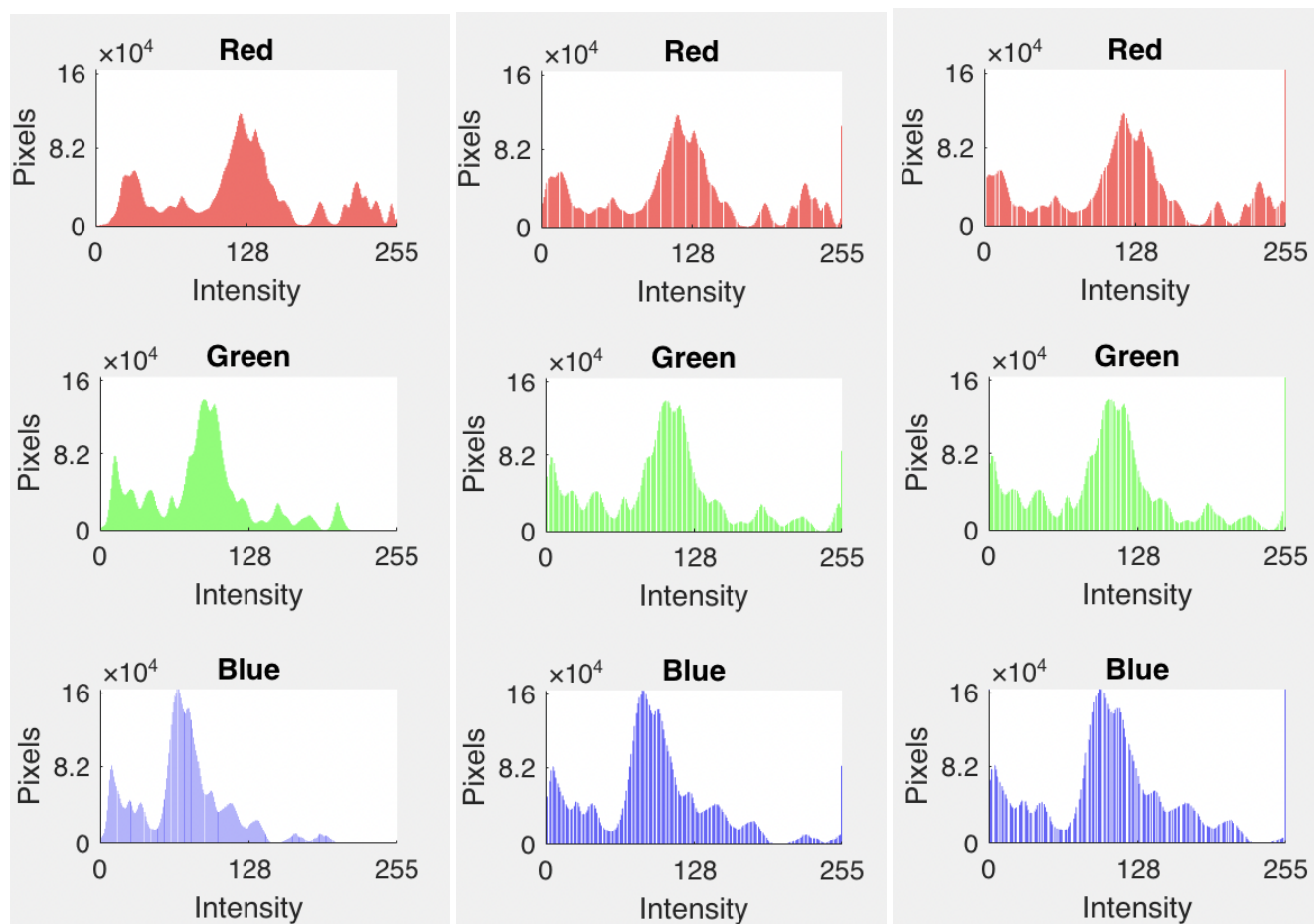


Figure 6. Histograms of RGB Values for Various Saturated Images. These RGB histograms are collected from the original (left), 1% saturated (middle), and 2% saturated (right) image of the color correction chart, provided in Fig. 2 (left). Note how increasing the saturation pulls more pixel values to the extremities of the individual RGB histograms while the remaining pixel values fill in the space in-between.

Comparing images

A visual comparison of an image of the color checker chart taken with an Android phone under the Hungary soft white bulb after using the various color corrections is provided in **Figure 7**.

In order to accurately and quantitatively compare these images, the RGB values from each of them needed to be recorded for comparison. This was done by “sampling” each square in an image. This code follows the same format as the cropping code that was used for the multivariable fit.



Figure 7. Corrections of an Image from Fig. 2 (left) Using Various Correction Techniques. This figure consists of the original (top left), multi-variable fit (top middle), manual white balance (top right), automatic white balance (bottom left), and 1% saturation (bottom right) methods. Note that, due to its use of the actual chart RGB values, the multi-variable fit image is the most accurate and can, therefore, be used when visually comparing the images for accuracy.

Once the RGB values for each correction method and the original images are collected, the comparisons of the values can begin. A separate code is written for the cross-comparisons. The average values are sorted by correction type and into RGB components so they can be appropriately compared. This is also done for the standard deviation values, σ , which act as one of the primary metrics for comparison. The equation for σ is provided in **Equation 3**:

$$\sigma = \sqrt{\frac{\sum(x_i - \mu)^2}{N}}. \tag{Equation 3.}$$

The standard deviation for red, green, and blue is automatically calculated by MATLAB. Here, x_i is one of the RGB values corresponding to a singular pixel in the image. If the standard deviation is for red, then the red value for this pixel will be used. The same can be said for the green and blue standard deviations. The variable μ is the average RGB value, again correlating to the color that the standard deviation is being calculated for. This difference is calculated, squared, and summed with other squared differences for all of the pixels in the selected image area. This sum is divided by N , which corresponds to the number of pixels in the cropped image, or sampled square. The square root of this quotient provides the standard deviation, σ , as seen in **Equation 3**.

All other squares from images with the same color correction are compared against one another. If the RGB values of one square fall into the range of maximum and minimum RGB values for another set by the standard deviations (with red being compared against red, green against green, and blue against blue), then the squares are considered a match. If one or more of the RGB values of the first do not fall into the respective ranges of the second, then the squares do not match. The next step is to then check if the colors should match. This is done by comparing the assigned specific color that is saved for the square that the data is taken from. If they are the same, then the colors should match and this indicates a false negative. If not, then the colors should not match and are a true negative. If the RGB values of the first square fall into the range for the second, then a matching specific color comparison would come out to be a true positive. If the values match but the specific color does not, then the result is a false positive.

This process is repeated until all squares within a correction type have been compared with one another. Again, this overall cycle of comparisons is completed for within each correction type. At the end, the percentage of true positive is cal-

culated for each type by dividing the true positive count by the sum of the true positive and false negative counts. The percentage of true negative is then calculated by dividing the true negative count by the sum of the true negative and false positive. Overall, all of these comparisons and data saving were repeated for various standard deviations, or sigma.

The true value comparisons, calculated separately, follows a similar format as the cross comparisons. The data is imported and saved into arrays in the same manner as in the cross-comparison code. The code is also ran for the same range of sigma. However, instead of comparing data from squares against other squares with the same color correction type, each square is only compared with the actual RGB chart values. In addition, the true value comparisons could not be used for either set of 500 photos since their true values are unknown.

Another code follows the same format as the standard deviation comparison code but is written for the Euclidean color difference comparison described earlier in the Methods and Procedures section. Instead of seeing if one data set for an image square falls within a specific number of standard deviations of another, the code calculates the Euclidean difference of the squares' colors using Equation 1. After checking if the calculated difference falls within a prescribed maximum difference, the remaining code follows that of the standard deviation comparisons, determining if the results of the squares should and do match to calculate the true/false positive/negative rates. This is also initially tested for multiple Euclidean distance values.

RESULTS

To determine the number of standard deviations (σ) that will be used for the comparisons of each set of photos, the results at various sigma from the gold standard, or multi-variable fit, method must first be considered. Since the gold standard data represents the "best case scenario," the opposite end of the spectrum, the original photo data, must also be considered when choosing an appropriate number of σ . This data helps gauge at what point too many standard deviations are being used because this would result in unreasonably high percentages for the original photos, particularly in the true positive percentages. A summary of the cross-comparisons of original photos and photos corrected using the multi-variable fit at various sigma is provided in Table 1.

Table 1. Standard Deviation True Positive and True Negative Results for the Original Photos and the Gold Standard Multivariable Color Correction of the Pure Color Chart

σ	Original Images				Gold Standard			
	True Positive		True Negative		True Positive		True Negative	
	Cross	True Value	Cross	True Value	Cross	True Value	Cross	True Value
2	2.69	0.35	99.98	91.61	81.60	85.76	100.00	91.67
3	6.41	3.82	99.93	91.58	91.54	93.40	99.99	91.65
4	11.01	6.94	99.84	91.47	95.61	97.22	99.86	91.64
5	16.32	14.24	99.67	91.35	97.41	97.92	99.49	91.34
6	22.76	20.14	99.45	91.06	98.52	99.31	98.83	90.70
7	29.26	26.04	99.12	90.79	99.12	99.65	98.00	89.99
8	35.73	33.33	98.67	90.41	99.50	99.65	96.86	88.98

Considering the results found for the gold standard color correction in Table 1, it would appear that around 4σ - 5σ is necessary to achieve the 95% accuracy desired, which equates to the accuracy of 2σ in a 1-dimensional normal distribution. This also follows with the results for the original photos in Table 1, where these numbers of σ correlate to data prior to when the original data results begins to rapidly improve. However, assuming that the RGB values are all independent, one could also argue that 3σ , alone, should encompass $99.7\%^3 = 99.1\%$ of the data. Therefore, going beyond this number of standard deviations would be unreasonable, even if there is a small dependence on one another between the RGB values. This also agrees with the overall trend of both data sets, as the average of the true positive and true negative cross-

comparison results for the gold standard at 3σ remains around 95% while the gold standard’s true color average is about 92.5%. This is also reasonable for the original data set because this number of σ still falls before the major improvements in results. Thus, three was chosen for the number of standard deviations to be used in comparisons of any following data.

While using standard deviation comparisons is a valid method to compare data, an issue arises when using this method alone for the textured photos. The data provided in **Table 1** result from pure color chart photos, which do not have large standard deviations. However, the added texture in the real-life photos, as demonstrated in **Figure 3**, naturally increases the standard deviation of the RGB values within a photo due to variations in color across each square. With this in mind, the Euclidean color distance comparison, described in the Methods and Procedures section, was also used as a comparison metric using the average RGB values collected for each photo and correction type. **Table 2** provides the results of the Euclidean distance comparison for the original photos and gold standard method.

Table 2. Euclidean Color Distance True Positive and Negative Results for the Original Photos and the Gold Standard Multivariable Color Correction of the Pure Color Chart

$d_{Euc.}$	Original Images				Gold Standard			
	True Positive		True Negative		True Positive		True Negative	
	Cross	True Value	Cross	True Value	Cross	True Value	Cross	True Value
20	17.35	12.73	99.77	99.68	96.57	96.99	99.99	100.00
30	33.88	29.63	99.15	99.09	99.48	99.31	99.99	99.69
40	48.39	52.08	97.79	97.80	99.97	100.00	97.48	97.56
50	59.42	67.36	95.81	95.79	99.97	100.00	95.15	95.12
60	68.66	78.01	93.23	93.03	100.00	100.00	92.43	92.63
70	76.44	86.57	89.93	89.53	100.00	100.00	86.67	86.81
80	83.17	90.74	86.03	85.37	100.00	100.00	81.06	81.11

As seen in **Table 2**, the gold standard method has the highest average true positive and true negative rate for both the cross-comparisons and true color comparisons when the Euclidean color distance is 30. This color distance is also the point where the original photos true positive rates are consistent between the cross-comparison and true color comparison results. The same can be said about the true negative results across both comparison types. For this reason, a Euclidean color distance of 30 was initially considered for the following corrected photo comparisons.

To get a sense of how each method would perform with real-life, or textured, images, the second set of photos mentioned in the methodology was taken to make such comparisons. However, since the actual average RGB values for each square in the images are unknown, both the gold standard method and true value comparisons are not used. In addition, only the 3σ determined using white balance and the original photos in the previous data set was used for this new set of standard deviation comparisons. Furthermore, an automatic white balance was added to comparisons since a grayscale is not initially provided for the manual white balance in photos for individual squares. A range of 0.0%-3.0% saturation via histogram manipulation is provided in these comparisons to consider how their performances vary with real-life photos and determine the best performance.

The cross-comparison results for the real-life photos with and without a black and white background at 3 sigma are provided in **Table 3**. Looking at the squares without the black an white background, alone, the only white balance that can be considered is the automatic white balance. This method performs a minimum of 5.5% worse than any of the other methods, including the original photo, in the true positive comparisons. In contrast, its true negative percentage is greater than any of the histogram manipulation percentages and is second only to the original image. While this does appear to reflect poorly on the histogram manipulation technique, it is important to remember that the textured squares have higher standard deviations than solid colored squares. As a result, there is more likely to be a significant false positive count, resulting

in a lower true negative rate. This is one of the justifications for later using the Euclidean distance comparison technique.

Looking at the overall trends between in these comparisons, 0.5% maintained one of the highest true positive rates, while 1.5% retained one of the highest true negative rates of the tested percentages. This factored into the choice to make 1.0% histogram manipulation the main focus when comparing against other correction methods while including the black and white background, as it is the middle-ground of these two percentages. However, since this choice is based on general trends, the Euclidean distance comparisons was also considered before making this decision. As explained later in this section, the Euclidean comparisons also affirmed the 1% saturation choice.

Despite the apparent shortcomings of white balance without the black and white background, it is important to note that this is an incomplete comparison because manual white balance could not be used in the individual square photos without a grayscale present. Taking this issue into consideration, along with the purposes of applying these methods to the image analysis of birds, the final set of photos mentioned in the Methods and Procedures were taken with black and white backgrounds for comparison. This is also to the benefit of the histogram manipulation method, which works on the assumption that there are pixels to the extremities of the RGB value range. Since black and white lie at these points in the RGB value range, this would provide a metric in the image to aid the histogram manipulation method in its color correction. This data for 3σ is also included in **Table 3**.

Table 3. Summary Table of Standard Deviation Cross-Comparisons of Real-Life Square Photos at 3 Sigma

Correction Type	True Positive		True Negative	
	W/O Black and White	W/ Black and White	W/O Black and White	W/ Black and White
Original	59.01	84.98	68.13	64.20
Auto WB	53.43	82.93	68.01	70.92
Manual WB	N/A	88.67	N/A	63.46
0.0% Saturation	61.13	86.78	66.71	61.82
0.5% Saturation	65.06	94.42	60.27	61.37
1.0% Saturation	64.11	93.08	60.36	62.95
1.5% Saturation	63.04	92.88	60.61	62.61
2.0% Saturation	62.14	92.41	61.11	62.35
2.5% Saturation	61.36	92.19	61.64	62.57
3.0% Saturation	60.43	91.78	62.05	62.61

The set of photos with black and white backgrounds provides a more complete understanding of how the white balance methods perform in comparison to the original and saturated photos. With the black and white background, the automatic white balance performed about 6% worse than the manual white balance in the true positive rates and 7% better in the true negative rate comparisons. This method also performs worse than the original photos in both rates for the square photos, with the exception of the true negative with a black and white background. The manual white balance, on the other hand, generally performs better in comparisons with the true positive percentages and worse with the true negative rate.

Across the table, 1.0% saturation generally performs among the best of the methods presented. While its true negative results are up to 7% lower than the automatic white balance photos, which did either the best or the second best in both the true negative comparisons, the saturation via histogram manipulation method consistently maintained at least a 4.3% gain on the other non-saturation methods in the true positive rates. The low true negative rates are particularly understandable when considering the large standard deviations with textured photos, which would lead to more false positives. While 0.5% saturation does maintain a higher true positive rate in these photos than the other saturations, it remains 1.5% from the 1% saturation rate. This is a similar difference to that between the two for the true negative rate, where 1% saturation

has the highest value. This, combined with the trends seen without the black and white background, adds to the justification for using 1% saturation.

It is also important to note that manual white balance does not perform the best in a single category, despite it never having the worst rate at any point. Regarding the standard deviation comparisons alone, 1.0% saturation is notably the best correction method of those compared. One may notice that in addition to the improvement in white balance and 1.0% saturation methods, the original photos also improve from the previous set. This is because this set of photos was taken separately from the previous, which resulted in variations in lighting and other conditions between the sets of photos. This, however, is not the sole cause of improvements in any of the color correction methods. While the original photos improved by a rate up to about 15%, the saturation and automatic white balance methods improved on a scale of about 20% - 30%. In addition, the original photos worsened in true negative rates, while the correction methods, with the exception of the 0.0% saturation, improved in those rates. A similar trend can be seen with the Euclidean distance comparisons.

Although the results of **Table 2** initially suggested that a Euclidean distance of 30 should be used for other comparisons, low rates in the positive and negative comparisons at this distance for textured photos suggested that this choice was flawed. Like with the standard deviation choice, the Euclidean distance for these comparisons must also take into account the large standard deviations in the real-life photos. For this reason, a larger Euclidean distance should be considered to provide a more fair comparison of the correction techniques. A Euclidean distance of 60 was chosen for the real-life comparisons because this is the point where the average of the true positive and true negative rates were at the highest for each correction type. The results from the Euclidean distance comparisons at a distance of 60 are provided in **Table 4**.

Again, the best histogram manipulation results remains in the 0.5%-1.5% range. The 0.5% saturation results have one of the highest true positive rates in both comparisons of the saturation method, remaining behind only to automatic white balance and 0.0% saturation in the square photos without a black and white background. The results of the higher percent histogram manipulations are higher in the true negative comparisons, but the true negative rate of the 1.5% saturation is within 0.5% of that of the 3.0% saturation.

While 0.5% saturation performed well in the Euclidean difference calculations, 1.0% saturation was still chosen for the final comparison set. This is because the results of the standard deviation comparisons, as explained before, suggest that 1.0% saturation would be a good compromise between 0.5% and 1.5% saturation. In addition, as seen in **Table 4** for the data without the black and white background, 1.0% saturation performs as consistently, although at lower true positive rates, as 0.5% saturation. Therefore, 1.0% remains a reasonable choice for the histogram manipulation method.

Table 4. Summary Table of Real-Life Square Cross-Comparisons with a Euclidean Distance of 60

Correction Type	True Positive		True Negative	
	W/O Black and White	W/ Black and White	W/O Black and White	W/ Black and White
Original	42.54	72.81	85.50	82.99
Auto WB	37.87	76.27	84.26	85.61
Manual WB	N/A	75.20	N/A	82.29
0.0% Saturation	43.30	70.30	85.24	82.96
0.5% Saturation	37.36	81.82	86.78	84.89
1.0% Saturation	35.02	80.44	87.27	86.07
1.5% Saturation	33.64	78.68	87.58	86.71
2.0% Saturation	32.30	76.69	87.66	87.09
2.5% Saturation	31.58	75.53	87.76	87.66
3.0% Saturation	30.64	74.12	87.70	88.02

With Euclidean distance, the 1.0% saturation method also maintains the best results across the comparisons with the black and white background. However, unlike in the standard deviation comparisons, 1.0% saturation performs the best across all comparisons and percentage rates, with the exception of other saturation methods which differ in success rates between each percentage type. While the manual white balance has higher true positive rates than the original photos by at least 2.0%, it also consists of the lowest true negative rates of the three methods. The difference between the original and manual white balance true negative rates is less than 1.5% across both comparisons, but the results demonstrate that the 1.0% saturation method is the most effective and consistent of the three methods in this photo set. Automatic white balance does perform better than either of these correction types but maintains lower values than the 1% saturation.

While the code used to produce the images from which **Tables 3** and **4** were the same throughout, the addition of the black and white background made a significant difference in the results. This particular difference is dependent on the processes behind the correction techniques. As described previously, in the histogram manipulation technique, a given percentage of the first and last incidences of an RGB value is assumed to be 0 and 255, respectively. When black and white are not present in the image, this may lead to over-saturating the image, leading to the poorer results seen in **Table 3** and **4**. Conversely, when black and white are present, the portions of the image containing these colors should be adjusted to these extremes. Although not all whites and blacks are perfectly (0, 0, 0) and (255, 255, 255) in the RGB color space, the presence of these colors provides a more accurate metric that the correction method may adjust the image in relation to.

As mentioned in the analysis of the individual square photos in **Tables 3** and **4**, manual white balance is also dependent on a grayscale being present to accurately adjust the image. The lack of success in the manual white balance results demonstrates that the manual white balance correction is considerably less viable and precise than the histogram manipulation method, even when attempts to make this option more applicable is made. Again, while these changes do improve the automatic white balance method, the difference is not enough to make this method more consistent than the saturation method.

Although both methods of statistical comparison reach the same conclusion, it is worth noting that the standard deviation method does so biasing towards true positive rates while the Euclidean distance method biases towards true negative rates. This is likely a result of the difference in how average and standard deviation values of the RGB values are accounted for in each comparison type. The standard deviation method includes a wide band, as a result of the large standard deviations in textured photos, to compare the RGB values between two squares. As a result of this, there is going to be a higher rate of positive results when using this comparison. This means that both the true positive and false positive rates are likely to increase, resulting in a higher true positive rate and a lower true negative rate. On the other hand, while there is a range determined for the Euclidean distance method, this range is not dominated by the high standard deviation values of the textured photos. As a result, in comparison to the standard deviation method, there is more likely to be a decrease in positive rates for the Euclidean distance approach. This, as a result, decreases the true positive rates while increasing the true negative rates.

CONCLUSIONS

Our motivation for testing color techniques is to find a technique or multiple techniques that could be used in SIA¹ to aid the eye by increasing the contrast, and to consistently adjust colors so that color comparisons can be made independent of lighting. Our preferred technique involving color saturation was used not only for these purposes but it was also used to increase the contrast of frames in the standalone application BatCount² thereby aiding foreground object detection in videos.

Although the results between data sets vary, the final set that was taken using photos based on the purposes of these color correction comparisons in SIA demonstrated that 1.0% saturation via histogram manipulation performed the best of the presented methods, excluding other saturations. The gains in the percent true positive for 1.0% saturation were more significant than the losses in its percent true negative when comparing it to white balance and the original photos in the stan-

dard deviation comparisons. With the Euclidean difference comparisons in the final data set, however, a saturation value of 1.0% consistently performs among the best across these comparisons.

It is important to note, however, that the success of the 1.0% saturation is partially dependent on its intended use. **Tables 3 and 4** illustrate that, when a chart is present without a black and white background, manual white balance does significantly better in the true positive comparisons and within 1.0% of the true negative results of 1.0% saturation. Therefore, the saturation method is not always the “best” method for color correction — it simply best serves the purposes of color correction in SIA. Additionally, please note that our comparison of lighting sources was intentionally treated in a statistical manner. Any subsequent analysis of color comparisons in different lighting using the same techniques and metrics will presumably reach similar conclusions but will likely not find our identical findings.

Despite its shortcomings, the histogram manipulation method does maintain a few advantages over other methods. The multi-variable fit function is impractical in its application to everyday photos due to its reliance on known RGB values in an image. One may consider taking an image with a color checker chart to achieve this level of accuracy, but this makes the process more tedious and reduces one’s ability to take action shots. In a similar manner, the difficulties illustrated in the second set of photos points to the issue of how limited the manual white balance method is. Again, one could take photos with a color checker chart present, but this is impractical and tedious, as explained with the multi-variable fit function. The automatic white balance method is applicable, but results in the second data set also demonstrates that it is less consistent than other methods, including both the 1.0% saturation method and, in some instances, the original image. Additionally, the 1% saturation works best if there is some black and white in the background. Without this colors can saturate in an unnatural way as discussed in ¹. But unlike with white balance a gray scale region doesn’t have to be identified.

In the future, a wider data set may also be considered. In the first set with the pure color charts, a variety of cameras were used to test the overall and more universal performance of correction techniques. In the photos for the following sets, however, all of the photos were taken with the same iPhone camera. Since cameras vary in quality across different devices, including various cell phones, it would be worth comparing how these corrections compare across different cameras — both in general and for specific camera types.

Furthermore, comparisons between the proposed technique and methods described from previous literature may also be compared. Since the best performance of the upper and lower percentage histogram manipulation method occurred when black and white aspects were added to the background, adding a color matching card into images for histogram manipulation using this card would be a reasonable change, especially since it is smaller than a color checker chart. However, the difference in run time in using this method may outweigh any improvements in color correction from the proposed method. Other approaches may include using a neural network. While this may also seem like a favorable option with color correction, this approach is not as frequently used because it takes more time to train. Thus, it is also more expensive. There are many other techniques that may be worth testing in the future, but careful considerations must be made before doing so. Each method has its own advantages and disadvantages and it is important to focus on and emphasize ideas that would best work for the purposes of SIA.

ACKNOWLEDGEMENTS

This research was supported by the National Science Foundation Infrastructure Innovation for Biological Research: Intuitive Sampling, Tracking and Counting Software for Biological Sciences (Award Number 1916850).

REFERENCES

1. Bentley, I., Ralston, J., Garman, S., Hershberger, O., Probst, C.M. and Washer, C. (2023) Introducing the Scientific Image Analysis Application: A Free and User-Friendly Program for Extracting Bioinformatics From Digital Images. IEEE 2023 CCWC Conference Proceedings, <https://ieeexplore.ieee.org/document/10099135>.
2. Bentley, I., Kuczynska, V., Eddington, V., Armstrong, M., and Kloepper, L. (2023) Bat-Count A software program to count moving animals. PLoS ONE 18(3) e0278012,

<https://journals.plos.org/plosone/article?id=10.1371/journal.pone.0278012>.

3. Bibikov, S.A., Zakharov, R. K., Nikonorov, A. V., Fursov, V. A., and Yakimov, P. Y. (2011) Detection and color correction of artifacts in digital images, *Optoelectronics, Instrumentation, and Data Processing*, 47(3), 226-232, <https://doi.org/10.3103/S8756699011030046>.
4. Noordin, M. J., Mat Isa, N. A., and Lim, W. H. (2016) Saturation avoidance color correction for digital color images, *Multimedia Tools and Applications*, 76(7), 10279-10312, <https://doi.org/10.1007/s11042-016-3620-y>.
5. Gasparini, and Schettini, R. (2003) Color correction for digital photographs, *12th International Conference on Image Analysis and Processing, 2003.Proceedings*, 646-651. <https://doi.org/10.1109/ICIAP.2003.1234123>.
6. Kwok, N.M, Shi, H. Y., Ha, Q. P., Fang, G., Chen, S. Y., and Jia, X. (2013) Simultaneous image color correction and enhancement using particle swarm optimization, *Engineering Applications of Artificial Intelligence*, 26(10), 2356-2371, <https://doi.org/10.1016/j.engappai.2013.07.023>.
7. H. Niu, Lu, Q., and Wang, C. (2018) Color Correction Based on Histogram Matching and Polynomial Regression for Image Stitching, *2018 IEEE 3rd International Conference on Image, Vision and Computing (ICIVC)*, 257-261. <https://doi.org/10.1109/ICIVC.2018.8492895>.
8. Bilcu, R. C. (2011) Multiframe Auto White Balance, *IEEE Signal Processing Letters*, 18(3), 165-168. <https://doi.org/10.1109/LSP.2011.2105476>.
9. Feng, L., Jian, S., and Yongzhao, Z. (2004) A fast color correction method based on image analysis, *Third International Conference on Image and Graphics (ICIG'04)*, 108-111. <https://doi.org/10.1109/ICIG.2004.3>.
10. Sengupta, D. Biswas, A., and Gupta, P. (2020). Non-linear weight adjustment in adaptive gamma correction for image contrast enhancement, *Multimedia Tools and Applications*, 80(3), 3835-3862. <https://doi.org/10.1007/s11042-020-09583-1>.
11. Mathworks (2021) Contrast Enhancement Techniques, *MathWorks Help Center*, <https://www.mathworks.com/help/images/contrast-enhancement-techniques.html>.
12. Hu, Y. (2012) Automatic White Balance Based on Gaussian Decomposition, *Applied Mechanics and Materials*, 263-266, 2542, doi:<https://doi.org/10.4028/www.scientific.net/AMM.263-266.2542>.
13. Zhang, J., and Chen, G. X. (2013) Research on the color correction algorithm of images based on histogram matching, *Applied Mechanics and Materials*, 469, 256, doi:<https://doi.org/10.4028/www.scientific.net/AMM.469.256>.
14. Rosebrock, A. (2021) Automatic color correction with OpenCV and Python, *pyimagesearch*, <https://pyimagesearch.com/2021/02/15/automatic-color-correction-with-opencv-and-python/>.
15. Manansala, J. (2021) Image Processing with Python: Color Correction using Histogram Manipulation, *The Startup*, <https://medium.com/swlh/image-processing-with-python-histogram-manipulation-on-digital-images-d4fb426d3513>.
16. Xie, X. M., Wang, C. M., and Zhang, A. J. (2013) Color image enhancement methods based on matlab, *Applied Mechanics and Materials*, 300-301, 1664, doi:<https://doi.org/10.4028/www.scientific.net/AMM.300-301.1664>.
17. Choudhury, A. and Medioni, G. (2010) Color Constancy Using Standard Deviation of Color Channels, *2010 20th International Conference on Pattern Recognition*, 1722-1726, <https://doi.org/10.1109/ICPR.2010.426>.
18. Handayani, H. H., and Wahiddin, D. (2018) Digital Image Analysis of Beef Color Using Euclidean Distance Method, *2018 Third International Conference on Informatics and Computing (ICIC)*, 1-5, <https://doi.org/10.1109/IAC.2018.8780457>.
19. Rahayu, Widyawati, M. N., and Suryono, S. (2021) Euclidean distance digital image processing for jaundice detect, *IOP Conference Series. Materials Science and Engineering*, 1108(1), 12022, <https://doi.org/10.1088/1757-899X/1108/1/012022>.
20. Neto, M., Wangenheim, A. von, Pereira, E. B., and Comunello, E. (2010) The Use of Euclidean Geometric Distance on RGB Color Space for the Classification of Sky and Cloud Patterns, *Journal of Atmospheric and Oceanic Technology*, 27(9), 1504-1517, <https://doi.org/10.1175/2010JTECHA1353.1>.
21. Abasi, Amani Tehran, M., and Fairchild, M. D. (2020) Distance metrics for very large color differences, *Color Research and Application*, 45(2), 208-223, <https://doi.org/10.1002/col.22451>.

22. Gijsenij, Gevers, T., and Lucassen, M. (2009) Perceptual analysis of distance measures for color constancy algorithms, *Journal of the Optical Society of America. A, Optics, Image Science, and Vision*, 26(10), 2243-2256, <https://doi.org/10.1364/JOSAA.26.002243>.
23. Nikon, DSLR Camera Basics: White Balance, *Nikon: DSLR Camera Basics*, <https://imaging.nikon.com/lineup/dslr/basics/17/index.htm>.
24. Image Analyst (2012), Color Checker Chart, *MathWorks File Exchange*, <https://www.mathworks.com/matlabcentral/fileexchange/38236-color-checker-chart>.
25. The MathWorks Inc., MATLAB and Image Toolbox Release 2021a, (accessed Nov 2021).
26. MathWorks (2021) Create Customizable Rectangular ROI, *MathWorks Help Center*, <https://www.mathworks.com/help/images/ref/drawrectangle.html>.
27. MathWorks (2021) Crop Image, *MathWorks Help Center*, <https://www.mathworks.com/help/images/ref/imcrop.html>.
28. Mahmoud Afifi, chromadapt: Adjust color balance of RGB image with chromatic, *MATLAB Central File Exchange*, <https://www.mathworks.com/matlabcentral/fileexchange/66682-chromadapt-adjust-color-balance-of-rgb-image-with-chromatic> (accessed Jul 2021).
29. Mathworks (2021), Comparison of Auto White Balance Algorithms, *MathWorks Help Center*, <https://www.mathworks.com/help/images/comparison-of-auto-white-balance-algorithms.html>.
30. C. Ahmet, Multivariable Polynomial Regression, *Github*, https://www.mathworks.com/matlabcentral/fileexchange/34918-multivariate-polynomial-regression?s_tid=FX_rc3_behav (accessed Jul 2021).
31. MathWorks (2021), Adjust Image Intensity Values or Colormap, *Mathworks Help Center*, <https://www.mathworks.com/help/images/ref/imadjust.html>.

ABOUT THE STUDENT AUTHORS

Kyra Obert recently graduated with a B.S. in Physics and a minor in Mathematics in May 2022.

Maria Schudt will graduate with a B.S. in Physics in May 2023. Following this, she will transfer to the University of Notre Dame as part of a 4+1 program to receive a B.S.E. in Mechanical Engineering in May 2024.

PRESS SUMMARY

Color correction is used to adjust digital photographs in order to reduce the effect of environmental factors, such as lighting. This manuscript analyzes the precision and accuracy of upper and lower percentage histogram manipulation, which involves saturating an image by a specified percentage of its pixels using its RGB histogram. It is compared against the commonly used white balance method, corrections using generated multi-variable equations for RGB values, and original images to determine when improvements or deteriorations in corrections are made in using this proposed method. The findings demonstrate that the histogram manipulation method is effective in comparison to these other methods because it does not require sampling of calibration regions and it is the most consistent method in the correction of photos with significant gray scale regions.

Overexpression of *MMACHC* Prevents Craniofacial Phenotypes Caused by Knockdown of *znf143b*

Isaiah Perez, Nayeli G. Reyes-Nava, Briana E. Pinales, & Anita M. Quintana*

Department of Biological Sciences, University of Texas at El Paso, El Paso, TX

<https://doi.org/10.33697/ajur.2023.081>

Students: iperez22@miners.utep.edu, nreyesnava2@miners.utep.edu, bepinales@utep.edu

Mentor: aquintana8@utep.edu*

ABSTRACT

ZNF143 is a sequence-specific DNA binding protein that regulates the expression of protein-coding genes and small RNA molecules. In humans, ZNF143 interacts with HCFC1, a transcriptional cofactor, to regulate the expression of downstream target genes, including *MMACHC*, which encodes an enzyme involved in cobalamin (*cbl*) metabolism. Mutations in *HCFC1* or *ZNF143* cause an inborn error of cobalamin metabolism characterized by abnormal *cbl* metabolism, intellectual disability, seizures, and mild to moderate craniofacial abnormalities. However, the mechanisms by which *ZNF143* mutations cause individual phenotypes are not completely understood. Defects in metabolism and craniofacial development are hypothesized to occur because of decreased expression of *MMACHC*. But recent results have called into question this mechanism as the cause for craniofacial development. Therefore, in the present study, we implemented a loss of function analysis to begin to uncover the function of ZNF143 in craniofacial development using the developing zebrafish. The knockdown of *znf143b*, one zebrafish ortholog of *ZNF143*, caused craniofacial phenotypes of varied severity, which included a shortened and cleaved Meckel's cartilage, partial loss of ceratobranchial arches, and a distorted ceratohyal. These phenotypes did not result from a defect in the number of total chondrocytes but were associated with a mild to moderate decrease in *mmachc* expression. Interestingly, expression of human *MMACHC* via endogenous transgene prevented the onset of craniofacial phenotypes associated with *znf143b* knockdown. Collectively, our data establishes that knockdown of *znf143b* causes craniofacial phenotypes that can be alleviated by increased expression of *MMACHC*.

KEYWORDS

ZNF143; *MMACHC*; Vertebrate abnormalities; Cobalamin; *cblX-like syndrome*; Chondrocytes; Neural crest cells; Hyosymplectic

INTRODUCTION

Mutations in *ZNF143* have been associated with inborn errors of cobalamin (*Cbl*) metabolism. For instance, Pupavac and colleagues¹ reported mutations in *ZNF143* in a 16-month-old male patient with numerous clinical manifestations including methylmalonic acidemia and homocysteinemia which is indicative of *cbl* deficiency. Such manifestations are consistent with *cblX* (MIM 309541)² and *cblC* (MIM 609831) syndrome, two subtypes of *cbl* deficiency. Previous studies have demonstrated that mutations in *HCFC1* decrease expression of *MMACHC*, a downstream target gene whose mutations causes *cblC*. Interestingly, ZNF143 interacts with HCFC1 to regulate *MMACHC* expression.³ This interaction occurs through binding of the ZNF143 DNA-binding domain (DBD) with the HCFC1 Kelch domain.⁴ Consequently, mutations in either *HCFC1*, *ZNF143*, and *MMACHC* result in an inborn error of *Cbl* metabolism.

ZNF143 is a sequence-specific transcriptional activator that regulates protein-coding genes and small RNA molecules. In fact, two domains residing in the protein spur transcription selectively at either small RNA or mRNA promoters.⁵ The phenotypes associated with mutations in ZNF143 in model systems have not been comprehensively studied, however, in zebrafish, loss of *znf143b* results in numerous abnormalities including defects in the heart, blood, ear, and midbrain hindbrain boundary.⁶ Craniofacial phenotypes were not documented or characterized even though facial phenotypes have been observed across other subtypes of inborn errors of cobalamin metabolism⁷. Therefore, the focus of this study is to determine the effects of reduced *ZNF143* expression on facial development. Interestingly, zebrafish *znf143b* has a 71% overall amino acid sequence identity with the human protein. The conserved protein domains include the DBD, mRNA gene activation domain, and small RNA gene activation domain.⁶

HCFC1 encodes a transcriptional co-factor which lacks a DNA binding domain but interacts with transcription factors that include THAP11 and ZNF143.⁸ Mutations in *HCFC1* result in a broad array of clinical manifestations including craniofacial

abnormalities. In fact, knockdown of the zebrafish ortholog, *hcf1b*, resulted in craniofacial abnormalities which are in part mediated by downregulation of *mmachc* expression.³ Knockdown of *hcf1b* caused an impairment in the differentiation of cranial neural crest cells (NCCs) which produce many facial cartilage structures. Given that mutations in *HCFC1* cause craniofacial defects via *mmachc* expression, it is likely that mutation or knockdown of *HCFC1* interacting partners can also result in craniofacial abnormalities.⁹ For instance, mutations in *THAP11* have been associated with *cbfX*-like manifestations including craniofacial abnormalities. Quintana and colleagues⁹ have reported that knockdown of *thap11* causes defects in zebrafish facial development. Based on these data and the interaction between *ZNF143* and *HCFC1*, we hypothesized that knockdown of *znf143b* will result in craniofacial abnormalities and downregulation of *mmachc*; consequently, ascertaining a mechanism by which *znf143b* regulates vertebrate facial development.

Here, we demonstrate that knockdown of *znf143b* results in abnormal craniofacial development in zebrafish. Morphant animals presented with an array of craniofacial defects which included a shortened and cleaved Meckel's cartilage, distortion of the ceratohyal, and a partial loss of ceratobranchial cartilages. In view of these defects, we analyzed chondrocytes, a derivative of NCCs, which contribute to cartilage formation. Flow cytometry found equal numbers of total chondrocytes in animals injected with *znf143b* MO and 3-dimensional rendering of chondrocytes did not indicate gross morphological defects. However, morphants had decreased expression of *mmachc* and cartilage phenotypes were effectively prevented using a human *MMACHC* transgenic allele. Collectively, these data suggest a function for *znf143b* in craniofacial development.

METHODS AND PROCEDURES

Zebrafish maintenance

Embryos were produced by crossing AB wild type, Tupfel Long Fin, *Tg(col2a1a:EGFP)*¹⁰, or *Tg(ubi:MMACHC)*¹¹ adults. Fish were set up in a 2:3 or 2:2 ratio of females and males, respectively. Harvested zebrafish embryos were maintained in embryo medium at 28 °C. All animals were maintained and used in accordance with the guidelines from The University of Texas El Paso Institutional Animal Care and Use Committee protocol number 811869-5. Euthanasia and anesthetic procedures were performed according to the American Veterinary Medical Association guidelines, 2020 edition.

Morpholino injections

A validated antisense oligonucleotide morpholino (MO) was utilized to knockdown zebrafish *znf143b* expression (5' – GATCCATCCATTCATTCATCAAT – 3').⁶ Injections of MO and random control (RC) MO were performed at the single cell stage with a volume of 2 nL. A MO gradient from 0.20 mM (3.31 ng/embryo; N=34), 0.25 mM (4.14 ng/embryo; N=29), and 0.30 mM (4.97 ng/embryo; N=39) was performed. A final concentration of 0.30 mM was empirically derived, with an estimated 80% of morphant larvae affected at 5 days post fertilization (DPF). The injected embryos were incubated in E3 media at 28 °C and grown at 2- and 5- DPF for relative mRNA expression analysis and alcian blue staining, respectively. Morphant larvae were scored and allocated into groups based on the severity of craniofacial abnormalities ranging from mild, moderate, and severe. Morpholino injection was performed on 3 independent occasions with clutch mates obtained from independent carriers using equivalent numbers of total injected embryos/group. Carriers of *tg(ubi:MMACHC)* were mated and offspring were injected at the single cell stage with 0.30 mM of a translational blocking MO targeting *znf143b* or RC (GeneTools). Injected embryos were incubated at 28 °C and raised to 5 DPF for Alcian blue staining. Injection into the *tg(ubi:MMACHC)* was performed on two independent occasions with embryos obtained from independent male and female pairs with equivalent numbers of total injected embryos. Statistical analysis was performed using a Fisher's exact test between groups.

Staining of cartilage and imaging

Zebrafish larvae were collected at 5 DPF and were fixed in 2% paraformaldehyde in PBS, pH 7.5 at room temperature for 1 hour. Larvae were washed for 10 min with 100mM Tris pH 7.5/10mM MgCl₂ and were stained overnight at room temperature with Alcian blue stain pH 7.5 (0.4% Alcian Blue in 70% EtOH, 1 M Tris pH 7.5, 1M MgCl₂). Subsequently, larvae were rehydrated in 80% ethanol, 50% ethanol, 25% ethanol in 100 mM Tris pH 7.5 for 5 minutes each. Larvae were bleached in 3% H₂O₂ and 0.5% KOH for 10 min at room temperature. Two washes with 25% glycerol/0.1% KOH were subsequently performed at room temperature for 10 minutes. All samples were stored at 4 °C in 50% glycerol/0.1% KOH. Larvae were whole mounted to visualize the viscerocranium at 6.3x magnification in 100% glycerol.

RNA isolation and quantitative PCR (qPCR) analysis

Total RNA was extracted with TRIzol reagent (Fisher Scientific) from a pool of whole-body embryos (n=10) injected with RC or *znf143b* MO at a concentration of 0.30 mM (4.97 ng/embryo) at 2 DPF. Analysis was performed in two biological replicates with embryos injected from independent clutches. cDNA was created using the Verso cDNA Synthesis kit (Fisher Scientific) and equivalent concentrations of total RNA were utilized. qPCR was performed in technical triplicate using a Sybr green (Fisher Scientific) based approach with primer pairs as follows: *mmachc* (FWD: GCITTCGAGGTTTACCCCTTCC, REV: AGGCCAGGGTAGGGTCCTG) and *rp13* (FWD: TCCCAGCTGCTCTCAAGATT, REV:

TTCTTGGGAATAGCGCAGCTT). qPCR was performed with Applied Biosystems StepOne Plus system. Data analysis was performed using $2^{-\Delta\Delta ct}$ and the statistics of relative mRNA expression was performed using a T-test ($p < 0.001$).

Chondrocyte image processing

Chondrocyte imaging was limited to visualizing the hyosymplectic region across all larvae at 5 DPF. Whole larvae were angled on the right ventrolateral angle and mounted with 0.6% low agarose gel in a glass bottom petri dish (Fisher Scientific). We obtained confocal imaging with Zeiss LSM 700 at 40X magnification. For all groups, 12 to 21 Z-slices were obtained per image. IMARIS software was employed to generate 3D visualization output. 3D renderings were produced from 10 individuals/group which include non-injected, random control, and morpholino injected. Fiji, an open-source platform, was utilized to calculate angles between individual chondrocytes in the hyosymplectic region. To ensure the angles were measured in a single plane, ImageJ software was used to apply a Fire LUT to provide a fluorescent intensity gradient with equal pixel measurements. The angle tool was used to draw the center of three adjacent cells along the region of interest. Length measurements of chondrocyte nuclei and the hyosymplectic were performed using the LUT and tools featured in Fiji. Measurements were performed in 5 technical replicates and the average angle across samples was used to test for statistical significance.

Flow cytometry

To enumerate chondrocytes, we utilized the *Tg(col2a1a:EGFP)* reporter line injected with a RC or *znf143b* morpholino at 0.30 mM. Whole larvae were dissociated by adapting a previous protocol from Bresciani and colleagues.¹² For each group, a pool of five larvae were dissociated using 500 μ l of digestion mix (460 μ l of 0.25% trypsin-EDTA and 40 μ l of Type I Collagenase-100 mg/ml) at 30 °C. Larvae were fully homogenized via harsh pipetting. Dissociation was stopped by adding 800 μ l of lamb serum (Fisher Scientific) and centrifuged (7.0 x g) for five minutes at room temperature. Cells were resuspended in 800 μ l of 1X phosphate buffered saline (Fisher Scientific) and centrifuged for five minutes to wash the cells. Cells were resuspended in 500 μ l of 1X phosphate buffered saline (PBS) and filtered (utilized 70 μ M filter). Analysis was performed with Kaluza software at a fixed rate of 10,000 cell events for 3 minutes. A total of 10,000 events was collected per biological replicate (2 biological replicates were performed).

RESULTS

znf143b mediates craniofacial development and *mmachc* expression.

To perform a functional analysis of *ZNF143*, a transient knockdown of *znf143b* was performed. An antisense MO was previously designed to target the translation start site of *znf143b*, consequently, disrupting the translation of *znf143b* in zebrafish embryos. At 5 DPF, *znf143b* morphants were stained with Alcian blue to visualize the craniofacial development. Knockdown of *znf143b* resulted in a shortening of the Meckel's cartilage, partial loss of the ceratobranchial arches, and distortion of the ceratohyal (**Figure 1A-D**). Not all injected larvae replicated with the exact defects; however, roughly 84% ($n = 16/19$) of embryos injected with 0.30 mM of MO presented with abnormal craniofacial development (**Figure 1F**). All affected morphants ($n=16$) demonstrated with a shortened and cleaved Meckel's cartilage. We calculated that 16% ($n = 3$) of the total morphant embryos injected developed mild defects, while 21% ($n = 4$) had moderate defects. Interestingly, morphant animals with moderate defects developed heart edema in a similar fashion as those severely afflicted animals. The prevalence of a distorted ceratohyal was noted more in animals with severe defects. All morphant animals were categorized based on severity of structures shown in **Table 1**.

Category	Phenotypes
Mild	Shorten/Cleave Meckel's Cartilage (MC)
Moderate	Shorten/Cleaved MC, torn palatoquadrate, distorted ceratohyal, heart edema
Severe	Shorten/Cleaved MC, loss of ceratobranchial arches, inverted ceratohyal, heart edema

Table 1. Phenotypic categorization of craniofacial defects observed in *znf143b* MO injected larvae.

Pupavac and colleagues¹ reported reduced expression of *MMACHC* in a patient with a mutation in *ZNF143*. Mutations in *MMACHC* are known to cause a multiple congenital anomaly syndrome that is attributed to defects in cobalamin metabolism. Mild to moderate facial dysmorphism had been documented in patients with mutations in *MMACHC*.¹³⁻¹⁵ In addition, mutations in *HCFC1* that cause *cbX* syndrome are also characterized with facial dysmorphism. Therefore, we hypothesized that *ZNF143* interacts with *HCFC1* to regulate the expression of *MMACHC*. As shown in **Figure 1G**, knockdown of *znf143b* caused a statistically significant 20% decrease in *mmachc* expression ($p=0.0002$).

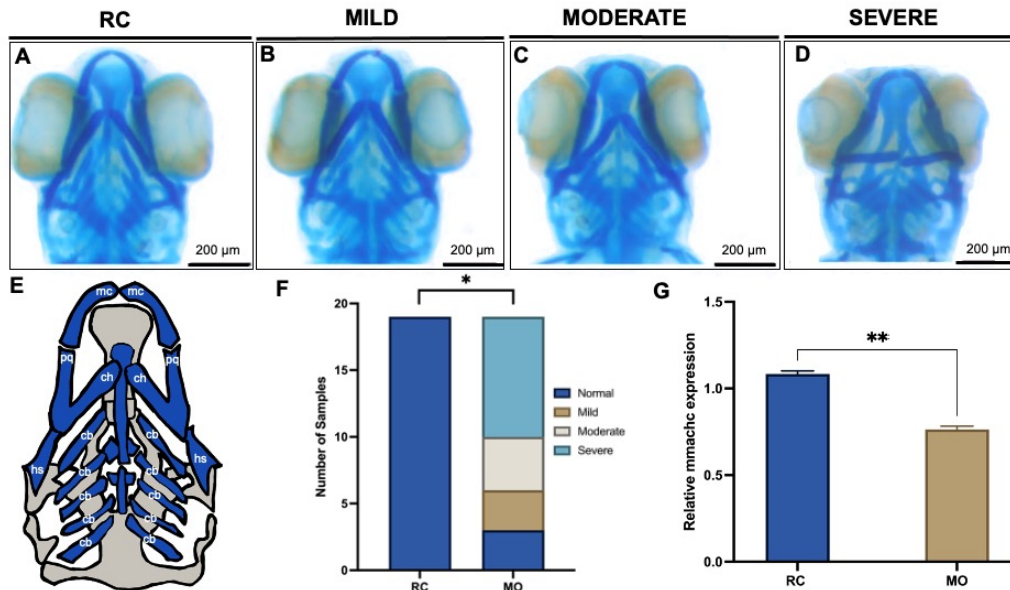


Figure 1. Loss of *znf143b* causes a spectrum of craniofacial abnormalities and a decreased expression of *mmachc*. (A-F) Alcian-Blue stain reveals heterogeneous craniofacial defects at 5 days post-fertilization (DPF) in *znf143b* morphant larvae (MO) when compared to random control (RC) injected fish. E) Viscerocranium cartilage structures of zebrafish: Meckel’s Cartilage (mc), Palatoquadrate (pq), Ceratohyal (ch), Ceraoabranhial arches (cb), and Hyosymplectic (hs). F) Total number of RC (n=19) and MO (n=19) larvae categorized by craniofacial phenotypes. Fisher’s exact test determined a significant difference between total number of affected and not affected animals (*p>0.0001) when comparing morphant (MO) and control injected (RC) larvae. Data represented here and the numbers of animals are a single representative of 3 biological replicates. G) Quantitative PCR demonstrated decreased expression of *mmachc* in *znf143b* morphants when compared to random control larvae (**p=0.0002). Representative experiment from 2 biological replicates is shown in (G).

Tg(ubi:MMACHC) expression prevents facial phenotypes in znf143b morphants.

Given the facial defects observed in morphant animals, we hypothesized that over expression of *MMACHC* could restore craniofacial deficits in *znf143b* morphants. The *Tg(ubi:MMACHC)* allele expresses the human *MMACHC* open reading frame under the control of the zebrafish ubiquitin promoter and was validated elsewhere.¹¹ We injected *znf143b* or RC morpholinos into the *Tg(ubi:MMACHC)* transgenic allele and stained them at 5 DPF with Alcian blue. Expression of *MMACHC* prevented the onset of *znf143b* mediated facial phenotypes (Figure 2C). As in the knockdown experiments, there was a statistical difference between animals injected *znf143b* and RC morpholinos (*p = 0.0248). The RC group had three mildly affected animals amongst a pool of twenty. In contrast, 19 of 23 morphant animals with wildtype background presented defects at 5 DPF (Figure 2B). Shown in Figure 2D, the total number of morphant animals in the mild, moderate, and severe groups was significantly reduced by expression of *MMACHC*, indicating that over expression *MMACHC* prevented the onset of facial phenotypes (**p = 0.0001).

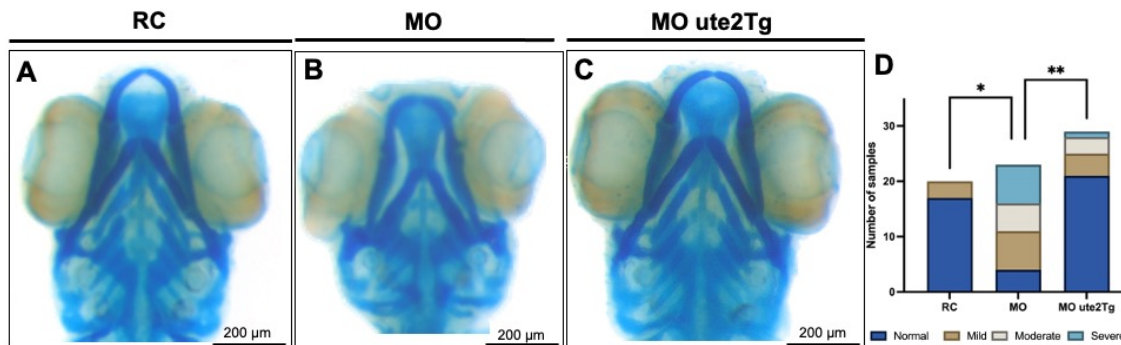


Figure 2. Prevention of craniofacial defects upon expression of *MMACHC* in *znf143b* morphant larvae. (A-C) Representative images of alcian-blue stained random control (RC) and *znf143b* (MO) injected larvae, in wildtype and *Tg(ubiquitin:MMACHC) (ute2Tg)* background at 5 days post fertilization (DPF). (A) RC animals showed normal craniofacial features. (B) MO injected larvae exhibited abnormal craniofacial phenotypes (i.e. shorten Meckel’s cartilage). (C) *znf143b* MO injection in animals with ubiquitous expression of *MMACHC (ute2tg)* prevented the craniofacial phenotypes induced by loss of *znf143b*. (D) Bar graph showing total number of RC (n=20), MO (n=23) and MO ute2Tg (n=29) larvae categorized by craniofacial phenotypes. Data represented here and the numbers of animals are a single representative of 2 biological replicates. Fisher’s exact test determined a significant difference between RC: MO injected animals (*p=0.0248) and MO injected animals: MO ute2Tg larvae (**p=0.0001).

znf143b does not exhibit abnormal chondrocyte stacking or defects in total cell number.

Knockdown of *znf143b* resulted in abnormal cartilage structures of the viscerocranium implicating a defect in neural crest cell (NCCs) developmental. Given the overt defects, we hypothesized abnormal development of chondrocytes, a derivative of NCCs that generate major skeletal structures of the viscerocranium. To test our hypothesis, we observed chondrocyte development in the hyosymplectic region using confocal microscopy and the *Tg(col2a1a:EGFP)* transgene. The hyosymplectic entails a region where the hyomandibula fuses with the symplectic rod and together secures the jaw skeleton to the neurocranium.¹⁶ It is formed from pharyngeal arch 2¹⁷, which also produces the ceratohyal. We observed the ceratohyal to be abnormally developed in morphant animals (Figure 1) and a recent publication from our laboratory demonstrated defects in chondrocyte development in a zebrafish mutant of *mmachc*.¹⁴ For these reasons, we imaged the developing hyosymplectic using confocal microscopy. We rendered 3D visualizations using Z-slices from high resolution confocal microscopy (Figure 3A-C). We measured the angle of 3 adjacent nuclei as a measure of chondrocyte intercalation as previously described.¹⁸ Angle measurements between three independent and adjacent chondrocytes was not statistically different between RC and morphant groups ($p = 0.9621$). Likewise, the length of the hyosymplectic was not significantly different between groups ($p = 0.3064$). We also sought to enumerate the total number of chondrocytes from whole larvae using flow cytometry. We did not detect a difference in the number of EGFP+ chondrocytes as shown in Figure D-D'' ($p=0.669818$). These data suggest that knockdown of *znf143b* does not affect number or intercalation of chondrocytes.

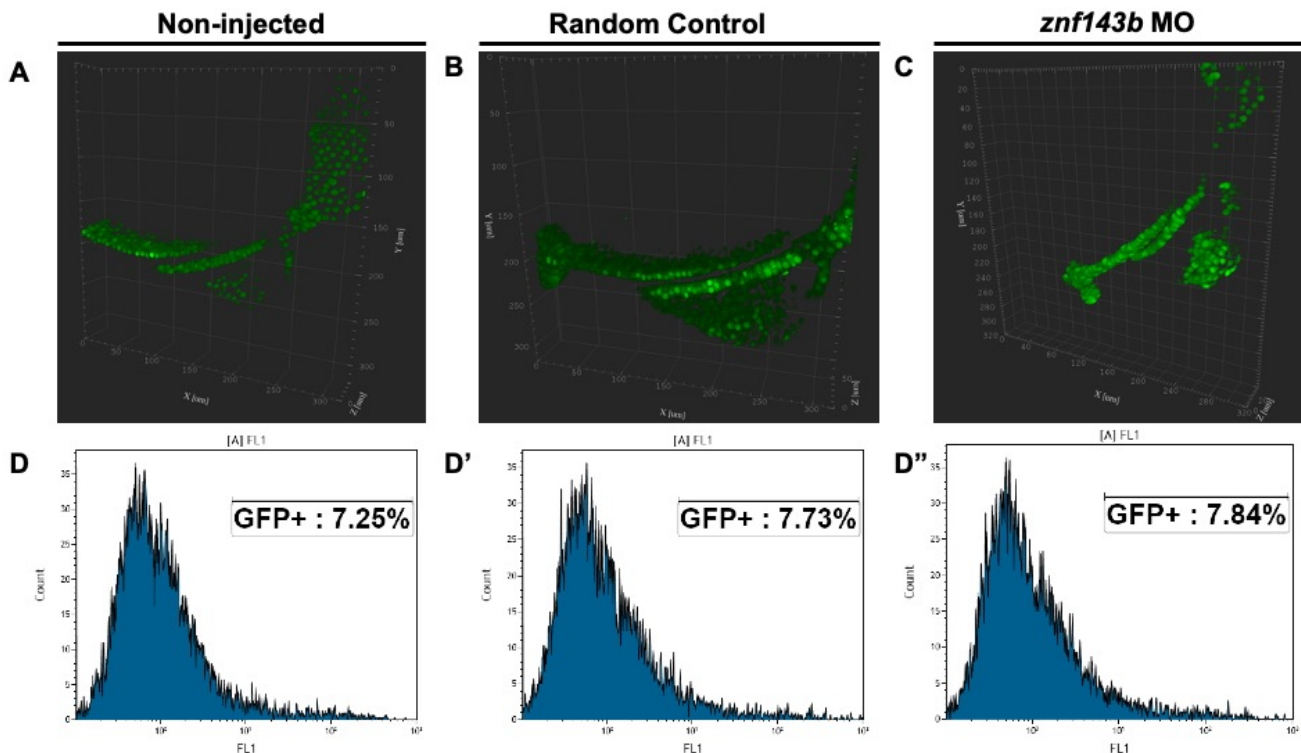


Figure 3. Knockdown of *znf143b* does not affect chondrocyte development in the hyosymplectic region or total chondrocyte cell number. (A-C) Representative 3D visualizations of the hyosymplectic (HS) region of injected larvae harboring the *Tg(col2a1a:EGFP)* allele at 5 DPF. (A) Non-injected animals showed normal extension of the HS region. Normal chondrocyte development of the HS was observed in random control group (B) and *znf143b* MO injected animals (C). Standard T-test found no statistical difference between random control and *znf143b* MO injected groups regarding chondrocyte angle ($p = 0.9621$) and hyosymplectic length measurements ($p=0.3064$). We quantified the number of chondrocytes across all groups with the *Tg(col2a1a:EGFP)* using flow cytometry analysis. (D-D'') Histograms of a single representative replicate displaying the percentage of GFP+ cells. Two biological replicates were performed 5 DPF from $n=5$ larvae/group. No statistical difference in the number of chondrocytes was found according to standard T-test ($p=0.669818$).

DISCUSSION

A single clinical study has reported a biallelic pathogenic variant of *ZNF143* that causes a *cbIX-like* syndrome.¹ The subject presented with increased levels of methylmalonic acid and homocysteine indicative of cobalamin deficiency. Additional phenotypes include intractable epilepsy, bilateral cleft palate, microcephaly, wide spaced eyes, progressive encephalopathy, and hypotonia.¹ These phenotypes are also observed in patients with mutations in *cbIC* disorder which is caused by mutations in *MMACHC*.¹⁹⁻²⁰ However, mild and moderate facial defects¹³⁻¹⁵ are not classic phenotypes associated with *cbIC*. Interestingly, *HCFC1* interacts with *ZNF143* to modulate the expression of *MMACHC* and mutations in *HCFC1* cause *cbIX* syndrome, which is very similar phenotypically to *cbIC*. Previous studies from Quintana and colleagues support a role for *HCFC1* and *MMACHC* during zebrafish craniofacial development.^{2,9} Similarly, our transient knockdown of *znf143b*, zebrafish ortholog of *ZNF143*,

caused reproducible craniofacial abnormalities in early zebrafish development. Interestingly, *znf143b* morpholino injected into embryos harboring an *MMACHC* transgene prevented morpholino induced craniofacial phenotypes. These data further support a role for *MMACHC* in facial development.^{2,9,21} However the function of *MMACHC* in *cbl* disorders is likely to be more complex because NCC specific expression of *MMACHC* in a mouse model of *cbfX* syndrome does not restore facial phenotypes.²¹ These data suggest there may be some species-specific mechanisms at play as it relates to *MMACHC* function. Moreover, the function of *MMACHC* may not be autonomous to NCCs, and thus, a global expression strategy may be required to restore phenotypes present in *HCFC1* and *ZNF143* loss of function assays. Finally, *HCFC1* and *ZNF143* regulate an immense number of target genes⁴ so it remains possible that *MMACHC* is not the sole genetic mediator of facial development in these *cbl* related disorders.

It is known that NCCs give rise to numerous tissues including chondrocytes of the viscerocranium.²² Thus, it is plausible that the craniofacial abnormalities observed in our morphant larvae are caused by abnormal NCC development, specifically cranial NCCs. However, our limited analysis of chondrocyte development and chondrocyte number did not show abnormal organization or defects in the total number of chondrocytes. We only studied a single time point, a single NCC marker, and a single region of the developing viscerocranium. Morphants were affected in various cartilaginous elements. These include Meckel's cartilage and the ceratohyal, both of which were dramatically affected. Future studies that analyze these other regions with additional time points and/or additional markers of NCC development may uncover phenotypes in chondrocyte and NCC development.

ZNF143 is a ubiquitously expressed transcriptional activator²³ and is largely involved in cellular and molecular processes that include but are not limited to cell growth, proliferation, cell cycle regulation, DNA repair, and progenitor cell identity.²⁴⁻²⁶ We therefore, analyzed the total number of chondrocytes using flow cytometry, which were normal. One possible explanation for the normal overall cell number we observed could be that although the expression of *ZNF143* is ubiquitous, the function of *ZNF143* is tissue specific. Thus, *ZNF143* could regulate facial development independent of proliferation, cell number, or cell cycle regulation. Future studies should aim at studying alternative cellular mechanisms to elucidate the putative role of *ZNF143* in NCC development. Alternatively, analysis of chondrocyte migration using live imaging could be performed. Previous studies have shown that migration is enhanced after knockdown of *ZNF143* in colorectal cancer cells.²⁷

Finally, mutation of *ZNF143* causes accumulated levels of homocysteine and methylmalonic acid.¹ This biochemical manifestation was not explored in *znf143b* morphants. Some patients with cobalamin disorders present with facial phenotypes and abnormal biochemical levels. However, it is not known if the accumulation of metabolites contributes to craniofacial abnormalities. As of now, we know that knockdown of *hcf1b*, a zebrafish ortholog of *HCFC1*, has no apparent changes in the levels of homocysteine and methylmalonic acid indicating normal metabolism of cobalamin.² Given its interaction with *HCFC1*, we can hypothesize that a knockdown of *znf143b* may show similar biochemical phenotypes in the zebrafish. Such a finding would implicate that craniofacial defects observed by knockdown of *ZNF143* or *HCFC1* are partially driven by *MMACHC* yet independent of cobalamin metabolism. Future work in this area is warranted.

CONCLUSION

In sum, our study functionally profiles the role of *ZNF143* in early craniofacial development using a zebrafish model. A morpholino mediated knockdown resulted in an array of craniofacial defects that include a shortened and cleaved Meckel's cartilage, distorted palatoquadrate and ceratohyal, and partial loss of the ceratobranchial cartilages. Alongside these apparent facial defects, we detected a decrease in the expression of *mmachc* mRNA. Injection of the *znf143b* MO into a transgenic allele overexpressing human *MMACHC* prevented the formation of craniofacial phenotypes suggesting some interplay between *ZNF143* and *MMACHC* during craniofacial development. Further, we found no abnormal development of chondrocytes in the hyosymplectic region and normal levels of total chondrocytes.

ACKNOWLEDGMENTS

Financial Support for this project was provided by NIDCR grant number R03 DE029517 given to Dr. Anita M. Quintana, NIMHD grant No 5U54MD007592 to the University of Texas El Paso, NIGMS linked awards R15GM118969, TL4GM118971, and UL1GM118970 to the University of Texas at El Paso. The content is solely the responsibility of the authors and does not necessarily represent the official views of the National Institutes of Health. The authors thank UTEP Core facilities for providing instruments for flow cytometry and imaging analysis of chondrocytes and mRNA expression analysis.

REFERENCES

1. Pupavac, M., Watkins D., Petrella F., Fahiminiya S., Janer A., Cheung W., Gingras A.C., Pastinen, T., Muenzer J., Majewski J., Shoubridge, E.A., Rosenblatt D.S. (2016) Inborn Error of Cobalamin Metabolism Associated with the Intracellular Accumulation of Transcobalamin-Bound Cobalamin and Mutations in *ZNF143*, Which Codes for a Transcriptional Activator, *Hum Mutat* 37, 976–982. <https://doi.org/10.1002/humu.23037>

2. Yu, H. C., Sloan, J. L., Scharer, G., Brebner, A., Quintana, A. M., Achilly, N. P., Manoli, I., Coughlin, C. R., 2nd, Geiger, E. A., Schneck, U., Watkins, D., Suormala, T., Van Hove, J. L., Fowler, B., Baumgartner, M. R., Rosenblatt, D. S., Venditti, C. P., & Shaikh, T. H. (2013) An X-linked cobalamin disorder caused by mutations in transcriptional coregulator HCFC1, *Am J Hum Genet* 93, 506–514. <https://doi.org/10.1016/j.ajhg.2013.07.022>
3. Quintana, A.M., Geiger E.A., Achilly N., Rosenblatt D.S., Maclean K.N., Stabler, S.P., Artinger B.K., Appel B., Shaikh T.H. (2014) Hcfc1b, a zebrafish ortholog of HCFC1, regulates craniofacial development by modulating mmachc expression, *Dev Biol* 396, 94–106. <https://doi.org/10.1016/j.ydbio.2014.09.026>
4. Michaud, J., Praz, V., James Faresse, N., Jnbaptiste, C. K., Tyagi, S., Schütz, F., & Herr, W. (2013) HCFC1 is a common component of active human CpG-island promoters and coincides with ZNF143, THAP11, YY1, and GABP transcription factor occupancy, *Genome Res* 23, 907–916. <https://doi.org/10.1101/gr.150078.112>
5. Huning, L., & Kunkel, G. R. (2020) Two paralogous znf143 genes in zebrafish encode transcriptional activator proteins with similar functions but expressed at different levels during early development, *BMC Mol Cell Biol* 21, 3. <https://doi.org/10.1186/s12860-020-0247-7>
6. Halbig, K.M., Lekven, A.C. & Kunkel, G.R. (2012) The transcriptional activator ZNF143 is essential for normal development in zebrafish, *BMC Mol Biol* 13, 3. <https://doi.org/10.1186/1471-2199-13-3>
7. Cerone, R., Schiaffino, M.C., Caruso, U., Lupino, S., & Gatti, R. (1999) Minor facial anomalies in combined methylmalonic aciduria and homocystinuria due to a defect in cobalamin metabolism, *J Inherit Metab* 22, 247–250. <https://doi.org/10.1023/a:1005521702298>
8. Sloan, J. L., Carrillo, N., Adams, D., & Venditti, C. P. (2008) Disorders of Intracellular Cobalamin Metabolism, In M. P. Adam (Eds.) et al., *GeneReviews®*. University of Washington, Seattle.
9. Quintana, A. M., Yu, H. C., Brebner, A., Pupavac, M., Geiger, E. A., Watson, A., Castro, V. L., Cheung, W., Chen, S. H., Watkins, D., Pastinen, T., Skovby, F., Appel, B., Rosenblatt, D. S., & Shaikh, T. H. (2017) Mutations in THAP11 cause an inborn error of cobalamin metabolism and developmental abnormalities, *Hum Mol Genet* 26, 2838–2849. <https://doi.org/10.1093/hmg/ddx157>
10. Askary, a., Mork, L., Paul, S., He, X., Izuhara, A.K., Gopalakrishnan, S., Ichida, J.K., McMahon, A.P., Dabizljevic, S., Dale, R., Mariani, F.V., Crump, J.G. (2015) Iroquois Proteins Promote Skeletal Joint Formation by Maintaining Chondrocytes in an Immature State, *Dev Cell* 35, 358–365. <https://doi.org/10.1016/j.devcel.2015.10.004>
11. Paz, D.*, Pinales, B.E.*, Castellanos, B.S.*, Perez, I., Gil, C.B., Jimenez-Madriral, L., Reyes-Nava, N.G., Castro, V.L., Sloan, J.,L., and Quintana, A.M. (2023) Abnormal chondrocyte development in a zebrafish model of cblC syndrome restored by an MMACHC cobalamin binding mutant, *Differentiation* 131, 74–81. <https://doi.org/10.1016/j.diff.2023.04.003> * indicates equal contribution
12. Bresciani, E., Broadbridge, E., & Liu, P. P. (2018) An efficient dissociation protocol for generation of single cell suspension from zebrafish embryos and larvae, *MethodsX* 5, 1287–1290. <https://doi.org/10.1016/j.mex.2018.10.008>
13. Biancheri, R., Cerone, R., Schiaffino, M. C., Caruso, U., Veneselli, E., Perrone, M. V., Rossi, A., Gatti, R. (2001) Cobalamin (Cbl) C/D deficiency: clinical, neurophysiological and neuroradiologic findings in 14 cases, *Neuropediatrics* 32, 14–22. <https://doi.org/10.1055/s-2001-12217>
14. Cerone, R., Schiaffino, M.C., Caruso, U., Lupino, S., Gatti, R. (1999) Minor facial anomalies in combined methylmalonic aciduria and homocystinuria due to a defect in cobalamin metabolism, *J Inherit Metab Dis* 22, 247–250. <https://doi.org/10.1023/a:1005521702298>
15. D’Alessandro, G., Tagariello, T., Piana, G. (2010) Oral and craniofacial findings in a patient with methylmalonic aciduria and homocystinuria: review and a case report, *Minerva Stomatol* 59, 129–137.
16. Mork, L., & Crump G. (2015) Zebrafish Craniofacial Development: A Window into Early Patterning, *Curr Top Dev Biol* 115, 235–269. <https://doi.org/10.106/bs.ctdb.2015.07.001>
17. Birkholz, D.A., Olesnicki Killian, E.C., George, K.M., & Artinger, K.B. (2009) prdm1a is necessary for posterior pharyngeal arch development in zebrafish, *Dev Dyn* 238, 2575–2587. <https://doi.org/10.1002/dvdy.22090>
18. Shull, L.C., Lencer, E.S., Kim, H.M., Goyama, S., Kurokawa, M., Costello, J.C., Jones, K., Artinger, K. B. (2022) PRDM paralogs antagonistically balance Wnt/ β -catenin activity during craniofacial chondrocyte differentiation, *Development* 149, dev.200082. <https://doi.org/10.1242/dev.200082>
19. Lerner-Ellis, J.P., Tirone, J.C., Pawelek, P.D., Dore C., Atkinson, J.L., Watkins, D., Morel, C. F., Fujiwara, T. M., Moras, E., Hosack, A.R., Dunbar, G.V., Antonicka, H., Forgetta, V., Dobson, C. M., Leclerc, D., Gravel, R.A., Shoubridge, E.A., Coulton, J. W., Lepage, P., Rommens, J.M., Morgan, K., Rosenblatt, D. S. (2006) Identification of the gene responsible for methylmalonic aciduria and homocystinuria, cblC type, *Nat Genet* 38, 93–100. <https://doi.org/10.1038/ng1683>
20. Carrillo-Carrasco, N., Chandler, R. J., Venditti, C. P. (2012) Combined methylmalonic acidemia and homocystinuria, cblC type. I. Clinical presentations, diagnosis, and management, *J Inheri Metab Dis* 35, 91–102. <https://doi.org/10.1007/s10545-011-9364-y>
21. Chern, T., Achilleos, A., Tong, X., Hill, M.C., Saltzman, A.B., Reineke, L.C., Chaudhury, A., Dsagupta, S.K., Redhead Y., Watkins, D., Neilson, J.R., Thiagarajan P., Green J.B.A., Malovannaya, A., Martin, J.F., Rosenblatt, D.S., & Poche, R.A. (2022)

- Mutations in Hcfc1 and Ronin result in inborn error of cobalamin metabolism and ribosomopathy, *Nat Commun* 13, 134. <https://doi.org/10.1038/s41467-021-27759-7>
22. Suzuki, T., Sakai, D., Osumi, N., Wada, H., & Wakamastu, Y. (2006) Sox genes regulate type 2 collagen expression in avian neural crest cells, *Dev Growth Differ* 48, 477–486. <https://doi.org/10.1111/j.1440-169X.2006.00886.x>
 23. Huning, L., & Kunkel, G.R. (2021) The ubiquitous transcriptional protein ZNF143 activates a diversity of genes while assisting to organize chromatin structure, *Gene* 769, 145205. <https://doi.org/10.1016/j.gene.2020.145205>
 24. Ye, B., Shen, W., Zhang, C., Yu, M., Ding, X., Yin, M., Wang, Y., Guo, X., Bai, G., Lin, K., Shi, S., Li, P., Zhang, Y., Yu, G., & Zhao, Z. (2022) The role of ZNF143 overexpression in rat liver cell proliferation, *BMC Genomics*, 23, 483. <https://doi.org/10.1186/s12864-022-08714-2>
 25. Izumi, H., Wakasugi, T., Shimajiri, S., Tanimoto, A., Sasaguri, Y., Kashiwagi, E., Yasuniwa, Y., Akiyama, M., Han, B., Wu, Y., Uchiumi, T., Arai, T., Nishio, K., Yamazaki, R., Kohno, K. (2010) Role of ZNF143 in tumor growth through transcriptional regulation of DNA replication and cell-cycle-associated genes, *Cancer Sci* 101, 2538–2545. <https://doi.org/10.1111/j.1349-7006.2010.01725.x>
 26. Ye, B., Yang, G., Li, Y., Zhang, C., Wang, Q., & Yu, G. (2020) ZNF143 in Chromatin Looping and Gene Regulation, *Front Genet* 11, 338. <https://doi.org/10.3389/fgene.2020.00338>
 27. Paek, A.R., Lee, C.H., & You, H.J. (2014) A role of zinc-finger protein 143 or cancer cell migration and invasion through ZEB1 and E-cadherin in colon cancer cells, *Molecular Carcinog* 53 Suppl, E161–168. <https://doi.org/10.1002/mc/22083>

ABOUT STUDENT AUTHORS

Isaiah Perez earned a Bachelor of Science in Microbiology from the University of Texas at El Paso in December 2022. Currently, he is part of the Graduate Research Employee Program (GREP) working with Dr. Stephen C. Ekker and his research team at the Mayo Clinic. He will transition to the Mayo Clinic Graduate School of Biomedical Science to begin his graduate studies in the Regenerative Sciences Ph.D. program. His long-term goal is to become a principal investigator. For this project he was mentored by Dr. Quintana.

PRESS SUMMARY

ZNF143 interacts with HCFC1 to modulate the expression of downstream targets including MMACHC – an enzyme that binds to and processes cobalamin (or vitamin B12). Mutations in *HCFC1* or *ZNF143* cause an inborn error of cobalamin metabolism characterized by metabolic defects, intellectual disability, seizures, and mild to moderate craniofacial abnormalities. Although not a prevalent phenotype, the function of ZNF143 in craniofacial phenotypes is unknown. Here, we characterize the role of ZNF143 in facial development via a knockdown of *znf143b*, a zebrafish ortholog. Our study demonstrates that ZNF143 regulates craniofacial development which can be partially prevented by over expression of MMACHC.

